Towards the development of plant-made PsVs as potential delivery vehicles for therapeutic HPV vaccines

by

Amy René Edwards

Dissertation presented for the degree of Master of Science

Department of Molecular and Cell Biology

University of Cape Town

July 2023

Supervisors: Dr Albertha van Zyl and Associate Professor Inga Hitzeroth

Declaration

I Amy R Edwards understand that plagiarism is using someone's work and pretend it is one's own, which is not acceptable.

I confirm that this **Dissertation presented for the degree of Master of Science in the Department of Molecular and Cell Biology** is my own work and has not been copied from anyone's work (published or unpublished).

I have used Harvard referencing style for citation and referencing. Each contribution to, and quotation in, this **Dissertation** from the work(s) of other people has been attributed and has been cited and referenced.

I further confirm that where required, **permission** was obtained for all images and figures used in this **Dissertation** and is stated as such, and where permission was not required, the original author was cited.

I have not allowed, and will not allow, anyone to copy my work with the intention of passing it off as his or her own work.

Signature: Signed by candidate

Date: 18/03/2024

Acknowledgements

To my wonderful supervisors, Dr Alta van Zyl and Associate Professor Inga Hitzeroth, for the opportunity to undertake this project and the unfaltering support you provided me for its duration. Your counsel and advice throughout this project have been invaluable. Alta, thank you for your continuous encouragement and patience, particularly during the writing process, and for always being there when I needed your guidance the most. This dissertation would not have been possible without you.

I would also like to thank Prof. Ed Rybicki, Dr Ann Meyers, and Dr Jennifer Stander for their invaluable expertise and guidance throughout the project despite not being my supervisors. Your time is highly appreciated.

I am incredibly grateful to all the members of the Biopharming Research Unit, both past and present, who have helped me in some way during my time in the lab. Thank you for being such a great team to work with and for making the lab a safe, inviting environment. A special thank you to Natalie Nel for her guidance and unyielding friendship.

Thank you to Prof. Rainer Fischer for the pTRAc vectors, Dr Neil Christensen for the monoclonal antibodies, Dr John Schiller's group for the pSHELL and pYSEAP plasmids, and Dr Georgia Schäfer for the HEK293TT cells.
A big thank you to Mohammed Jaffer for the assistance with transmission electron microscopy and for always managing to help me visualise grids, even during his busiest weeks.

Thank you to Shakiera Sattar for the tissue culture training and continued assistance with the BSLII laboratory equipment.

Thank you to the National Research Fund (NRF) for funding this project and to the NRF and Poliomyelitis Research Fund (PRF) for the bursaries that supported me financially for the duration of my master's degree.

To my endlessly supportive family, thank you for all your love and care. You are the glue that holds me together. A special thank you to my amazing mother, Lianne, for always being my biggest supporter and best friend. I am eternally grateful for everything you've done and continue to do for me. Without your love and care, I would not have made it this far.

To my beautiful friends, thank you for always supporting my academic endeavours despite not having a clue about what my research entails.

Finally, to my dear partner, Rowan, thank you for coming into my life during this degree and changing it forever. For helping me edit, bringing me endless snacks and cups of tea, and for giving me the strength to keep going when I didn't think I could – thank you.

Table of Contents

List of Abbreviations:

APC	antigen presenting cell(s)
BCIP	5-bromo-4-chloro-3-indolyl-phosphate
BeYDV	Bean yellow dwarf virus
BGH	bovine growth hormone
BM	basement membrane
bp	base pair(s)
BPV	Bovine papillomavirus
cDMEM	complete Dulbecco's Modified Eagle Medium
CHO	Chinese hamster ovary
CIN	cervical intraepithelial neoplasia
CMV	Cytomegalovirus
CO_2	carbon dioxide
CRPV	Cottontail rabbit papillomavirus
CTL	cytotoxic T lymphocyte(s)
DC	dendritic cell(s)
DMEM	Dulbecco's Modified Eagle Medium
DNA	deoxyribonucleic acid
DPBS	Dulbecco's phosphate buffered saline
dpi	days post infiltration
DTT	dithiothreitol
ECM	extracellular matrix
EDTA	ethylenediaminetetra-acetic acid
ELISA	enzyme-linked immunosorbent assay(s)
ER	endoplasmic reticulum
FBS	fetal bovine serum
g	gram(s)
GMP	Good Manufacturing Practice
HBV	Hepatitis B virus
HEK	human embryonic kidney

HIV	Human immunodeficiency virus
HPV	Human papillomavirus
hr	hour(s)
HSNaOAc	high salt sodium acetate
HSPBS	high salt phosphate buffered saline
HSPG	heparin sulphate proteoglycan(s)
kb	kilobase(s)
kDa	kilodalton(s)
kg	kilogram(s)
kV	kilovolt(s)
LA	Luria agar
LB	Luria broth
LIR	long intergenic region
M	molar
mA	milliamperes
MAb	monoclonal antibody
MES	2-morpholinoethanesulfonic acid
mg	milligram(s)
min	minute(s)
mL	millilitre(s)
mm	millimeter(s)
mM	millimolar
NAb	neutralising antibody
NaCl	sodium chloride
NaOAc	sodium acetate
NBT	nitro-blue tetrazolium
ng	nanogram(s)
nm	nanometre(s)
OD	optical density
ori	origin of replication

OVA	ovalbumin
PAGE	polyacrylamide gel electrophoresis
PBS	phosphate buffered saline
PCR	polymerase chain reaction
polyA	polyadenylation signal
PsV	pseudovirion(s)
PV	papillomavirus
PVX	Potato virus X
RCA	rolling circle amplification
RE	restriction enzyme(s)
SDS	sodium dodecyl sulphate
SEAP	secreted alkaline phosphatase
SIR	short intergenic region
SIV	Simian immunodeficiency virus
T-DNA	transfer DNA
TEM	transmission electron microscopy
vir	virulence
VLP	virus-like particle(s)

Symbols

α	alpha
β	beta
Ω	Ohm(s)
µF	microfarad(s)
µg	microgram(s)
µL	microliter(s)
µm	micrometre(s)
µM	micromolar
°C	degrees Celsius
%	percentage

Abstract

Infection with human papillomavirus (HPV) is the leading cause of cervical cancer, the fourth most common cancer in women globally. Cervical cancer results in an estimated 604,000 new cases and 342,000 deaths each year, with the majority of these cases reported in sub-Saharan Africa. HPV-16 is a high-risk oncogenic subtype and, along with HPV-18, is associated with >70% of all cervical cancers. While current vaccines can prevent infection with high-risk HPVs, they cannot induce regression of persistent infections, thus the development of vaccines that function therapeutically is required. DNA vaccines are ideal candidates for therapeutic treatment; however, naked DNA vaccines are associated with ineffective presentation to antigen presenting cells (APCs). This limitation can be overcome by using pseudovirions (PsVs) as vaccine delivery vehicles. HPV PsVs are highly immunogenic synthetic viral particles consisting of L1 and L2 capsid proteins, which self-assemble to package pseudogenome DNA. Pre-existing immunity to high-risk HPVs through natural infection and vaccination, however, preclude their use as delivery vehicles for DNA vaccines. The development of non-human papillomaviruses (PVs) PsVs for gene delivery is a novel alternative. PV PsVs are conventionally produced in mammalian cells. However, plants have demonstrated potential as an alternative platform for rapid PsV production due to their scalability and cost-efficiency. Therefore, the aim of this study was to investigate plant-based production of bovine papillomavirus 1 (BPV-1) PsVs encapsidating a HPV-16 therapeutic DNA vaccine candidate, and to assess their infectivity in mammalian cells.

Initially, strategies to optimise *Agrobacterium*-mediated transient expression of BPV-1 L1 and L2 capsid proteins in *Nicotiana benthamiana* were explored. Approaches such as an increased acetosyringone concentration for recombinant *Agrobacterium* induction, a heat-shock treatment of post-infiltrated plants, and an extended *in planta* maturation were investigated. A pseudogenome encoding secreted embryonic alkaline phosphatase (SEAP) was co-infiltrated with BPV-1 L1- and L2-encoding expression vectors. L1 protein expression and particle assembly were confirmed with western blotting and transmission electron microscopy (TEM) respectively. However, no SEAP expression was observed following infection of HEK293TT cells with the plant-made

particles and none of the strategies investigated were conclusively found to increase BPV-1 PsV yield.

Several geminivirus-derived self-replicating reporter plasmids encoding a HPV-16 shuffled E7 (E7SH) sequence were constructed using In-Fusion cloning. These constructs were co-expressed in *N. benthamiana* with expression vectors encoding BPV-1 or HPV-35 L1 and L2 proteins. HPV-35 was chosen as it has been shown to encapsidate a Zera®E7SH DNA vaccine in plants for delivery to mammalian cells *in vitro*. Following purification, rolling circle amplification (RCA) analysis showed successfully encapsidation of the E7SH-based pseudogenomes within the plant-made PsVs. However, TEM showed that PsV yields were low and no E7 expression was observed following infection of HEK293TT cells with the plant-made PsVs. These results indicated that encapsidation efficiency of PsVs produced in plants is low. BPV-1 and HPV-35 PsVs were also produced in HEK293TT cells and comparative analyses with plant-made particles revealed that, while the pseudogenomes were successfully encapsidated in the PsVs produced in both systems, only the HEK293TT-made PsVs effectively delivered their packaged DNA into mammalian cells. These findings demonstrate the ability of PsVs to self-assemble and encapsidate pseudogenome DNA *in planta* while also revealing potential limitations of plant-based PsV production. For plant-made PsVs to reach their potential in gene delivery, further optimisation and characterisation of plant-based PV PsV expression is required.

1 Chapter 1: Literature review

1.1 Introduction to papillomaviruses

Papillomaviruses (PVs) belong to *Papillomaviridae*, a family of viruses which arose 330 million years ago in Africa during the Carboniferous period of the Palaeozoic era (Rector & Van Ranst, 2013). Papillomaviruses are therefore one of the most ancient, as well as one of the largest vertebrate virus families known, with over 240 distinct types classified across 37 genera (Bernard, 1994; Cubie, 2013; Van Doorslaer, 2013). They are a highly diverse group of viruses ubiquitous to the animal kingdom, having been known to infect over 20 different mammalian species, in addition to reptiles and birds (Doorbar, 2005).

PVs are small oncogenic viruses that are known to cause hyperproliferative lesions, such as papillomas and warts, through infection of mucosal and cutaneous epithelia (O'Brien & Saveria Campo, 2002). The virions specifically target keratinocytes and the virus' infectious life-cycle depends on the differentiation of these keratin-producing epidermal cells (Campo & Roden, 2010). This has significant implications for the host's immune response.

Papilloma virions consist of a circular double-stranded DNA genome enclosed in a non-enveloped shell (Schwarz et al., 1983). The viral capsid is comprised primarily of the major structural protein, L1, arranged in 72 capsomeres within a T=7 icosahedral assembly (Baker et al., 1991; Trus et al., 1997). A minor L2 structural protein is also present, although at a 1/30th ratio to that of L1. Although the structural relationship between L1 and L2 is largely unknown, it is theorized that L2 is mostly embedded within the L1 lattice (Kirnbauer et al., 1993).

The genome ranges in size from 6.9kb to 8.6kb and is highly stable due to packaging with host cell histone proteins. It is distinctly organised into early-expressed (E1 – E7), late-expressed (L1 and L2) regions, and the long control region (LCR) (Van Doorslaer, 2013). The early genes are translated into proteins which are implicated in viral infection and replication (E1, E2, and E4), as well as oncogenic transformation (E5,

E6, and E7) (Brentjens et al., 2002). The late region codifies the capsid proteins, expressed to self-assemble and simultaneously encapsidate the viral genome. While the LCR does not code for any proteins, it carries the origin of replication (*ori*) and sequences that regulate viral replication and transcription (Van Doorslaer, 2013).

The L1 open reading frame (ORF) is the most conserved across the PV types. PVs are currently phylogenetically classified based on nucleotide sequence identity of this structural protein (de Villiers et al., 2004). Papilloma virion genomes are defined as a novel type if there is less than 90% L1 sequence homology with other PV types, and as a novel subtype with between 90-98% homology with another type. PVs with over 60% L1 ORF similarity are grouped together into genera (Bernard et al., 2010). Members of the same genus often display analogous host, habitat, and behavioural characteristics (Munday, 2014). PVs are known to be extremely host-specific with cross-species infection being a rare occurrence (Munday et al., 2007). An exception to this is the bovine delta-papillomaviruses which are well-known to infect multiple ruminant species (Munday, 2014).

1.2 HPV

Since its first isolation in 1949 by Strauss et al, human papillomavirus (HPV) has become universally recognized as a major human pathogen (Brentjens et al., 2002). HPV is the most extensively studied within the PV family, with over 100 serotypes identified (Bernard, 2005).

1.2.1 HPV classification

In addition to classification based on L1 sequence homology, several other identification systems to define and subtype human papillomaviruses are currently utilized. HPVs are also classified according to their tissue tropism, ability to induce oncogenic transformation, and disease manifestation (Tyring, 2000). HPV serotypes can be defined as dermatotropic, with an affinity towards colonization of the epidermis, or mucosotropic, with an affinity towards mucous membranes. Presentations of the viral infections within these cellular microenvironments allow classification as non-genital cutaneous and genital mucosal. Finally, the potential for oncogenesis further identifies the virus as either low or high-risk (Brentjens et al., 2002).

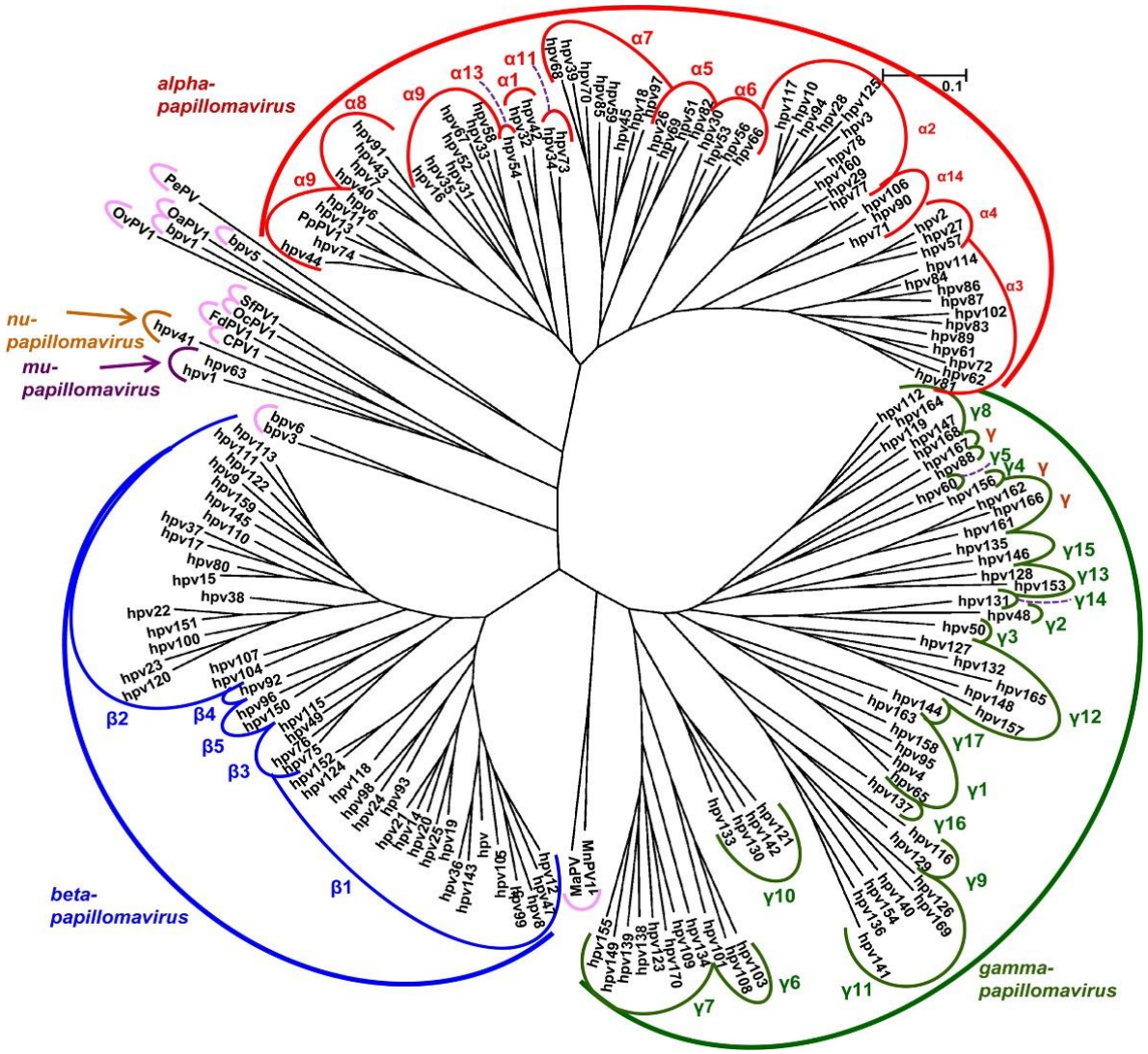

Figure 1.1: Phylogenetic classification of human papillomaviruses. Phylogenetic tree analysis characterising papillomavirus genera and species based on L1 sequence homology. PV types shown with pink are single animal papillomaviruses. Image from de Villiers (2013) with permission.

These characteristics can be combined to form a hierarchical system of papillomavirus classification that reflects the virus' evolution (Figure 1.1). As a result, five genera of HPVs exist of which two are notable (Doorbar, 2006). Alpha and Beta genera encompass 90% of all currently classified HPVs (Ramoz et al., 2002). Beta HPVs are classically associated with benign cutaneous infections. Those belonging to the Alpha genus are further subdivided into three groups – high-risk, low-risk, and cutaneous. High and low-risk types are known to colonize the genital mucosa while cutaneous viruses predominantly cause common warts and are seldom associated with cancer (Doorbar, 2016). A subset of genital-mucosal infecting HPVs targets the cervical

epithelium and an even smaller subset of these is associated with neoplasia that leads to cancer. Those that are potentially oncogenic are characterized as high-risk (hrHPV) (Beutner & Tyring, 1997). These types are implicated in 99.7% of global cervical cancer cases and include HPV-16/18/31/35/39/45/51/52/56/58/66 and -68 (zur Hausen, 2002). HPV-16 and -18 are the most prevalent of the hrHPVs and are present in over 70% of all cervical cancer cases (Moody & Laimins, 2010).

1.2.2 HPV and cervical cancer: Aetiology

A group of high-risk mucosatropic HPV types are recognized as the aetiological agent of cervical cancer (Bosch et al., 2002). The role of human papillomaviruses in cervical cancer was first suspected in 1976 by Meisels and Fortin when they discovered the presence of papillomavirus infection in cervical smears (Meisels & Fortin, 1976). Their findings were swiftly supported by the detection of papilloma virions in dysplastic cervical lesions (Della Torre et al., 1978). Suspicions were further confirmed when high-risk HPV subtypes 16 and 18 were isolated and cloned from cancer biopsies (Dürst et al., 1983). A few years later, cervical cancer cell lines revealed a high degree of E6 and E7 viral gene expression (Schwarz et al., 1985). Before the turn of the century, epidemiological studies and advances in molecular technology had provided indisputable evidence of the causal relationship between certain human papillomaviruses and cervical cancer (Bosch et al., 2002). The vast heterogeneity of HPV and its aetiological nature had been uncovered.

1.2.3 HPV mechanism of infection

Most infections caused by high-risk HPV types are asymptomatic and are usually acquired by young adults following the commencement of sexual activity (de Martel et al., 2012). HPV is thus classified as a sexually transmitted disease (Doorbar, 2016). Incidence of infection reaches a peak with hosts up to the age of 25 and then decreases thereafter, as the immune system clears the virus (Forman et al., 2012). However, HPV infections are known to be persistent rather than transient and may take months or years to resolve (Moscicki et al., 2012). Although most cases clear without causing any serious disease, persistent infections can have severe implications for the host.

Viral persistence, if accompanied by heightened E6 and E7 expression, can lead to the accumulation of genetic mutations resulting in chromosomal abnormalities (Roman & Munger, 2013). The site of infection is a strong determinant for whether this dysregulated level of gene expression results simply in limited cell proliferation or low to high-grade neoplasia (Doorbar, 2016). High-risk HPVs cause cancer at highly specific epithelial sites, namely the cervical transformation zone, the anal transformation zone, and the oropharynx. The cervical transformation zone is defined as the epithelial region where the stratified cells of the ectocervix progress into the columnar cells of the endocervix (Egawa et al., 2015). The virus' capacity to induce gene expression dysregulation within the host is dependent on the presence of these dividing basal cells at these specific regions.

Studies have observed, however, that upon infection HPV virions bind preferentially to the basement membrane (BM) rather than the cervicovaginal epithelia (Roberts et al., 2007). Moreover, efficient binding of virions to the BM is dependent on the disruption of the epithelial integrity of the genital tract (Cladel et al., 2008). Injury via physical or chemical means results in removal of the upper epithelial layers, allowing direct exposure to the BM (Auewarakul et al., 1994). Ulceration at the site of infection is therefore vital for the establishment of HPV pathogenesis. It is thought that virions then associate with their host cells at a later stage (Kines et al., 2009).

1.2.4 HPV structure

HPV genomes generally consist of 8000bp and eight or nine overlapping genes, with slight variation across genera (Brentjens et al., 2002). Their genome structure reflects that of all those described within the *Papillomaviridae* family – an ordered distribution of early and late transcribed zones with a single control region (Figure 1.2). The early genes, labelled E1 – E8, encode proteins with specific roles in viral transcription and replication (Frattini et al., 1996). Many of the early gene ORFs overlap to allow formation of polycistronic mRNA. Notably, E6 and E7 oncogenes are expressed as bicistronic mRNA which allows coupled oncoprotein expression (Stacey et al., 2000). Late genes, L1 and L2, encode the major and minor proteins and form the distinct T=7 papillomavirus capsid described above (Tyring, 2000). Each gene encodes for a specific function in the attachment, entry, intracellular trafficking, and eventual

dissemination of the HPV virions within and from host cells. Expression of these genes, and their associated function, is dependent on the virus' phase of infection within the host (Schiller et al., 2010).

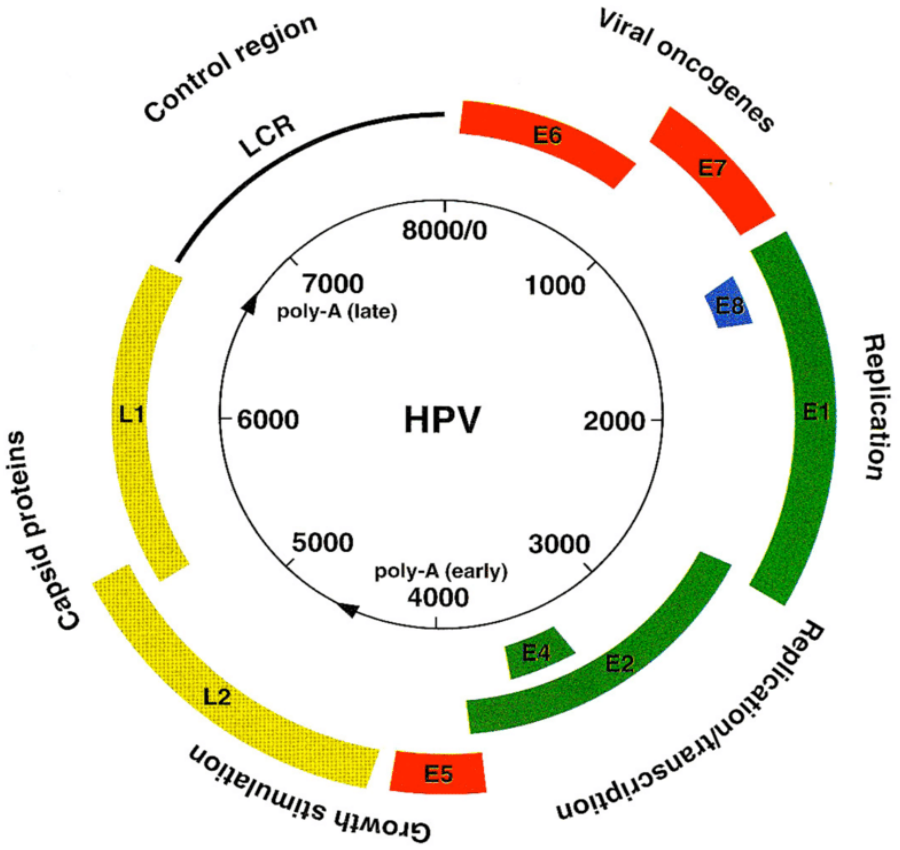

Figure 1.2: Genome organisation and protein function of HPV. The genome is made up of seven early genes (E1 – E8), two late genes (L1 and L2), and a long control region (LCR) consisting of transcriptional and replicational regulatory elements. Solid bars indicate ORFs. Image from Antonishyn (2007) with permission.

1.2.5 HPV lifecycle

1.2.5.1 Cell entry

Entry of PVs into host cells is receptor mediated. Due to the high level of conservation of the major L1 capsid protein across papillomaviruses, the binding moiety on the surface of host cells is also relatively well conserved (Qi et al., 1996). Capsid proteins across PV types have been shown to compete for binding to the same receptor on cells (Roden et al., 1994). Although the exact nature of this process is unknown, it is widely accepted that viral uptake is facilitated by heparin sulphate proteoglycans (HSPG) (Shafti-Keramat et al., 2003). Following initial attachment of L1 to HSPG, the

viral capsid undergoes a string of conformational changes at the cell surface (Selinka et al., 2007). L2, previously hidden within the L1 pentamers, becomes exposed to furin cleavage at the N-terminus (Kines et al., 2009). This cleavage is thought to be necessary for virion internalisation as it results in the unveiling of a secondary binding site on L1. Thus, it appears that efficient viral internalization also depends on the presence of secondary receptors, possibly α6 integrin (Evander et al., 1997). From this point, the process of cell entry is relatively slow and non-conserved for HPV types. Most types, however, undergo clathrin-coated endocytosis (Day et al., 2003). Particles then disassemble within endosomes to unsheathe the viral DNA, which is then transferred to the nucleus by L2 (Day et al., 2004).

1.2.5.2 Genome maintenance

From this point, within the basal cell layer, the virus enters a phase known as genome maintenance (Figure 1.3). Within this phase, the viral genome maintains its stability as a low copy number episome, without integrating itself into the host cell genome (Doorbar, 2006). This low level is maintained through expression of E1 and E2 genes (Wilson et al., 2002). It has been postulated that a low level of E6 and E7 expression also occurs at a later point of this stage of infection to drive cells into S-phase. The specific pattern of this expression is, however, unclear (Crum, 1998).

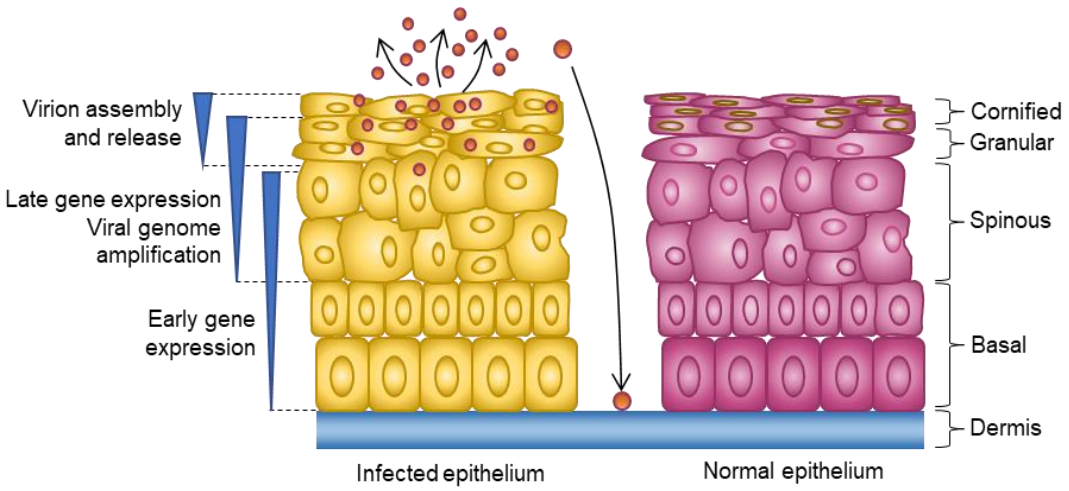

Figure 1.3: The HPV life cycle. Uninfected epithelium is shown on the right and HPV-infected epithelium is shown on the left. The virus enters the skin and infects basal keratinocytes at the basement membrane. The viral genome then replicates with the epithelial cells, allowing daughter cells to migrate upwards. Virus particles are shed from the top layer of the epidermis, from the cornified epithelial cells (red spheres). Image adapted from Moody and Laimins (2010).

1.2.5.3 Genome amplification and viral synthesis

Viral replication occurs in the mid to upper epithelium and is regulated by the differentiation-dependent late promoter. Activation of the promoter leads to up-regulation of E1-E5 genes, all of which play vital roles in viral genome amplification. This has no direct effect on any oncogenic transformation that may be developing (Middleton et al., 2003).

Following genome replication, viral synthesis occurs in the upper epithelium (Ozbun & Meyers, 1998). Expression of the capsid proteins is also controlled by the late promoter, with L2 minor capsid protein production preceding that of the L1 major capsid protein (Florin et al., 2002). This is followed by self-assembly of HPV particles within nuclear structures of upper epithelial cells. Here, 360 copies of L1 interact with ~12 copies of L2 to form an icosahedral shell with a single copy of the amplified viral genome enclosed (Modis et al., 2002). L1 protein expression alone is sufficient for virus-like particle self-assembly, but the inclusion of L2 proteins is necessary for both packaging of genetic material and infectivity (Stauffer et al., 1998; Zhou et al., 1993).

1.2.5.4 Viral shedding

HPVs are non-lytic and thus, to be successful, must be released from the infected epithelial cells when they reach the surface layer of the epidermis (Doorbar, 2005). This internal virion retention, coupled with viral molecular mechanisms that limit epitope display in the lower epithelium, inhibits immune cell detection (Marchetti et al., 2002). Following shedding, the virus particles must withstand the conditions of the extracellular environment. They achieve this through desiccation tolerance, before reinfection of new host cells (Roden et al., 1997).

1.2.5.5 Productive proliferation

At some point after infection, the ordered expression of viral products is either replaced by productive proliferation or viral clearance. In uninfected hosts, basal cells would depart the cell cycle following migration into the suprabasal cell epithelium. They would then undergo terminal differentiation to form a physical epidermal barrier against the environment (Madison, 2003). Under viral infection conditions, the basal cells lose restraint of the cell cycle and terminal differentiation is stunted (Sherman et al., 1997).

Persistence of infection leads to the development of squamous epithelial lesions (SILs). In the cervix these are classified as cervical intraepithelial neoplasia (CIN). The development of low-grade neoplasia (CIN 1) can then progress to high-grade CIN 2/3 which can further develop into invasive cervical malignancies (zur Hausen, 2002). Progression of neoplasia is directly correlated with increased E6 and E7 expression (Doorbar et al., 2012). It is not fully understood how E6 and E7 expression from the viral episome becomes dysregulated but changes in hormone signalling and epigenetic modifications are thought to play a role (Ding et al., 2009; Gariglio et al., 2009).

When expressed, E7 stimulates cell cycle progression by associating with the retinoblastoma protein (pRb). This association triggers several downstream effects that ultimately result in activation of host cyclins required for mitotic progression and S-phase entry (Munger & Howley, 2002). The effects of E7 are complemented by those of E6. E6 proteins function to associate with p53, a protein that initiates cell-cycle arrest to allow DNA repair and cell apoptosis if necessary (Ozaki & Nakagawara, 2011). In high-risk HPV types, this E6 to p53 association drives the ubiquitination and subsequent degradation of p53. The combined effects of these oncoproteins result in uncontrolled cell division and the accumulation of random DNA mutations (Doorbar, 2005).

The viral dysregulation associated with CIN 2/3+ development is considered to facilitate episomal integration of the viral genome into fragile sites within the host cell chromosome (Doorbar et al., 2012). Linearisation of the viral episome during genomic integration results in the disruption of the E2 gene. When expressed, E2 acts as a transcriptional repressor of E6 and E7. Disruption of E2, coupled with host genome integration, therefore results in the constitutive expression of the oncogenes. The genomic instability that results from this constant expression leads to cancer (Chabeda et al., 2018; zur Hausen, 2002).

1.3 HPV and cervical cancer: Burden

According to 2020 statistics, cervical cancer is the fourth most diagnosed cancer and the fourth leading cause of cancer-related death in women worldwide. In 2020 alone, an estimated 604,000 new cases emerged, and 342,000 deaths were reported (Sung et al., 2021, p. 214). Cervical cancer is the leading cause of cancer death in 36 countries and the most frequently diagnosed cancer in 23 countries (Sung et al., 2021, p. 216). In the context of South Africa, cervical cancer leads in cancer-caused deaths and its frequency of diagnosis is second only to breast cancer (Figure 1.4) (De Vuyst et al., 2013; "Global Cancer Observatory: Cancer Today," 2020). Global estimates are misleading, however, as there are significant disease burden disproportionalities between regions, and between countries. Sub-Saharan Africa (SSA), the region with the highest cervical cancer incidence rate, accounts for the majority of annually reported cases and deaths (Sung et al., 2021, p. 233). Within these developing countries, incidence rates are 7 to 10 times that of more developed regions such as North America, Europe, and Australia ("Global Cancer Observatory: Cancer Today," 2020). Wide disparities in the Human Development Index (HDI) and poverty rates between these developed and developing regions account for over 52% of variations in incidence and mortality (Singh et al., 2012).

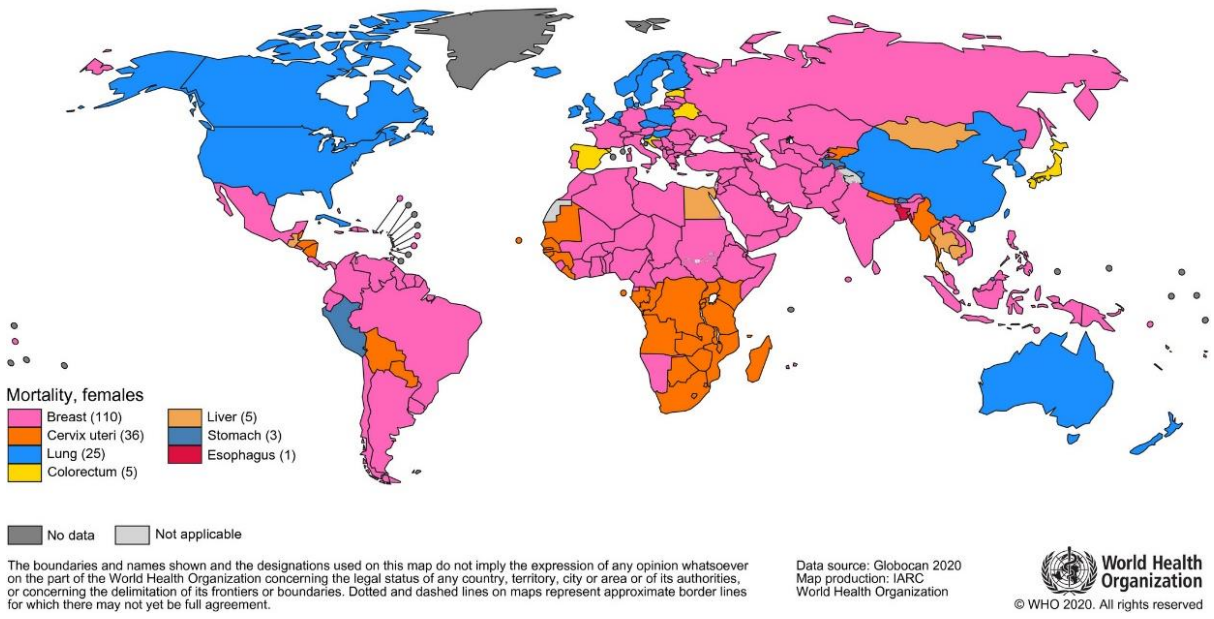

Figure 1.4: Most common cause of cancer death by country in 2020 in women. Colours in the legend represent type of cancer most prevalent in each country. Source: WHO (2020).

Although HPV infection is necessary for cervical cancer development, with 12 high-risk types being classified as group 1 carcinogens, its presence alone is not sufficient (Walboomers et al., 1999). Known cofactors of HPV infection include smoking, a high fertility rate, long term use of hormonal contraceptives, and, significantly, co-infection with other sexually transmitted diseases (STDs) like human immunodeficiency virus (HIV) and *Chlamydia trachomatis* (Sung et al., 2021). South Africa leads the globe in both HIV incidence and mortality, and this significantly contributes to the country's elevated cervical cancer burden (Rikhotso et al., 2022).

Over the last few decades, most parts of the world have seen a steady fall in cervical cancer incidence and mortality rates. This decline is attributed to the combined effects of factors such as improvements in genital hygiene, diminishing prevalence of STDs, increased socioeconomic levels, and highly effective preventative measures (Prendiville & Sankaranarayanan, 2017). Not all countries have reflected this trend, however, with consistently rising rates reported in seven of eight SSA countries, including South Africa (Jedy-Agba et al., 2020).

Cervical cancer is deemed to be almost entirely preventable. This is due to the implementation of highly successful primary and secondary prevention strategies, such as HPV vaccination of both adolescent females and males, and regular cancer screening (Bray et al., 2005). Australia has demonstrated the power of national vaccination strategies with the implementation of a government-funded school vaccination program in 2007. The quadrivalent vaccine was initially rolled out to girls aged 12-13, then to those between 13-26 years old, and was finally extended to include boys in 2015 (Dyda et al., 2019; Garland et al., 2011). This intensive strategy has resulted in protective coverage of 90.9% of females and 86.9% of males born from 2002 onwards (Smith et al., 2021). The measures employed in Australia are resource-dependent and can be costly, however, and have not been equitably employed across regions (Sung et al., 2021). Less than 30% of low- and middle-income countries (LMICs) have effectively implemented national HPV vaccination programmes compared with over 80% of high-income countries ("Global HPV Vaccine Introduction Overview," 2020). This socioeconomic gap is further widened by the lack of cervical screening in LMICs. This is especially apparent for SSA countries, where only a median of 17% of women have been screened (Lemp et al., 2020).

Although the current statistics for LMICs are grim, they are not beyond intervention. In 2018, the Director-General of the World Health Organisation (WHO) called for the global elimination of cervical cancer through the implementation of a three-stage strategy that could result in the prevention of over 62 million deaths within the next century (Canfell et al., 2020). The strategy would involve (1) the vaccination of 90% of all girls by age fifteen, (2) two screenings of 70% of women between 35-45 years old, and (3) the treatment of 90% of all precancerous lesions detected via screening ("WHO Director-General Calls for All Countries to Take Action to Help End the Suffering Caused by Cervical Cancer," 2018). In countries with a low HDI, the eradication of cervical cancer could take until the end of the 21st century. In contrast, high-income countries are expected to achieve this goal in the next 40 years (Brisson et al., 2020).

1.4 HPV vaccine development

1.4.1 Virus-like particles as vaccines

Virus-like particles (VLPs) are structures made up of viral structural proteins which lack the presence of virulent genetic material and replication capabilities. VLPs are based on the ability of structural antigens to spontaneously assemble into repeated arrangements following DNA expression (Noad & Roy, 2003). This assembly can be achieved in a diverse range of production systems. Their size and morphology are dependent on the viral proteins incorporated (Fifis et al., 2004). They are safe due to the absence of infectious viral genes, and elicit strong immunogenic responses due to their repetitive, high-density presentation of epitopes. VLPs therefore have strong potential in vaccine development against a multitude of diseases caused by viral infections (Grgacic & Anderson, 2006).

The particulate nature of VLPs allows for potent T-cell induction through interactions with dendritic cells (DCs). These antigen-presenting cells (APCs) phagocytose antigens in the cytosol, and subsequently process and display the peptides for stimulation of both cytotoxic T cells and helper T cells. This cross-presentation drives pathogen clearance in hosts (Chen & Lai, 2013). With a size range of 20-300nm in diameter, VLPs are ideal for DC uptake and antigen processing. Just a single VLP provides APCs with thousands of antigenic materials to process and present for

immune cell activation (Fifis et al., 2004). Moreover, VLPs of 20-200nm are capable of rapid diffusion into lymph nodes, where they can be directly presented to B and T lymphocytes (Roozendaal et al., 2008).

In addition to efficient stimulation of T cells, VLPs can also effectively induce B cells. Their arrangement of repetitive epitopes makes VLPs a primary target for vigorous B cell recognition (Bachmann & Zinkernagel, 1996). Particulate antigens induce oligomerization of epitope-specific immunoglobins (Ig) on B cell surfaces (Bachmann & Zinkernagel, 1997). This Ig cross-linking triggers a signal-cascade that initiates B cell and T helper cell proliferation, neutralising antibody production, and long-lasting B cell memory (Chen & Lai, 2013). These immune-stimulating mechanisms have made VLPs a highly successful vaccine platform.

1.4.2 Prophylactic HPV VLP vaccines

For years following the discovery of high-risk HPV types and their role in cervical cancer development, researchers endeavoured towards the development of a safe and practical papillomavirus vaccination platform. The virus' inability to grow in culture, as well as the downfalls of live attenuated vaccines, made this challenging (Hagensee et al., 1993). Attention was thus turned towards the use of the L1 major structural protein in VLP vaccine development. The bacterial expression system used, however, resulted in malformed purified particles that failed to elicit a neutralising antibody response in animal models (Schiller & Davies, 2004). In papillomavirus infection, neutralising antibodies (IgG and IgM) are believed to be the primary mechanism for viral inhibition (Day et al., 2010). For the correct assembly and immunogenicity of HPV VLPs, a eukaryotic expression system is required (Kirnbauer et al., 1992). Subsequent studies found that L1 VLPs purified from eukaryotic cells stimulate neutralising antibody production against PVs in model animal systems (Christensen et al., 1996). These findings led to the development and commercialisation of three VLP-based HPV vaccines, Cervarix™ (GSK), Gardasil 4® (Merck) and Gardasil 9® (Merck). Cervarix™ is a bivalent vaccine against high-risk types 16 and 18 and is produced in baculovirus-infected insect cells. Gardasil® was originally a quadrivalent vaccine which protected against types 6, 11, 16, and 18, and was expressed in recombinant yeast cells. In 2014, Merck released Gardasil 9®, an updated iteration of their original 4vHPV

vaccine. The newer version is 9-valent, protects against the four original types as well as HPV-31, 33, 45, 52, and 58, and is also expressed in yeast cells. Ongoing clinical trials have repeatedly demonstrated a high level of prophylactic efficacy ranging from 96-100% after three 10-50μg intramuscular injections. Furthermore, antibody titres generated from HPV VLP vaccines are 10-fold higher than that of natural infection and provide long-term protection (Harper et al., 2006; Mao et al., 2006).

There are, however, limitations associated with these vaccines and their expression platforms. Firstly, the target population is pre-adolescent and adolescent girls, before commencement of sexual activity. This is a notoriously difficult age-group to target due to low levels of contact with healthcare services (Schiller & Müller, 2015). An additional constraint is the need for three injections over at least six months. School-based vaccination programs have been crucial for effective immunisation rates and are associated with an 80% increase in vaccine dose completion (Hopkins & Wood, 2013). There is still limited vaccine uptake in developing countries, however, with only 8% of LMICs having introduced the vaccine by 2016 (WHO, 2016). Secondly, due to the highly specific immune response to L1 proteins, there is limited coverage to the HPV types incorporated in the vaccines. Cross-neutralising titres are inadequately low, at less than 1/100th that of type-specific titres (Schiller et al., 2012).

There are also limitations to the expression systems used for recombinant protein production. Several factors such as plasmid instability, low protein yield, and protein hyper-glycosylation have limited the use of yeast, specifically *Saccharomyces cerevisiae*, in commercial assembly (Baghban et al., 2019). The baculovirus-insect system is also limited in that VLPs can only undergo simple post-translational modifications (PTMs). Furthermore, co-expression with baculovirus particles can complicate downstream processing, and are associated with regulatory and safety concerns (Harrison & Jarvis, 2006).

These vaccines are also expensive to produce and deliver, with cold chain requirements restricting broad-scale distribution (Hancock et al., 2018). Adjuvants included in vaccines to enhance VLP immunogenicity also increase costs and render the product thermolabile (Rosales & Rosales, 2017). While some manufacturers have lowered the price to increase accessibility, the vaccines and their delivery are still

prohibitively costly for most LMIC countries ("GAVI injects new life into HPV vaccine rollout," 2013).

Lastly, and most notably, while VLP-based vaccines effectively induce a humoral immune response, these immunogens do not induce cell-mediated immunity necessary for viral clearance or regression of cervical lesions (Wang & Roden, 2013). Their use is thus restricted to HPV-naïve individuals. The VLPs elicit neutralising antibodies exclusive to L1 and, in established HPV proliferation, expression of structural proteins is lost (Kumar et al., 2015). As a result of these limitations, high cervical cancer incidence and mortality rates remain a serious global concern.

1.4.3 Therapeutic HPV vaccines

While a humoral response is sufficient for prevention of HPV infection, a cell-mediated immune response is necessary for elimination of established infections (Figure 1.5). Cell-mediated immunity is achieved through the facilitation of antigen presenting cells, the generation of cytotoxic T lymphocytes (CTLs), and the mediation of T helper 1 (Th1) cells (Yang et al., 2016).

Using ideal target antigens, therapeutic vaccines induce a robust cell-mediated response to drive disease regression and viral clearance. High concentrations of target antigens need to be attained for activation of APCs, such as dendritic cells (Hung et al., 2008). These cells transport the processed viral peptides to the lymph nodes, where they are presented to naïve T cells via major histocompatibility complex (MHC) I and II molecules. This activates their transformation into CD8+ cytotoxic T cells and CD4+ Th1 cells through association with MHC I and II stimulators, respectively. The activated Th1 cells then promote the proliferation and differentiation of the activated CTLs into effector cells (Skeate et al., 2016). These cells then target and kill HPV-infected tissue. The helper cells also function to secrete cytokines which aid in further activation of CD8+ T cells and their targeting of diseased cells (Hancock et al., 2018).

Vaccine candidates targeting E6 and E7 are most common due to the oncogenes' constitutive expression in CIN lesions, and their ubiquitous expression across hrHPV types (Khallouf et al., 2014). These oncoproteins are also ideal targets as their crucial

role in malignancy precludes them from immune cell escape through mutation (Lin et al., 2010). Conversely, E1 and E2 are useful targets for early infection, before genome integration, when they are expressed at higher levels than E6 and E7 (Chabeda et al., 2018). Moreover, several studies have demonstrated that these target antigens can be spliced together, and to L1 and L2 sequences, to form chimaeras (Bian et al., 2008; Da Silva et al., 2003; Greenstone et al., 1998; Kuck et al., 2006). These fusions can generate compounded or complementary humoral and cell-mediated immune responses (Monroy-Garcia et al., 2014).

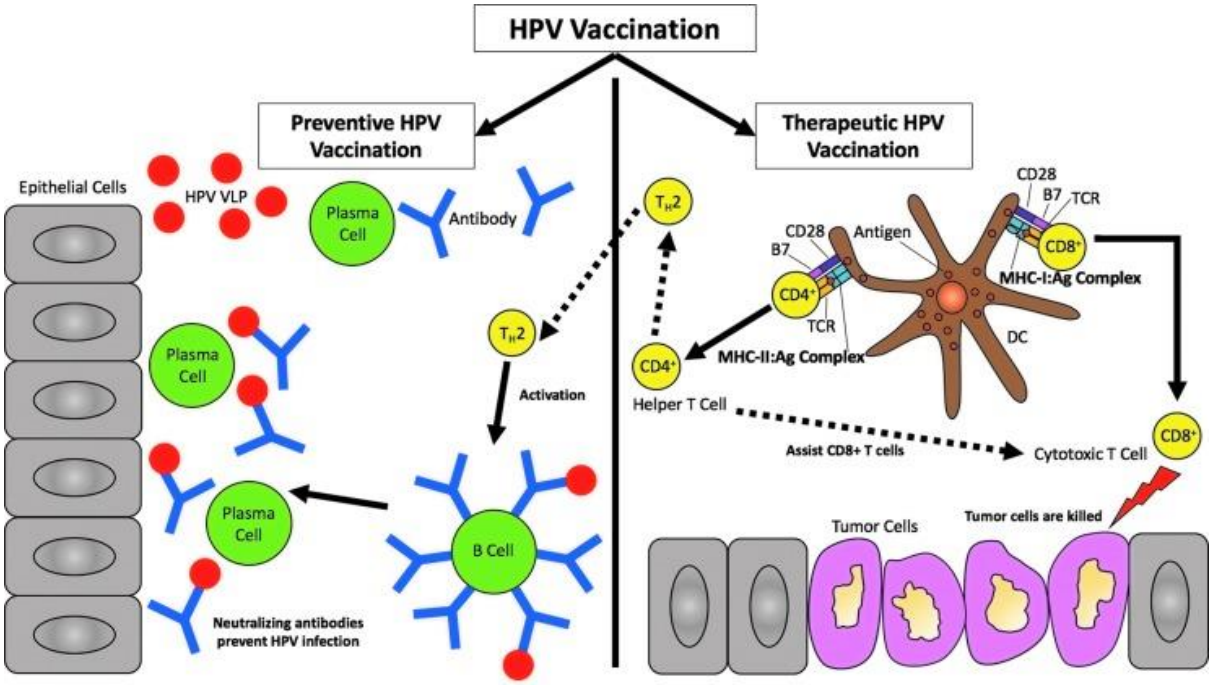

Figure 1.5: Type of immunity achieved through HPV vaccination. Preventative vaccination targets the humoral immune system via L1-based VLPs. A Th2 response results in the production of neutralising antibodies which protect against HPV infection. Therapeutic HPV vaccines, on the other hand, aim to induce cell-mediated immunity via induction of professional APCs. These go on to prime CD4+ and CD8+ T-cells through recognition with MHC class I and class II molecules. An antigen-specific cytotoxic T-cell response is activated, and tumour cells are targeted and killed. Image from Cheng et al. (2018) with permission.

Therapeutics targeting HPV can be classified as live vector-, nucleic acid-, protein-, peptide-, or cell-based vaccines (Dadar et al., 2018). Nucleic acid vaccines comprising of DNA have emerged as a particularly promising approach. While numerous studies and clinical trials across these categories have shown promising results, no therapeutic HPV vaccines have currently been approved for human use (Gardella et al., 2022).

Chemotherapy and radiotherapy are often employed in conjunction with candidate vaccines to enhance vaccine potency and strengthen lesion clearance efforts (Huang et al., 2010). Mice model studies involving the combination of low-dose radiation and an E7-based DNA vaccine showed heightened CD8+ T cell activity and increased tumour susceptibility. This therapeutic strategy led to increased long-term survival rates (Tseng et al., 2009). The mechanisms of these synergistic effects, however, have not yet been defined (Knoff et al., 2014).

1.4.4 DNA vaccines

DNA vaccines consist of plasmid DNA encoding a strong promoter, the antigen of interest, and a transcriptional termination sequence. The DNA is delivered into the host's tissue for uptake by APCs whereby it can induce an adaptive cell-mediated immune response (Hancock et al., 2018).

DNA vaccines are advantageous in that they are safe, thermally stable, easy to produce with high purity, and do not stimulate antibody production. The absence of humoral induction allows for recurrent administration without loss of efficacy (Gurunathan et al., 2000). These vaccines also allow for the combined delivery of multiple antigens in a single formulation, through the addition of more plasmids (Kubler et al., 2015). Furthermore, cellular expression of DNA-based antigens is maintained for longer periods than with RNA or protein molecules (Donnelly et al., 1997). The benefits associated with DNA vaccines, united with their potential to control HPV infection, make this therapy an attractive prospect (Cheng et al., 2018).

There is the possible risk of oncogenic transformation associated with DNA plasmids encoding oncogenic proteins. This has been addressed with the use of altered E6 and E7 genes that have been disarmed of their virulent potential (Chabeda et al., 2018). Potency of DNA vaccines largely depends on their transfection efficiency. In turn, efficacy of transfection relies mainly on the method of DNA delivery (Barber, 2011; Hancock et al., 2018).

Intramuscular (IM) and intradermal (ID) delivery are the most conventional forms of DNA vaccine administration (Huang et al., 2010). IM injection commonly results in the

transfection of DNA into somatic cells, such as myocytes. DNA uptake is followed by transgene expression and subsequent presentation of the antigens to CD8+ T cells. Presentation through myocytes often results in a non-efficacious immune response as these cells are not professional APCs and, therefore, are not capable of inducing strong specific cytotoxic T cell activity (Lin et al., 2010). In contrast to IM delivery, ID delivery is associated with transfection of professional APCs, through direct interaction with Langerhans cells in the epidermis (Hancock et al., 2018). As a result, this delivery mechanism is much more likely to stimulate specific CD8+ T cells for a stronger immune response (Cheng et al., 2018).

The site of administration can be a limiting factor in the immunogenicity and specificity of the vaccines (Cheng et al., 2018). Many strategies have therefore been employed to optimize delivery of DNA therapeutics to enhance DC antigenic expression (Figure 1.6).

Antigenic potency can be improved through ID administration with a gene gun. With this high-velocity transfection device, DNA-coated micro-sized particles can be delivered directly to dendritic cells (O'Brien & Lummis, 2004). Gene gun delivery of HPV-16 E7 DNA has been shown to induce antitumour immunity, although not necessarily to a higher extent than with IM injection (Best et al., 2009; Chen et al., 1999).

Electroporation has also emerged as a promising approach to enhance immunogenic potency. The transfection efficiency of IM vaccination is improved when followed by low-voltage electrical currents at the site of administration (Yan et al., 2008; Yan et al., 2009). These charges introduce perforations in cell membranes for plasmids to enter through. This process also stimulates the release of pro-inflammatory cytokines which enhances establishment of an immune response through recruitment of immune cells to the site of injection (Keane-Myers & Bell, 2014). Best et al. (2009) demonstrated that electroporation-mediated IM delivery is associated with the highest CD8+ T cell levels when compared to IM injection alone or ID gene gun administration. A phase I clinical trial in HPV-16/18 CIN3+ women showed that IM injection, followed by electroporation, resulted in 94% of patients having increased HPV-16 E7 antibodies,

and 78% having HPV-specific CTL responses, with all participants showing increased HPV-18 E7 antibodies (Bagarazzi et al., 2012).

While electroporation at the site of IM vaccination has been successful in inducing heightened immune responses, participants described it as an invasive and painful process. It also requires the use of local anaesthesia and specialized equipment (Otten et al., 2004). Another promising strategy associated with comparably robust levels of APC activation is the use of pseudovirions (PsVs) in DNA vaccine delivery.

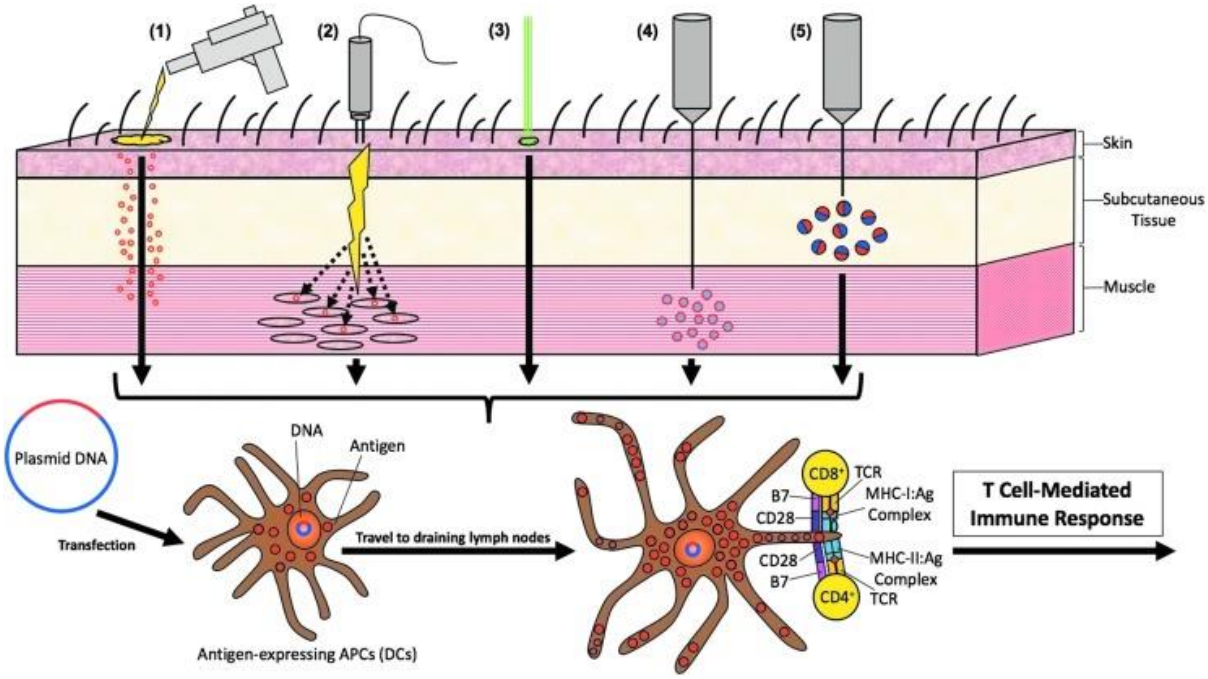

Figure 1.6: Routes of DNA vaccine administration. Alternative forms of vaccine administration have been developed to enhance antigen uptake by professional APCs for a stronger T cell-mediated immune response. Interactions between B7 and CD28 receptors on the T cells and APCs, respectively, assist this response. DNA vaccines can be delivered **(1)** intradermally using a gene gun, **(2)** intramuscularly followed by electroporation, **(3)** intradermally followed by laser treatment, **(4)** intramuscularly by injection with encapsulated nanoparticles, or **(5)** subcutaneously with HPV DNA combined with PEI600-Tat, which is a HIV-1 protein conjugated with a low molecular weight polymer. Source: Cheng et al. (2018) with permission.

1.4.5 Pseudovirions in gene delivery

Naked DNA vaccines are associated with inefficient transfection of APCs, resulting in ineffectual antigenic potency *in vivo*. Pseudovirions address this limitation through efficient encapsidation and delivery of plasmid DNA to target cells (Peng et al., 2011). Papillomaviruses are particularly promising vaccine vector candidates as they are

highly stable, capable of infecting mucosa, and can accumulate in large quantities (Buck et al., 2004; de Villiers et al., 2004).

Papillomavirus L1 and L2 capsid proteins are capable of self-assembling to package plasmid DNA as they would with episomal viral DNA. Expression of both capsid proteins is essential for DNA encapsidation (Kirnbauer et al., 1993). The resulting virus-like particle can act as a therapeutic DNA delivery vehicle to efficiently deliver encapsidated material into cells both *in vitro* and *in vivo* (Bayer et al., 2018; Ma et al., 2011). While PV PsVs mimic viral host cell infection, they do not contain viral genes and are thus non-replicative (Buck et al., 2004). Moreover, PV capsid proteins can encapsidate both non-PV and non-viral genetic material. Schiller et al. (2016) found that PVs have only a basic size discrimination mechanism for plasmid DNA incorporation, with no packaging signal necessary. This study additionally observed that particle capsomeres undergo cyclical disassembly and reassembly around DNA until a stable conformation is achieved. Analyses of BPV-1 have shown that plasmid DNA of size 4.7 – 8.6kb can be contained through L1 and L2 assembly (Bayer et al., 2018; Zhao et al., 1998). It has been observed, however, that plasmids around 5kb and 5.9kb are associated with higher encapsidation efficiencies than those above 6kb. In turn, plasmids of 6kb encapsidate more efficiently than those exceeding 7kb (Buck et al., 2004; Stauffer et al., 1998; Touze & Coursaget, 1998). In general, the smaller the sequence, the more likely it is to be packaged by capsid proteins.

HPV pseudovirions, particularly HPV-16, function well in gene delivery. This is partly due to their propensity to initially bind to basement membrane HSPGs that initiate viral capsid conformational changes which ultimately allows the delivery of encapsidated material into epithelial cells (Kines et al., 2009; Roberts et al., 2007). HSPGs play a crucial role in BM remodelling through wound healing. Tumours manipulate and exaggerate this characteristic of HSPGs to induce the physiology of an ‘over-healing’ wound (Schafer & Werner, 2008). This is achieved through overexpression and mutation of HSPG sulphation patterns on tumours. These changes stimulate the creation of an extracellular matrix (ECM) that emulates the BM (Hammond et al., 2014; Liu et al., 2002). This HSPG-enriched microenvironment promotes tumorigenesis but can also be exploited for PsV-mediated gene delivery. Kines et al. (2016) found that HPV-16 PsVs preferentially target a wide range of cancer cell lines *in vitro*, and

tumours *in vivo*, in an HSPG-contingent manner that leaves healthy cells untouched. These results suggest the potential use of HPV PsVs in broad-spectrum tumour targeting.

HPV pseudovirions have also been shown to effectively target the vaginal mucosa to deliver genes to the female genital tract in a multitude of animal models. Graham et al. (2010) observed that respiratory syncytial virus (RSV) M- and M2-derived antigens delivered intravaginally by HPV PsVs induced both antibody and M/M2-specific CD8+ T cell responses in mice equivalent to a 10,000-fold higher dose of naked plasmid DNA. Light emission and immunofluorescent microscopy, following immunization with HPV PsVs encapsidating reporter genes, additionally revealed that antigen expression is limited to the vaginal epithelium and is transient, lasting less than five days post-immunization (Graham et al., 2010). Peng et al. (2011) further demonstrated the value of HPV particles through vaccination studies with encapsidated ovalbumin (OVA) DNA in mice. Pseudovirion-based OVA delivery stimulated antitumour effects against OVA-expressing tumours and gave rise to the highest number of CD8+ T cells compared to other delivery methods and other antigen-specific vaccines. Most notably, OVA delivery with HPV-16 PsVs generated a T cell response 5-fold that of gene gun delivery and 10-fold that of naked DNA followed by electroporation (Peng et al., 2011). HPV PsVs have also demonstrated success in targeting the vaginal tract of non-human primate species. Gordon et al. (2012) showed that macaques intravaginally vaccinated with HPV-16, -45, and -58 PsVs containing simian immunodeficiency virus (SIV) Gag DNA elicited Gag-specific antibodies and CD8+ T cells both locally and systemically. The authors further demonstrated rapid expansion of the antigen-specific immune cells following challenge with SIV (Gordon et al., 2012).

1.5 Plant-based protein expression

The concept of plants as alternative bioreactors for pharmaceutical production was first put forward over 30 years ago. Pioneers of the biopharming field sought to overcome the three major drawbacks associated with conventional expression systems – safety, scalability, and expense (Edgue et al., 2017; Hiatt et al., 1989). Initial work focussed on stable transformation of tobacco plants (*Nicotiana tobacum*) for production of transgenic homozygous lines (Daniell et al., 2009; Thuenemann et al.,

2013). Plants are an attractive expression host due to their rapid, simple, scalable, and cost-effective growth as well as their ability to undergo post-translational modifications (PTMs) (Rozov & Deineko, 2022). PTMs, such as glycosylation and multimeric subunit assembly, are possible as plant cells have a eukaryotic endomembrane system closely related to that of mammalian cells (Chen et al., 2009; Lai et al., 2010). Moreover, plant systems are incapable of introducing contamination with bacterial toxins or animal viruses (Fischer & Buyel, 2020; Huebbers & Buyel, 2021).

Transgenic expression is, however, associated with shortfalls that limits its usage. The system is reliant on integration of transgenes into the host chromosome and is thus affected by genome position effects. Additionally, only a small proportion of DNA is successfully incorporated (Komarova et al., 2010). The generation and selection of stable transgenic plant lines is also time-consuming and resource-demanding, sometimes taking months to achieve (Rybicki, 2009; Sainsbury & Lomonossoff, 2014). Moreover, transgenic expression in plants is typically associated with low protein yields that rarely surpass 1% of total soluble protein (TSP) (Daniell et al., 2009). This lack of protein accumulation is most likely owed to siRNA-dependent or post-translational gene silencing of transgene mRNA that results in its degradation (Baulcombe, 2004; Voinnet et al., 2003).

Transient expression, whereby plant tissue is transiently transformed with plasmid DNA that remains episomal, overcomes the limitations associated with transgenic expression. High levels of proteins can be rapidly generated, within 1 – 2 weeks after gene delivery, with fewer requirements for infrastructure and biosafety containment (Chen et al., 2011; Merlin et al., 2014). There are a wide variety of plants and plant tissues utilized for transient protein production with the leaf and stem tissues of tobacco species, particularly *Nicotiana benthamiana*, being the most widely employed (Hefferon, 2017). The species is well-characterized, easy to grow, yields a large biomass, and has a lower protease profile than many other plant species (Kjemtrup et al., 2014). Moreover, tobacco species have a naturally high transformation efficiency due to a low exposure to plant pathogens resulting from their desert-biome origins. This lack of pathogen challenging has led to the development of a deficient host immune system that can be exploited to express exogenous antigens (Pietersen,

2019; Tremblay et al., 2010). The use of *N. benthamiana* as a transient expression system has been further popularized by the innovation of agroinfiltration, the most facile method for transient expression in plants.

1.5.1 Development of virus vaccine antigens in plants

The first successful plant-produced virus vaccine candidate was a Hepatitis B (HBV) surface antigen transgenically developed by Mason et al. (1992). Shortly after, foot-and-mouth disease viral proteins were successfully expressed on the surface of recombinant cowpea mosaic virus particles (Usha et al., 1993). The two decades that followed have seen major developments in the production of vaccine candidates in plants against a wide range of viruse. A leap in plant expression was made in 2006 when a veterinary vaccine against Newcastle disease virus (NDV) became the first ever licenced plant-produced purified injection vaccine ("News In Brief," 2006). The NDV vaccine candidate is based on expression of the antigenic haemagglutinin-neuraminidase (HN) surface glycoprotein produced in *N. benthamiana* (Thomas & Walmsley, 2018).

Plant production of HIV vaccine candidates has also seen impressive leaps with Zhang et al. (2002) successfully expressing the p24 capsid protein in transgenic tobacco plants to 3.5 mg/g of soluble leaf material. Meyers et al. (2008) achieved similar success with transient expression of a Gag-derived p17/p24 fusion protein in *N. benthamiana*. When expressed with a chloroplast localisation signal, purified fusion protein levels reached 5 mg/kg and elicited both a humoral and innate immune response in mice primed with *gag* DNA (Rybicki, 2010). Influenza vaccine research also saw great achievements in the development of vaccine candidates in plants. Over the last 70 years, influenza vaccines have been manufactured in chicken eggs. This is a complex process with a long timeframe and intense regulatory requirements. Additionally, the reliance on eggs poses a threat to global food security (Trombetta et al., 2019). To overcome this, novel strategies of influenza vaccine production have been explored. D'Aoust et al. (2008) investigated assembly of VLPs in *N. benthamiana* plants based on expression of haemagglutinin (HA) from H1N1 and H5N1 virus strains. The correctly trimerized HA VLPs yielded 50 mg/kg of soluble leaf. Furthermore, the H5 particles conferred complete immunogenic protection in mice

challenged with an otherwise lethal heterologous influenza virus strain. Further development of HA VLPs resulted in monovalent H5- and H7-based vaccine candidates, followed by the formulation of a quadrivalent HA VLP-based vaccine which successfully completed phase 1, 2, and 3 clinical trials (Landry et al., 2010; Pillet et al., 2015; Ward et al., 2020). These achievements inspired the development of a H1N1 VLP-based vaccine platform as part of the DARPA Blue Angel programme by Medicago Inc. (Québec) in 2012. Over 10 million vaccine doses were produced and purified from tobacco plants within a single month (Stander et al., 2022; Szondy, 2013).

Progress towards the commercial development of human virus vaccine antigens in plants has, however, been slow. The distinct lack of industry presence is largely due to focus being on the development of purification protocols and optimisation of expression and yields. Movement into the global industry has been further impeded by strict regulatory and clinical trial requirements. Despite this, the field has achieved some major advancements in molecular pharming, as well as the establishment of good manufacturing process (GMP) processes and facilities. This progress has exhibited applicability and feasibility within the commercial vaccine industry. This has recently been demonstrated through the authorisation of COVIFENZ®, a VLP-based COVID-19 vaccine produced by Medicago Inc., following enormous success in all stages of the human trials (*Medicago Covifenz COVID-19 vaccine*, 2022; Stander et al., 2022).

1.6 Study aims and objectives

The main aims of this study were to (1) express bovine papillomavirus type 1 (BPV-1) pseudovirions (PsVs) encapsidating a therapeutic human papillomavirus type 16 (HPV-16) Zera®E7SH DNA vaccine in *N. benthamiana* plants and (2) test their ability to deliver the encapsidated pseudogenome to mammalian cells. This was done in the pursuit of developing an affordable, safe, and effective therapeutic HPV-16 vaccine candidate. There are currently no therapeutic HPV vaccines nor any plant-produced HPV vaccines licensed for use in humans despite the desperate need for cervical cancer therapies in low- and middle-income countries, where high-risk HPV infections are rampant. Expansion of research into the expression and purification of an

efficacious HPV therapy, that is both cost-effective and scalable, is therefore of high importance.

The four main objectives of this study were to:

1 Optimise BPV-1 PsV expression, extraction, purification, and analysis.

2 Develop HPV-16 Zera®E7SH reporter constructs.

3 Perform head-to-head analyses of BPV-1 and HPV-35 PsVs containing HPV-16 E7SH reporter constructs in *N. benthamiana* and analyse their infectivity using reporter gene assays.

4 Perform head-to-head analyses of plant- and mammalian cell-produced BPV-1 and HPV-35 PsVs containing SEAP.

2 Chapter 2: Optimization of BPV-1 pseudovirion expression in *Nicotiana benthamiana*

2.1 Introduction

BPVs are well-described; approximately 23 of 160 known animal PV types are characterised as bovine in origin (Koch et al., 2018). BPVs are largely species-specific and infect the epithelia of ruminants such as cattle and giraffe (Campo, 2002). BPV-1, however, is known to cross species barriers and additionally colonise equid species such as horses, donkeys, and zebra (Bocaneti et al., 2016; Chambers et al., 2003). In cattle, BPV-1 and -2 are the aetiological agents of largely benign papillomas and are highly prevalent, with approximately 50% of cattle farmed in the United Kingdom bearing lesions (Bocaneti et al., 2016).

Like other PVs, BPVs have non-enveloped T=7 quasi-icosahedral capsids made up of 72 capsomeres consisting of L1 and L2 proteins associated in pentamers. These subunits self-assemble into viral particles that, when fully formed, are approximately 50-60 nm in diameter (Figure 2.1) (Baker et al., 1991; Chen et al., 2000; Wolf et al., 2010).

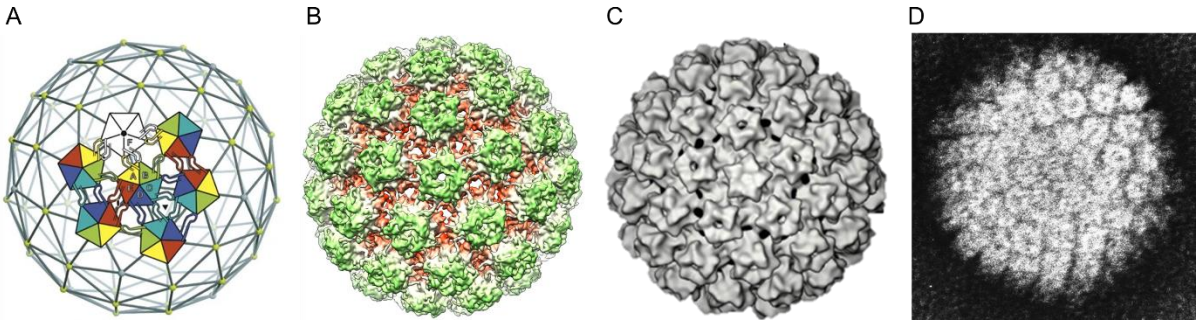

Figure 2.1: Structural features of bovine papillomavirus. A) Model illustrating the self-assembly of T=1 pentamers into T=7 icosahedral lattices to form the viral capsid. B) 3D density map of a fully assembled T=7 BPV capsid. **C)** 3D reconstruction of a BPV capsid. **D)** Electron micrograph of a papilloma virion of size 50-60 nm. Source: A, obtained with permission from Wolf et al. (2010); B, C, D, obtained from Wikimedia Commons.

BPV-1 L1 and L2 proteins have been shown to self-assemble into VLPs when recombinantly expressed in plants and these VLPs can elicit a strong immunogenic response in rabbit models (Love et al., 2012). Plant-produced BPV-1 L1/L2 particles

can encapsidate plasmid DNA between 4.8 and 8.8 kb in size (Pietersen et al., 2020; Zhao et al., 1998). Adams et al. (2023), however, found that a pseudogenome of 5.9 kb is optimal for efficient HPV PsV assembly in tobacco plants. While the L2 capsid protein is not necessary for the formation of VLPs, its presence is essential for the effective encapsidation of genetic material (Lamprecht et al., 2016; Ma et al., 2011).

2.1.1 *Agrobacterium*-mediated transient expression in plants

For genes to be transiently expressed in plant cells, they must first be effectively delivered. *Agrobacterium* tumefaciens (*A. tumefaciens*), a plant pathogen known to cause crown-gall disease, is well-established for its simple role in gene transfer (Tzfira et al., 2004). Its abilities lie in the presence of virulent T-DNA, a region of the tumour-inducing (Ti) plasmid, that, once induced, functions to transfer associated DNA to plant cells for transcription and translation (Chen et al., 2013).

Acetosyringone, a plant phenolic compound, can induce *vir* gene expression for T-DNA transfer (Tsai et al., 2009). This process is aided by heat-shock proteins which promote the accumulation of Vir proteins (Hiei et al., 1994; Lai et al., 2006). The inclusion of acetosyringone in recombinant *Agrobacterium* cultivation media is thus crucial for effective DNA transfer for transient expression in plants (Jeoung et al., 2002; Rogowsky et al., 1987). *Agrobacterium*-mediated transfer is also dependent on physical factors such as temperature, pH, light conditions, bacterial strain and density, and length of cultivation (Norkunas et al., 2018).

Recombinant *Agrobacterium*, transformed with an expression cassette carrying T-DNA, can be delivered into the extracellular spaces of *N. benthamiana* leaves by syringe or vacuum infiltration (Norkunas et al., 2018). Syringe infiltration involves the use of a needleless syringe to inject recombinant bacteria into the leaves (Potera, 2012). Due to its limited localisation, syringe infiltration allows for the introduction of multiple DNA constructs, possibly containing entirely different promoters and organelle targeting sequences, into a single leaf (Rybicki, 2010). This makes it an ideal small-scale method for optimisation of transgene expression without the need for specialised equipment (Chen et al., 2013; Vaghchhipawala et al., 2011). Syringe infiltration, however, lacks scalability. For infiltration of plants that cannot be syringe-infiltrated and

for large-scale expression analyses, vacuum infiltration is employed (Rivera et al., 2012). This method involves the use of a vacuum chamber holding infiltration media containing recombinant *Agrobacterium* strains into which the plant leaves are submerged. A vacuum pump is used to draw air out of the extracellular leaf spaces and replace it with the bacterial culture. Vacuum infiltration is a robust, highly scalable production platform for *Agrobacterium*-mediated expression in plants (Chen et al., 2013).

2.1.2 Non-human papillomavirus pseudovirions for gene delivery

PsVs based on HPV capsid proteins have displayed numerous advantages and experimental successes as gene delivery vehicles (Graham et al., 2010; Kines et al., 2015). Worldwide vaccination campaigns with Gardasil 4® and 9®, coupled with the high global rate of natural HPV infection, has, however, resulted in a large proportion of the global female population having existing immunity against HPV L1 and L2 capsid proteins. Neutralising antibodies would thus sequester PsVs composed of antigens to which the immune system has previously been exposed before the particles can reach dendritic cells for presentation to, and activation of, T and B lymphocytes for therapeutic effects. This protection is type-specific; however, due to the multivalent nature of the vaccine, many candidate types are precluded from use as gene delivery vehicles. Non-human PVs have therefore been explored for their ability to deliver DNA vaccines in humans (Bayer et al., 2018; "GAVI injects new life into HPV vaccine rollout," 2013).

In this chapter, optimisation of *Agrobacterium*-mediated BPV-1 L1/L2 PsV expression in *N. benthamiana* is described. Several iterations of a papillomavirus extraction protocol developed by Lamprecht et al. (2016) were tested to increase PsV production. This involved the co-infiltration of plants with recombinant *Agrobacterium* containing human codon-optimised BPV-1 L1 and L2, and pRIC3.0-mSEAP, a plant expression cassette containing a mammalian expression cassette encoding secreted embryonic alkaline phosphatase (SEAP). The following strategies were investigated: (1) increased concentration of acetosyringone for induction of *Agrobacterium vir* genes, (2) heat shock of whole plants after infiltration, and (3) an extended period of *in planta*

particle maturation following infiltration. These optimisation approaches were adapted from studies by Pietersen et al. (2020) to optimize expression of BPV-1 VLPs.

2.2 Materials and methods

2.2.1 Transient expression of BPV-1 hL1/hL2 PsVs in *N. benthamiana*

2.2.1.1 *Agrobacterium*-mediated infiltration of *N. benthamiana*

Previous studies investigating expression of HPV and BPV L1 and L2 in plants showed that human codon-optimisation of these structural proteins demonstrated increased levels of L1 protein expression and VLP assembly when compared to that of plant codon-optimised L1 and L2 (Edwards, 2019; Maclean et al., 2007). Genes encoding human codon optimised L1 and L2, referred to as hL1 and hL2 in this study, (BPV-1 Genbank ID: X02346) were synthesised by Genscript Biotech Corp (USA) with the sequences provided in pCC1 and pUC57 maintenance vectors respectively. The genes were sub-cloned into the pTRAc plant expression vector (Maclean et al., 2007) and the resulting pTRAc-hL1 and -hL2 constructs were electroporated into *Agrobacterium tumefaciens (A. tumefaciens)* strain GV3101::pMP90RK according to the method described by Shen and Forde (1989). A silencing suppressor sequence was not included for infiltration as previous studies conducted in the laboratory have shown that inclusion of a silencing suppressor does not significantly impact recombinant protein expression levels (Hitzeroth et al., 2018; Yanez et al., 2017). For transformation, 100 µL electrocompetent cells were mixed with 300 ng of recombinant plasmid DNA in a pre-cooled 1 mm gap electroporation cuvette and cooled on ice for 5min. Electroporation was then carried out at 1.8 kV, 25 µF, and 200 Ω, after which 900 µL LB media (Bertani, 1951) was added to the cuvette. The mixture was transferred to a microcentrifuge tube and incubated at 27°C for 2hr with agitation. Positive clones were selected on LB agar (Bertani, 1951) supplemented with rifampicin (50 µg/mL), kanamycin (30 µg/mL), and carbenicillin (50 µg/mL).

The reporter gene construct pRIC3-mSEAP is used in this study as a pseudogenome for encapsidation in BPV-1 hL1/hL2 particles. The construct is comprised of a self-replicating plant expression vector, pRIC 3.0, modified to include a mammalian expression cassette encoding secreted embryonic alkaline phosphatase (SEAP). The vector contains two short nucleotide sequences, LB and RB, which flank the region of the plasmid that is transferred into plant cells during *Agrobacterium*-mediated infiltration (T-DNA). Two long intergenic regions (LIRs) and Rep function to re-circularise the T-DNA for formation of the rolling circle replication complex (Khan,

2005). Self-directed replication of the replication complex within plants would result in a replicon of size 4.8 kb being encapsidated within self-assembled BPV-1 particles (Figure 2.2) (Kennedy, 2013). pRIC3-mSEAP was transformed into *A. tumefaciens* strain GV3101::pMP90RK (Lamprecht et al., 2016).

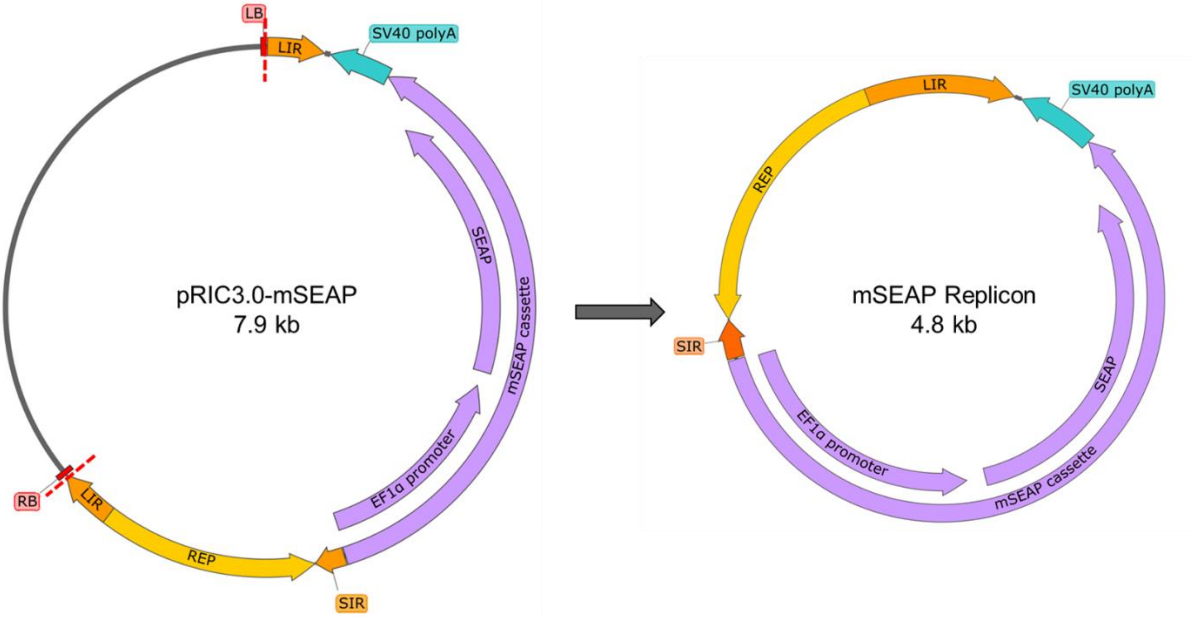

Figure 2.2: The pRIC3-mSEAP construct and corresponding replicon. Following replicational release of the T-DNA in plants, the pRIC3-mSEAP construct of 7.9 kb (left) re-circularises at the LIRs to form the mSEAP replicon of 4.8 kb (right). The purple elements indicate the SEAP cassette under the control of the E1 alpha promoter. Labels: LB (red), left border; RB (red), right border; LIR (orange), bean yellow dwarf virus (BeYDV) long intergenic region; SIR (orange), BeYDV short intergenic region; SV40 polyA (blue), SV40 polyadenylation signal; REP (yellow), BeYDV *rep* gene; and red dashed line, positions where T-DNA is enclosed and LIRs recombine.

For large-scale preparation of *Agrobacterium* cultures to produce BPV-1 PsVs, the method described for HPV-16 VLP production was followed (van Zyl & Hitzeroth, 2016). Frozen 2 mL glycerol stocks of recombinant *Agrobacterium* containing pTRAc as a negative control, pTRAc-BPV-1-hL1, pTRAc-BPV-1-hL2, and pRIC3-mSEAP were inoculated into 10 mL induction media [10 mg/mL Tryptone; 5 mg/mL NaCl; 5 mg/mL yeast extract; 10 mM MES, pH 5.6] supplemented with rifampicin (50 µg/mL), kanamycin (30 µg/mL), and carbenicillin (50 µg/mL) and incubated overnight at 27°C with agitation. The following day, the starter cultures were inoculated into 50 mL induction media supplemented with relevant antibiotics and grown overnight. The *Agrobacterium* cultures were scaled up the following day to a final volume of 500 mL induction media supplemented with the relevant antibiotics (excluding rifampicin) and

20 µM acetosyringone and grown overnight. Overnight cultures were combined and diluted to the required OD_{600} ratios in resuspension buffer [5 mM MES and 10 mM MgCl2.6H2O, pH 5.6] as stated in Table 2.1., followed by incubation with 200 µM acetosyringone at room temperature for 2hr prior to infiltration to allow induction of *Agrobacterium vir* genes. Plants were vacuum infiltrated with induced, diluted cultures and grown at 22°C under a 16hr light: 8hr dark daily cycle for 4 days (Maclean et al., 2007). VLP and empty pTRAc control cultures and plants were treated and infiltrated in the same manner as PsVs.

Table 2.1: Culture concentrations (OD_{600}) and combinations of recombinant *Agrobacterium* cultures required for expression of empty pTRAc, VLPs, and PsVs. Ratios are based on optimisation studies done by Chabeda (2017) and Pietersen (2019).

	pTRAc	pTRAc-hL1	pTRAc-hL2	pRIC3-mSEAP	Product
OD_{600}	0.25	-	-	-	Empty vector control
	-	0.25	0.05	-	VLP control
	-	0.25	0.05	0.70	PsVs

2.2.1.2 Extraction and purification of PsVs

Extraction and purification of BPV-1 particles was based on methods established for purification of HPV-16 PsVs (Lamprecht et al., 2016). A simplified diagram detailing the major steps of the protocol is shown in Figure 2.3. Plant leaves were harvested at 4 days post infiltration (dpi) and frozen at -80°C. Frozen leaf material was homogenised in 2x v/w high salt NaOAc (HSNaOAc) [0.1 M NaOAc/0.5 M NaCl, pH 5.2] using a T25 digital ULTRA-TURRAX® homogeniser (IKA®). Crude extract was incubated at 4°C for 2hr with gentle agitation and then filtered through 3 layers of Miracloth™ (Calbiochem®). The extract was further clarified by centrifugation at 10,000 *x g* using an Avanti J25TI® centrifuge (Beckman Coulter Inc.) at 4°C for 15min. Sucrose cushion gradients of 30% and 50% w/v sucrose solution were prepared in HSNaOAc and under-layered below the clarified supernatant in a 38.5 mL Thinwall Ultra-Clear Tube (Beckman Coulter Inc.) using a long syringe needle. Samples were pre-purified by density gradient ultracentrifugation at 174,500 *x g* using a SW32Ti rotor (Beckman Coulter Inc.) at 15°C for 45min. After centrifugation, the 5 mL 30% cushions were collected using a long syringe needle, pooled, and dialysed at 4°C overnight in dialysis tubing with a MW cut-off of 10 kDa (Sigma-Aldrich), in 60-100x v/v 1x high salt

PBS (HSPBS) [1x PBS/0.5 M NaCl, pH 7.4]. For density gradient purification 60% Optiprep™ (Sigma-Aldrich®) was diluted in 6x HSPBS [6x PBS/3 M NaCl, pH 7.4] to prepare a 50% stock solution which was further diluted in 1x HSPBS to make 39%, 33%, and 27% gradients. Dialysed samples were transferred to ultracentrifuge tubes and step gradients were under-layered using a long syringe needle. Density gradient ultracentrifugation was carried out at 174,500 *x g* using a SW32Ti rotor (Beckman Coulter Inc.) at 15°C for 3h30min to purify particles based on their densities. The bottom of each tube was punctured using a 21-gauge needle and 13x 1 mL fractions were collected from the bottom of the tubes. Fractions were immediately aliquoted and stored at -80°C until further analysis.

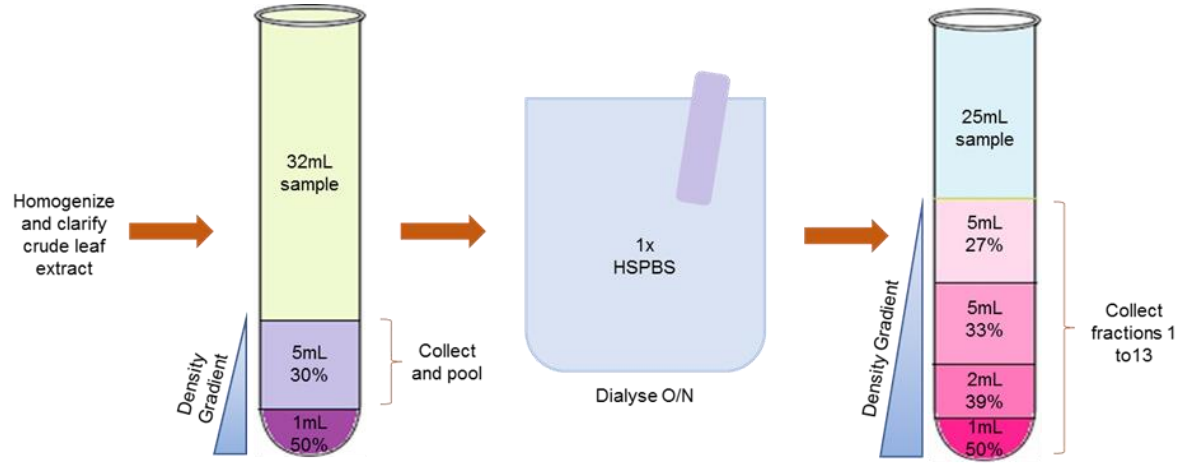

Figure 2.3: Schematic diagram showing the purification process for BPV-1-hL1/hL2 VLPs and PsVs

2.2.2 Optimisation of BPV-1 PsV expression

A flow chart demonstrating the strategies explored for expression of BPV-1 hL1/hL2 PsVs encapsidating mSEAP is shown in Figure 2.4. The following strategies were investigated to increase PsV production in plants: (1) increased concentration of acetosyringone for induction of *Agrobacterium vir* genes, (2) heat shock of whole plants after infiltration, and (3) an extended period of *in planta* particle maturation following infiltration.

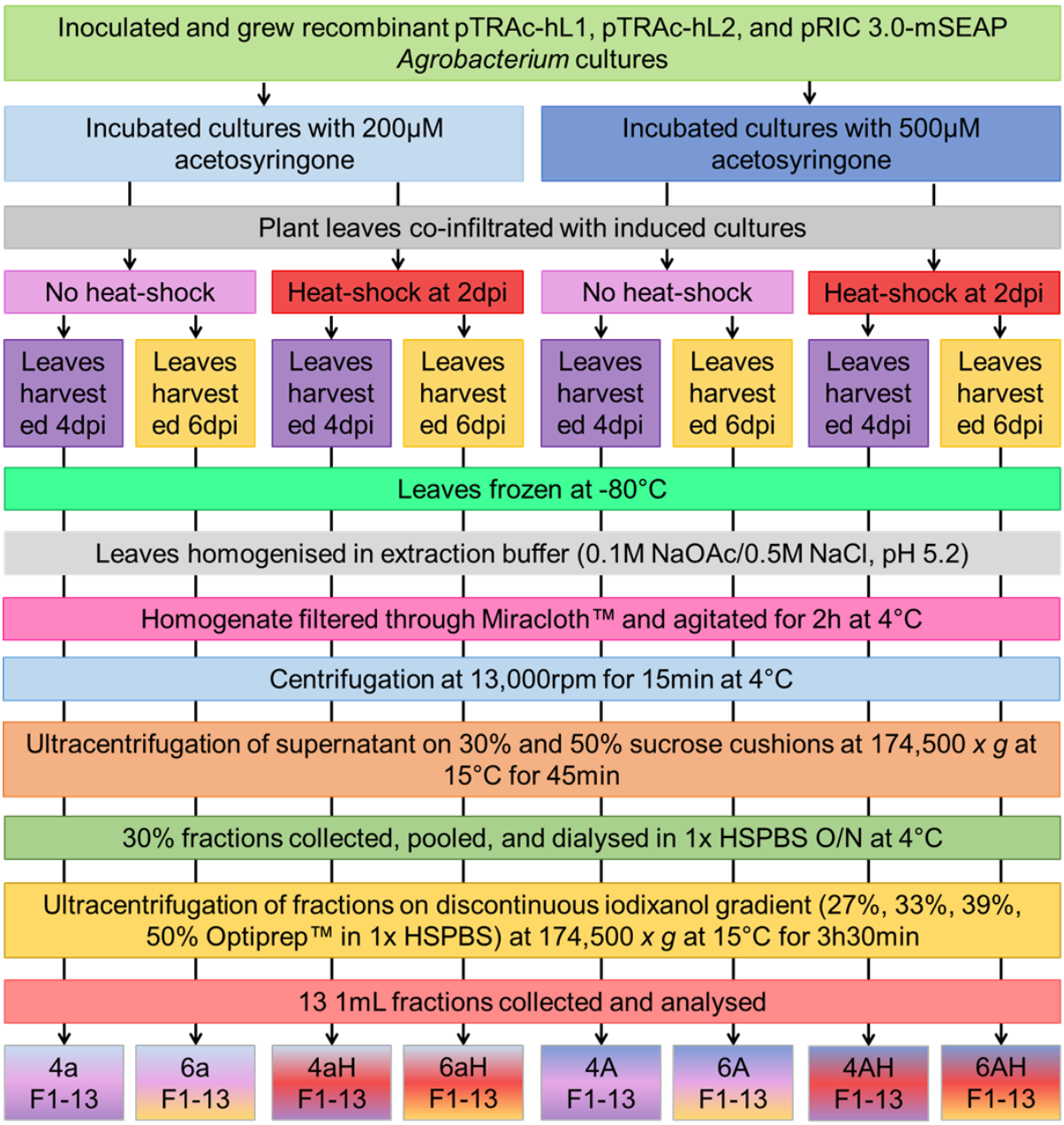

Figure 2.4: Flow chart of expression strategies investigated for plant-production of BPVP-1 hL1/hL2 PsVs

Strategies were combined to generate eight iterations of 10 plants each (using the same batch of plants). Protein expression and particle assembly was compared using dot blots, western blots, transmission electron microscopy (TEM), and SEAP assays. Extraction and purification of PsVs following optimisation was carried out as per the standard protocol described in section 2.2.1.2. A key of abbreviations used for the optimisation iterations explored in this chapter is provided in Table 2.2.

Table 2.2: Optimisation strategy abbreviations

Iteration label	Acetosyringone concentration (μM)	Heat shock	Length of *in planta* maturation
4a	200	No	4 days
4A	500		
4aH	200	Yes	
4AH	500		
6a	200	No	6 days
6A	500		
6aH	200	Yes	
6AH	500		

2.2.2.1 Higher acetosyringone concentration

The standard infiltration protocol utilized in the BRU is based on the method published by Maclean et al. (2007), this method uses 200 μM acetosyringone for *Agrobacterium vir* gene induction. A recent study investigating ways to improve *Agrobacterium*-mediation infiltration showed that recombinant gene expression was significantly enhanced by using 500 μM acetosyringone (Norkunas et al., 2018). Pietersen (2019) showed similarly promising results when using increased acetosyringone levels for *vir* gene induction. To explore whether an increased level of acetosyringone could result in increased expression of target genes, recombinant *Agrobacterium* cultures of pTRAc-BPV-1-hL1, pTRAc-BPV-1-hL2, and pRIC3-mSEAP were grown, diluted, and combined as described in section 2.2.1.1 and Table 2.1. The resulting cell suspension was halved, with one part supplemented with 200 μM acetosyringone and the other with 500 μM acetosyringone. These were incubated at room temperature for 2hr after which 40 plants were infiltrated for each.

2.2.2.2 Heat shock of whole plants

In addition to the promising results when using a higher acetosyringone concentration, both Norkunas et al. (2018) and Pietersen (2019) found that heat-shocking whole *N. benthamiana* plants at 2dpi increased transgene expression and particle formation. To determine whether a heat shock step would increase yields and particle integrity of BPV-1 PsVs, 20 plants for each acetosyringone concentration were incubated at 37°C for 30min at 2dpi.

2.2.2.3 *In planta* particle maturation

Previous studies have detected the presence of VLPs in plants harvested at 4dpi (Adams et al., 2023; Pietersen et al., 2020). It has been observed, however, that a longer period of *in planta* maturation can result in an increase in yield and uniformity of VLPs (Chabeda, 2017; Maclean et al., 2007). To test whether an extended maturation period generates improved PsVs, half of the plants of each iteration described above was harvested at 4dpi and the other half at 6dpi. In total eight expression strategies were tested and subsequently processed as per the protocol summarised in Figure 2.3.

2.2.3 Protein analysis of purified BPV-1 PsVs

2.2.3.1 Dot blot analysis

Dot blot analyses were employed as a rapid method for detection of L1 protein in purified fractions to determine (1) whether expression and purification was successful and (2) which fractions collected from gradients contained the highest concentration of L1 protein for further analysis. BioTrace™ NT nitrocellulose membrane (PALL®) was dotted with 4 µL of purified sample from each fraction and air dried. Blots were incubated in blocking buffer [1x PBS, 0.1% Tween20, 5% long life skim milk] at room temperature for 30min, after which primary antibody diluted in blocking buffer was added and incubated overnight at 4°C (or at 37°C for 1hr) with gentle agitation. For BPV-1 hL1 detection, a commercially available anti-BPV-1-L1 mouse monoclonal antibody [BPV-1/1H8 + CAMVIR, Abcam] was used at a concentration of 1:1000. Following overnight incubation, blots were washed 4x with blocking buffer at room temperature with gentle agitation, after which secondary antibody was added for overnight incubation at 4°C (or at 37°C for 1hr). For the secondary antibody, a commercially available anti-mouse IgG whole molecule-AP antibody produced in goat (Sigma-Aldrich®) was used at a concentration of 1:10,000. Following incubation in secondary antibody, blots were washed 4x with wash buffer (blocking buffer without milk added) at room temperature, then developed in 5-bromo-4-chloro-3-indolyl-phosphate (BCIP) and nitro-blue tetrazolium (NBT) phosphatase substrate (BCIP/NBT 1-component, KPL) for 45min – 1hr.

2.2.3.2 Western blot analysis

The best fractions, as determined on dot blots, were selected for western blot analysis. Samples were denatured in the presence of 5x sample loading buffer [10% SDS, 1M Tris-Cl pH 7.5, 100 mM EDTA, 50% glycerol, 4% β-mercaptoethanol, 0.1% bromophenol blue] to a final concentration of 1x at 95°C for 10min. The molecular weight marker used for all western blots in this study, unless otherwise stated, was the PageRuler Plus Prestained 10 to 250 kDa Protein Ladder (Thermo Fisher Scientific). Denatured samples were loaded on 10% SDS-PAGE polyacrylamide gels and separated by electrophoresis in a Tetra Cell System (Bio-Rad Laboratories) at 100V per gel for ~90min.

Proteins were transferred onto a nitrocellulose membrane pre-soaked in 1x transfer buffer [25 mM Tris base, 190 mM glycine, 20% methanol, pH 9.2] using a Trans-blot™ Semi-dry Transfer Cell (Bio-Rad Laboratories) at 15V for 1hr15min. Western blots were then processed using the same method as described for dot blot analysis in section 2.2.3.1.

2.2.3.3 TEM analysis

Transmission electron microscopy (TEM) was used to determine if PsVs were successfully assembled using the different strategies tested for expression and maturation. Carbon-coated copper grids were made hydrophilic by glow discharging at 25mA for 30s using a Model 900 SmartSet Cold Storage Controller (Electron Microscopy Sciences). Grids were incubated on 20 µL of sample for 3 min, washed 5x in double distilled water (dsH_2O), and negatively stained with 2% w/v uranyl acetate for 1min. Stained grids were visualized using a Tecnai 20 transmission electron microscope (FEI®) equipped with a LaB6 emitter and operated at 200 kV.

2.2.4 Reporter gene expression analysis

2.2.4.1 Growth and maintenance of HEK293TT cells

The HEK293TT cell line derived from human kidney cells was used for all mammalian tissue culture experiments. Cells were cultured in complete Dulbecco's Modified Eagle Medium (cDMEM) with 1% GlutaMAX (Thermo Fisher Scientific), supplemented with

10% Fetal Bovine Serum (Hyclone™ FBS, Separations), 1% non-essential amino acids (Sigma-Aldrich), Penicillin-Streptomycin (100 units/mL penicillin, 100 µg/mL streptomycin) (Thermo Fisher Scientific), and 250 µg/mL Hygromycin B (Sigma-Aldrich). Cells were incubated at 37°C in 5% CO_2 and 95% humidity. Cells were passaged when they reached 70 – 90% confluency at a seeding density of $1x10^5$ cells/mL.

2.2.4.2 Infection of HEK293TT cells

After successful demonstration of BPV-1 hL1 protein expression and PsV formation, it was necessary to test their ability to infect mammalian cells. This was done by measuring the amount of SEAP detected after infection of HEK293TT cells with the PsVs. HEK293TT cells that were 70 – 90% confluent were trypsinised with trypsin-EDTA (Sigma-Aldrich), resuspended in cDMEM, and diluted to $1x10^5$ cells/mL in cDMEM. Corning® Costar® 24-well plates (Merck) were seeded with $1x10^5$ cells per well and incubated overnight at 37°C in 5% CO_2 and 95% humidity. The following day, PsV fractions and a VLP fraction were diluted 1:5 in DMEM and added to cells in triplicate at 500 µL/well. For the cells only control, DMEM was added to cells in triplicate at 500 µL/well. For the positive SEAP control, 1 µg purified pRIC3-mSEAP plasmid DNA was incubated with 100 µL DMEM and 2 µL X-tremeGENE™ 9 Transfection Reagent (Sigma-Aldrich) at room temperature for 20min and added to cells in triplicate, according to the manufacturer's protocol. The cells were incubated for a further 72hr, after which SEAP activity was measured (Buck et al., 2006; Chabeda, 2017).

2.2.4.3 SEAP expression analysis

SEAP activity was assayed using the Great EscAPe™ SEAP Chemiluminescence Kit 2.0 (Clontech Laboratories, Inc.). The protocol was followed as per the manufacturer's instructions with slight modification to the volumes of cell culture medium, dilution buffer, and substrate buffer added, with 0.6x of the stated volumes used. Briefly, 15 µL cell culture medium was transferred in triplicate from infected cells to a white polystyrene 96-well plate (Porvair Sciences) and 45 µL kit dilution buffer was added to the samples. The plate was sealed with plastic film and aluminium foil and incubated at 65°C for 30min. The plate was then cooled on ice for 3min, equilibrated to room

temperature, and 60 µL SEAP substrate solution was added. The plate was incubated at room temperature for a further 30min, after which SEAP signal was detected at a wavelength of 477 nm using a GloMax® 20/20 Luminometer (Promega).

2.3 Results

2.3.1 Expression optimisation of BPV-1 PsVs in plants

To determine the co-expression conditions associated with the highest protein and particle yield of BPV-1 hL1/hL2 encapsidating mSEAP, approaches such as an increased acetosyringone concentration, inclusion of a heat-shock treatment, and *in planta* maturation were investigated. Leaves of *N. benthamiana* plants vacuum infiltrated with recombinant *Agrobacterium* cultures at a total OD_{600} of 1.0 were monitored over a 6-day period and representative samples of leaves harvested at days 4 and 6 post-infiltration are shown below in Figure 2.5. Leaves infiltrated with *Agrobacterium* cultures containing either pTRAc or BPV-1 pTRAc-hL1/hL2 harvested at day 4 post-infiltration were included as a negative empty vector control or positive VLP control respectively. Plants co-expressing hL1/hL2 with mSEAP showed signs of necrosis and chlorosis from day 4 with an increase in symptoms at day 6. Plants infiltrated with *Agrobacterium* cultures induced with 500 μM acetosyringone and treated with heat-shock displayed the highest level of necrosis. Both the negative and positive control plants showed no symptoms on day 4 post-infiltration. The time-trial was repeated, and physiological effects observed were like the results shown here.

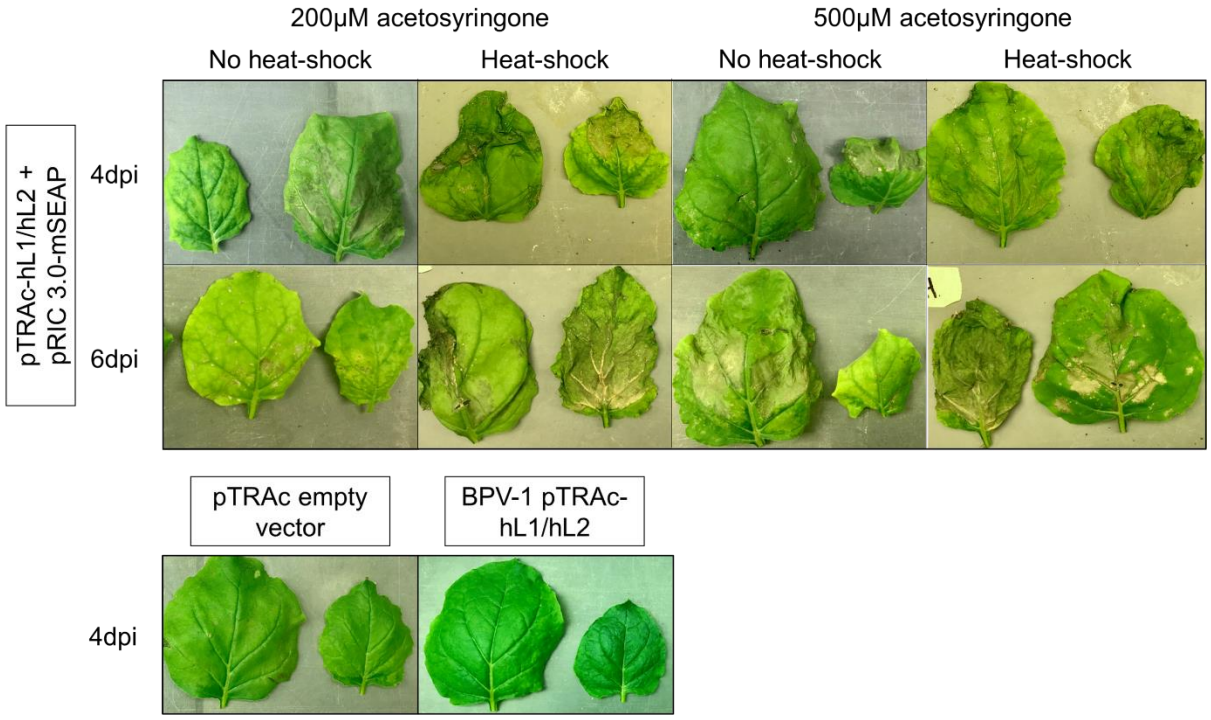

Figure 2.5: Physiological effects of pTRAc-hL1/hL2 and pRIC3-mSEAP co-expression. Representative leaf samples indicate changes in plant physiology across expression optimisation strategies with recombinant *Agrobacterium* containing pTRAc-hL1/hL2 and pRIC3-mSEAP infiltrated at OD_{600} values of 0.25, 0.05, and 0.7 respectively. Infiltration of recombinant *Agrobacterium* containing pTRAc empty vector and BPV-1 hL1/hL2 were included as plant expression controls.

2.3.2 Purification and analysis of BPV-1 L1 protein

PsVs were extracted from frozen leaf material in HSNaOAc and pre-purified on 30% and 50% sucrose cushions, after which 30% cushions were collected and pooled for further purification on discontinuous 27-50% Optiprep™ gradients in 1x HSPBS (Figure 2.3). Upon visual inspection of the sucrose gradients for the pTRAc and VLP controls, a clear layer corresponding to the 30% cushion was observed (Figure 2.6, red arrows). Upon visual inspection of the sucrose gradients for the PsV iterations, the 30% sucrose layer appeared cloudier and less defined with no discernible phenotypic differences observed amongst the PsV iterations. A dense green layer was apparent in the 50% sucrose cushion possibly indicating successful separation of plant material from the protein of interest. Visual inspection of the Optiprep™ gradients reveals the presence of an opaque band for the VLP control, 4a, 4A, 6a, and 6A (Figure 2.6, blue arrows) (Table 2.2 for abbreviations). This cloudy layer at the interface of the 27% and 33% gradients could indicate the presence of VLPs and PsVs. No opaque band was observed for the pTRAc negative control, and the heat-shock treated iterations,

namely 4aH, 4AH, 6aH, and 6AH. Fractions 1-13 collected from the discontinuous gradients (50% → 27%) were analysed for the presence of L1 protein on dot blots. Dot blot analysis showed that L1 protein was detected and distributed across fractions with peak L1 levels observed in fractions 8, 9, and 10 across the VLP control and PsV iterations. This suggests that VLPs and PsVs were isolated between the 27 - 33% Optiprep™ interface. L1 signals observed for heat-shock treated iterations 4aH, 4AH, 6aH, and 6AH were intense, indicating a higher concentration of particles in these fractions despite the lack of an opaque band observed in the gradients. Particularly low L1 signals were seen for 4A, 6a, and 6A possibly indicating a low yield of PsVs in these fractions. Based on these results, fractions 8-10 for each method tested were selected for western blot and TEM analysis. Fraction 11 was included for groups 6aH and 6AH due to the particularly strong signal observed in this fraction for both groups.

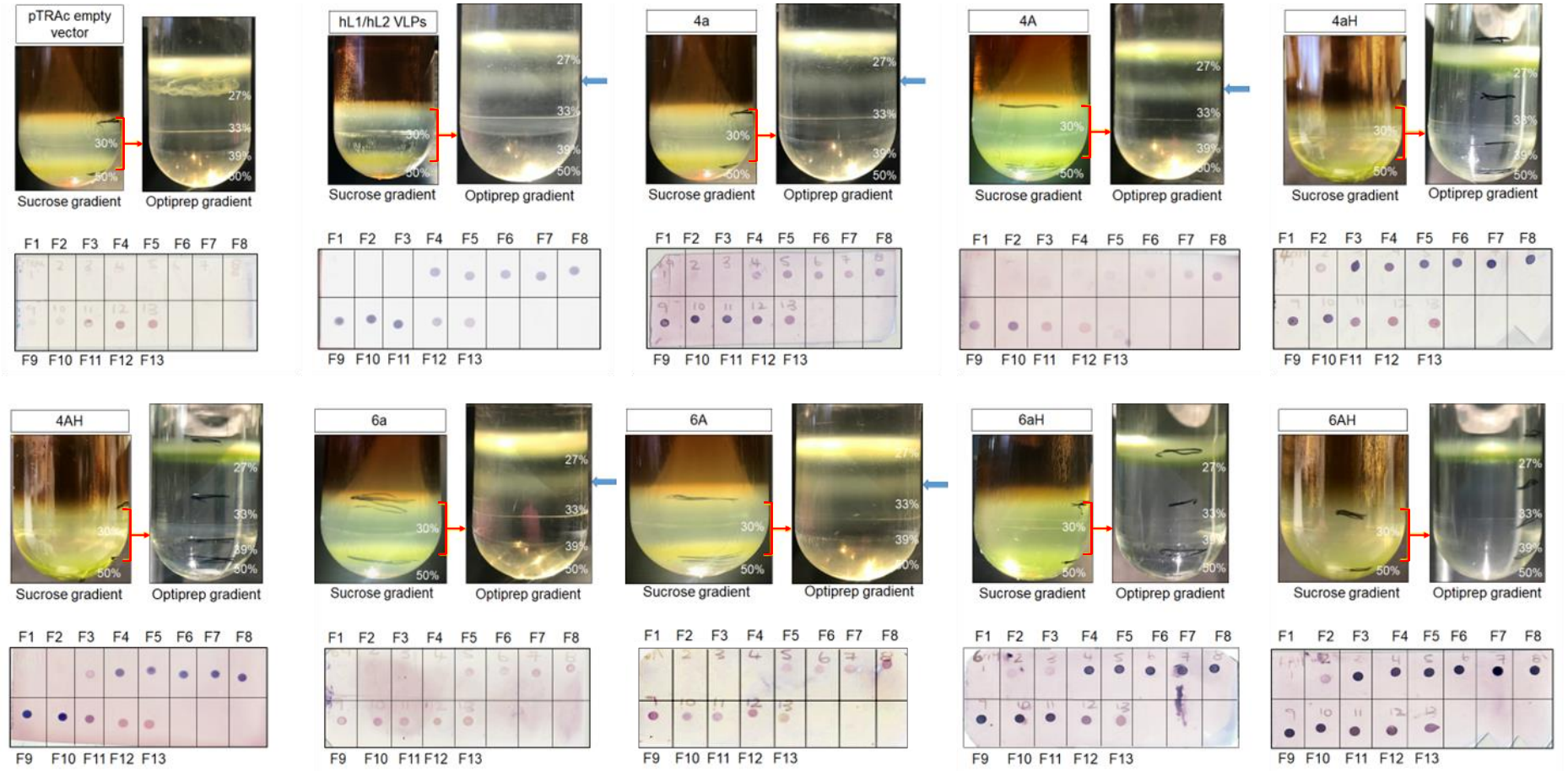

Figure 2.6: Comparison of purified BPV-1 PsVs expressed using different optimisation strategies. Discontinuous gradients and corresponding dot blots for PsVs are pictured. For each iteration, the left gradient image with the red arrow indicates 30% sucrose cushion that was pooled and purified on the Optiprep™ gradient. Purified L1 protein was probed with Camvir anti-BPV-1-L1 (1:1000). Labels: 4 & 6, days post infiltration; a, 200 µM acetosyringone; A, 500 µM acetosyringone; H, heat shock; F 1-13, purified fraction 1-13; and blue arrows, opaque bands observed.

Fractions 8-10 were resolved on 10% SDS-PAGE gels and BPV-1 hL1 was probed for western blotting with anti-BPV-1-L1 Mab Camvir (Figure 2.7). A band of 58 kDa (blue arrows) corresponding to hL1 was observed in the positive control, corresponding to VLP fraction 9. Similarly, BPV-1 hL1 was detected at ~58 kDa for groups 4aH (fraction 9 and 10, Figure 2.7B), 6A (fractions 8-10, Figure 2.7C), 6aH (fractions 8-11, Figure 2.7D), and 6AH (fractions 9-11, Figure 2.7D). Although BPV-1 hL1 is a ~55 kDa protein, it has been observed to migrate to 56-60 kDa in SDS-PAGE gels (Pietersen et al., 2020). No bands were observed in the negative control (pTRAc fraction 9, Figure 2.7A), and groups 4a, 4A, 4aH fraction 8, 4AH fractions 8-10, 6a fractions 8-10, and 6AH fraction 8. The strongest L1 signal was observed in 6A fraction 8 and 9, and 6aH fractions 10 and 11. A faint band of ~52 kDa (clear arrows) was observed in fractions with the strongest L1 signals, possibly representing a degradation product (Love et al., 2012). Protein smearing was also noted across fractions with L1 bands present, possibly representative of incomplete protein denaturation.

Following detection of BPV-1 hL1 in purified fractions by western blotting, fractions 8, 9 and 10 of each optimisation group was analysed for hL1 and hL2 assembly into capsids by TEM. Electron micrographs of the fractions shown in Figure 2.7 indicate the presence of structures that resembled T=1 VLPs and T=7 PsVs in literature (Love et al., 2012; Pietersen et al., 2020). For most groups, the highest concentration of assembled particles was detected in fraction 9. Fewer assembled particles were detected in fractions 8 and 10 for majority of the strategies (not shown), except for 6A F8, 4A F10 and 6aH F10. No particulate structures were observed for the negative pTRAc control indicating that empty pTRAc vectors cannot assemble into particles. In the positive control, a uniform population of 20-30 nm putative hL1/hL2 (white arrows) empty VLPs was observed. VLP-like particles were observed in all PsV expression optimisation groups, possibly indicating a low efficiency of pseudogenome encapsidation across the groups. Despite the absence of a band on the western blot, a high density of VLP-like particles was seen in 4a F9. Particles that resembled PsVs (yellow arrows) measuring 40-60 nm in size were observed for PsV strategies 4a, 4A, 6a, and 6A with none detected in the heat-shock strategies. While some PsVs appeared to be well-formed, circular, and characteristically doughnut-like, most were either ‘loosely’ packed structures or misshaped. Aggregates of L1 protein were observed in most of the preparations. Additionally, capsomeres of ~10 nm (black

arrows) were seen in some preparations with the highest density seen in heat-shock treated groups, particularly 6aH, possibly indicate that application of heat prevents the complete assembly of particles in plants.

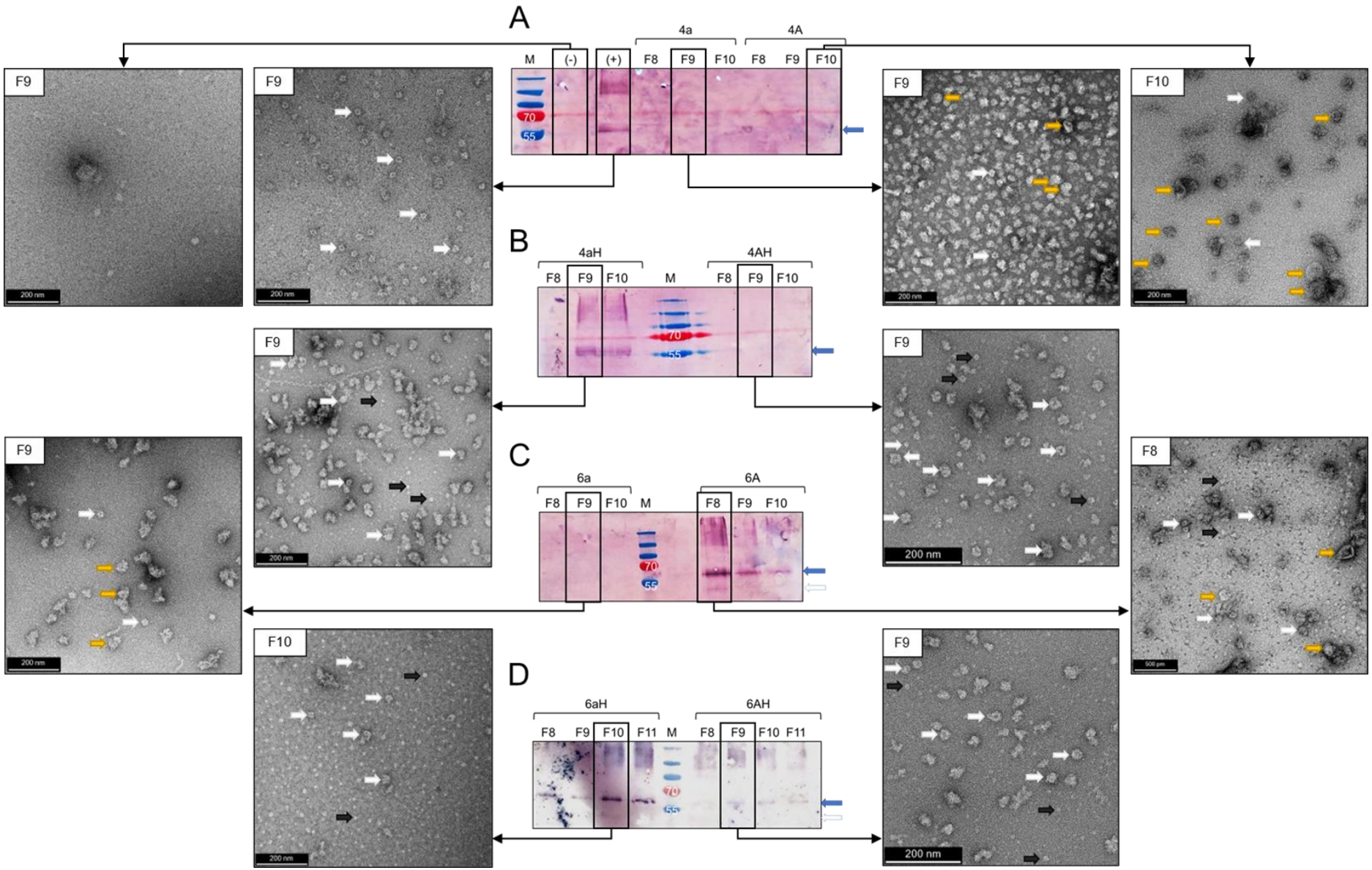
A
M
(-)
(+)
4a
4A
F8
F9
F10
70
55
B
4aH
4AH
C
6a
6A
D
6aH
6AH
F11
200 nm

Figure 2.7 (shown on previous page): Comparative western blots and transmission electron micrographs of plant-purified BPV-1 PsVs. Blots were probed with Camvir anti-BPV-1-L1 (1:1000). BPV-1 hL1/hL2 + mSEAP PsV fractions were negatively stained with 2% uranyl acetate. **A)** Western blot of purified control fractions and PsV fractions of non-heat shock treated plants harvested 4 dpi. **B**) Western blot of PsV fractions of heat shock treated plants harvested 4 dpi. **C)** Western blot of PsV fractions of non-heat shock treated plants harvested 6 dpi. **D)** Western blot of PsV fractions of heat shock treated plants harvested 6 dpi. Labels: M, molecular weight marker (kDa); (-), pTRAc empty vector negative control; (+), BPV-1 hL1/hL2 VLP positive control; 4, 6 – days post infiltration; a, 200 µM acetosyringone; A, 500 µM acetosyringone; H, heat shock; F 8-10, purified fraction 8-10; blue arrows, hL1 protein band (58 kDa); clear arrows, degraded protein(~52 kDa); white arrows, T=1 VLPs (20-30 nm); yellow arrows, T=7 PsVs (40-60 nm); and black arrows, capsomeres (10 nm). A scale bar (200 nm) is indicated at the bottom of each TEM image.

2.3.3 SEAP expression in mammalian cells

To determine whether the putative BPV-1 PsVs detected by TEM encapsidated functional mSEAP replicons and could deliver the pseudogenome to mammalian cells, a SEAP assay was performed. HEK293TT kidney-derived cells were infected with fractions 8-10 of each optimisation iteration in triplicate. Cells were transfected with pRIC3-mSEAP plasmid DNA as a positive SEAP expression control and uninfected cells (cells only) as well as BPV-1 hL1/hL2 VLP fraction 9 were used as negative controls. The supernatants of control and infected cells were assayed for SEAP expression 72 hr post-infection and results are shown below with error bars representing variability in SEAP expression across triplicates measured (Figure 2.8). A SEAP signal of ~40,000 RLUs was observed for the positive control (green bar) indicating that the gene encoded by pRIC3-mSEAP was successfully expressed and that the assay worked. As expected, very poor SEAP signals of >1,500 RLUs were detected in the negative controls. These low signals represent ‘background’ levels of SEAP expression. In relation to the signals detected for the negative controls, the SEAP signals observed for fractions 8-10 of the PsV optimisation groups were negative (>1,500 RLUs). These negative results could indicate an extremely low concentration of PsVs, a lack of encapsidated material within the capsids, or an inability of BPV-1 particles to effectively deliver encapsidated material to mammalian cells.

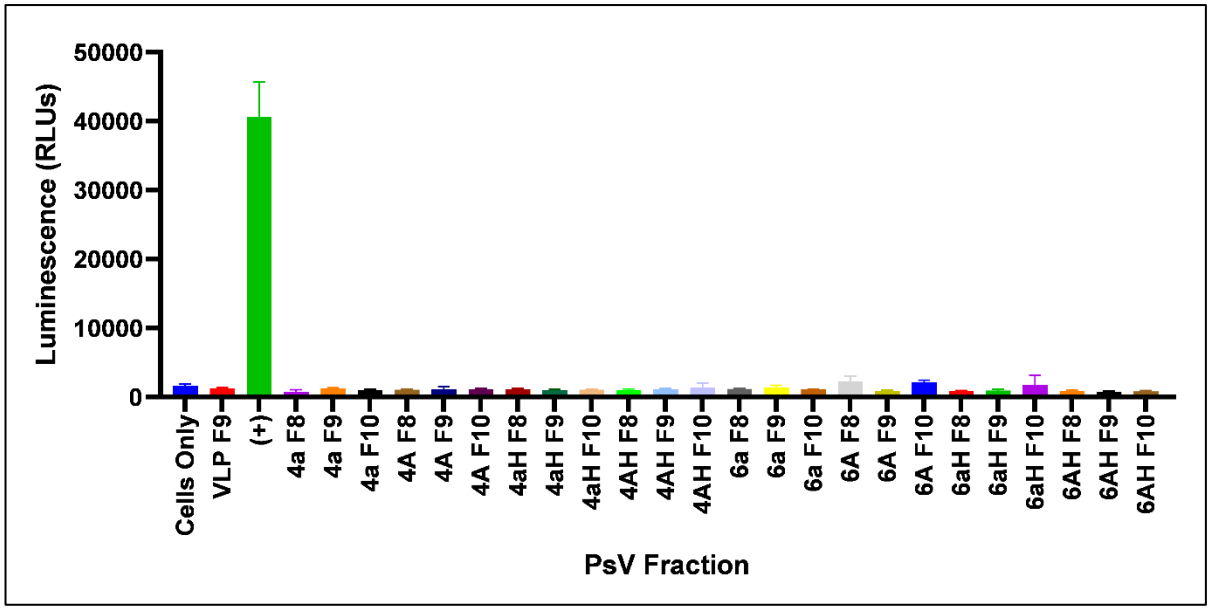

Figure 2.8: SEAP assay of BPV-1 PsVs. SEAP reporter gene expression as indicated by luminescence measured in relative light units (RLUs). (+): positive SEAP expression control.

2.3.4 Summary of BPV-1 PsV expression optimisation studies

Results of the optimisation studies based on analysis of fractions obtained after purification are summarised below in Table 2.4. Based on the results obtained in this chapter, the following methods were adopted for subsequent plant-based PsV purification: induction of recombinant *Agrobacterium* cultures with 200 µM acetosyringone, no heat-shock treatment at day 2 post-infiltration, and an *in-planta* maturation period of 5 days.

Table 2.4: Comparison of expression optimisation strategies. Labels: (+) and green: increase; (-) and red: decrease; (/) and yellow: no change. Colour intensity indicates degree of change.

Variable tested	Iterations compared	L1 expression	Particle yield & integrity	Comments	Method adoption
Increased acetosyringone concentration (200µM vs. 500µM)	4a vs. 4A	-	- -	Not enough evidence to suggest an increased acetosyringone concentration increases expression levels and T=7 particle formation	No
	4aH vs. 4AH	/	/		
	6a vs. 6A	+ +	+		
	6aH vs. 6AH	- -	+ +		
Heat shock at 2dpi	4a vs. 4aH	+	- -	Although L1 protein yield is higher in heat-shocked plant samples, yield and integrity of T=7 particles are compromised	No
	4A vs. 4AH	+	/		
	6a vs. 6aH	+ + +	-		
	6A vs. 6AH	Inconclusive	- -		
In planta maturation (4dpi vs. 6dpi)	4a vs. 6a	Inconclusive	- -	Protein yield is increased with longer maturation while T=7 particle yield is slightly decreased with no change in integrity	Partly
	4aH vs. 6aH	/	- - -		
	4A vs. 6A	+ +	/		
	4AH vs. 6AH	+	-		

2.4 Discussion

The use of plants as a transient expression platform for the production of recombinant proteins has long been investigated as an alternative to traditional expression systems (Huebbers & Buyel, 2021; Stander et al., 2022). Moreover, *Agrobacterium*-mediated transient expression within whole plants has been established as an efficient, scalable, and cost-effective method of viral protein production and assembly, with vast protein accumulation levels observed within days of the infiltration event (Fischer et al., 1999; Rybicki, 2009). This method has been especially useful for the assembly of VLPs in the development of vaccine antigens (Daniell et al., 2009). In this chapter, several methods to optimise transient expression of BPV-1 PsVs as viral antigens were explored. BPV-1 protein expression was investigated by comparing conditions previously established for HPV VLPs by Lamprecht et al. (2016) to conditions such as an increased concentration of acetosyringone for recombinant *A. tumefaciens vir* gene induction prior to infiltration, a heat-shock treatment of infiltrated plants, and an extended period of *in planta* maturation. Protein expression was confirmed with analysis of dot blots, western blots, TEM micrographs, and functionality of PsVs were evaluated by HEK293TT infection.

Previous studies in our laboratory have explored various optimisation strategies to improve plant-based papillomavirus protein expression. Maclean et al. (2007) examined the effects of codon optimisation on HPV-16 L1 expression and determined that human codon optimisation resulted in greater expression levels of higher-order L1 structures. Following this study, HPV-16 L1 yields were shown to increase by a further 50% when expressed with pRIC 3.0, a self-replicating viral vector, rather than pTRAc (Regnard et al., 2010). Pineo et al. (2013) and Chabeda (2017) investigated the use of silencing suppressors and chloroplast localisation on HPV-16 L1/L2/E7 chimaeras and found that both strategies resulted in increased protein accumulation. Pietersen (2019) further described an increase in BPV-1 L1/L2 VLP expression through implementation of various strategies, some of which are described here. Finally, for my Honours project I explored the use of both plant and human codon-optimised BPV-1 L1 and L2 gene sequences and found that human codon usage resulted in a higher accumulation of VLPs and PsVs than plant-optimised proteins (Edwards, 2019).

Incubation of recombinant *Agrobacterium* cultures with 500 µM acetosyringone, as opposed to 200 µM, as well as a brief heat-shock treatment of whole plants, has been observed to increase GUS protein expression in *N. benthamiana* (Norkunas et al., 2018). Additionally, a longer protein maturation step can increase recombinant protein yield in both *N. benthamiana* plants and HEK293TT cells (Buck et al., 2004; Chabeda, 2017; Dennis et al., 2018). A previous study in our laboratory has investigated these strategies in pursuit of enhanced BPV-1 PsV expression and reported an increase in both particle yield and structural integrity (Pietersen et al., 2020). While Pietersen et al. (2020)'s optimisation studies showed promising outcomes, there were some limitations with potential implications for reproducibility of the results. The conditions were not tested in conjunction with each other, and biomass was stored at -80°C for longer than ideal before protein extraction. Moreover, L1 protein expression levels and particle yields were relatively low and reporter gene encapsidation was not directly confirmed. Due to the aforementioned factors, the three methods adopted for BPV-1 PsV production in Pietersen et al. (2020) were further examined and optimised in this study.

Leaves of plants infiltrated for BPV-1 PsV production displayed strong signs of necrosis at 6 dpi while plants at 4 dpi appeared relatively healthy (Figure 2.5). The level of plant pathology observed at 6 dpi is consistent with previous studies in which transient expression of certain recombinant proteins, such as human growth hormone, hepatitis B surface antigen, and hemagglutinin, leads to accelerated plant death (Gils et al., 2005; Huang et al., 2006; Matsuda et al., 2012). This effect is likely caused by the accumulation of exogenous proteins in the ER leading to the formation of reactive oxidative species (ROS) which ultimately results in plant cell death, and could be indicative of recombinant protein degradation (Nosaki et al., 2021a; Nosaki et al., 2021b). Therefore, the results observed here indicate that an extended in planta maturation step could lead to increased levels of L1 protein degradation.

Dot blotting is a simple and rapid colorimetric technique for detection and qualitative estimation of protein expression levels (Sambrook et al., 1989; Towbin et al., 1979). Dot blots are intended for use as a preliminary protein expression assay and reveal limited information about protein yield. Furthermore, this technique reveals nothing about particle structure and assembly and is thus not a strong indicator of particle

yield. Dot blot analysis was implemented here for initial evaluation of the relative intensities of BPV-1 L1 expression between sample fractions and across conditions. Moreover, it was utilised to help determine which fractions should be further analysed by western blotting and TEM. As expected, L1 protein was detected in all the PsV optimisation groups with peak intensities observed in fractions 8-10, corresponding to the 27%-33% Optiprep™ interface (Figure 2.6). This BPV-1 L1 protein distribution is consistent with previous studies and could indicate the presence of particles of varying densities (T=1 VLPs closer to the 27% gradient and T=7 PsVs closer to the 33% gradient) (Love et al., 2012; Pietersen, 2019). Upon analysis of the relative intensity of protein dots across conditions, it appears the heat-shock treated samples have the highest L1 protein accumulation levels and the widest distribution of protein across fractions. These findings support those of previous studies that suggest a <40°C heat-shock treatment of plants leads to up-regulation of heat shock proteins (HSPs) that directly promote protein expression. HSPs function as molecular chaperones to deliver proteins to relevant cellular compartments as well as assist in protein folding and mRNA stabilisation (Park & Seo, 2015; Ul Haq et al., 2019; Wu et al., 2022). Moreover, a study by Tsai et al. (2009) suggests that small HSPs promote DNA transfer between *A. tumefaciens* and plant cells resulting in increased uptake of T-DNA into the cells. The heightened levels of L1 protein accumulation observed in the heat-shock treated groups is likely a result of up-regulated HSPs.

An unexpected observation reported in Section 2.3.2 relates to the gradient images that accompany the dot blots in Figure 2.6. An opaque band at the 27%/33% Optiprep™ interface was observed in the gradients of the non-heat-shock groups but was markedly absent in those of the heat-shock groups. This cloudy layer can be indicative of VLP and PsVs concentrated at that position (Chabeda, 2017; Pietersen, 2019). This observation could indicate a relatively low concentration of PsVs in the heat-shocked samples despite the heightened L1 protein levels detected.

To elucidate further information about L1 expression levels, western blotting was implemented. In this study, western blots confirmed the presence of BPV-1 L1 of size 58 kDa in a few of the optimisation iterations tested (Figure 2.7). Despite being a 55 kDa protein, L1 has been observed to migrate to 58 kDa thus this result was not unexpected (Pietersen, 2019). Additionally, a band of 52 kDa was detected,

suggesting proteolytic cleavage of L1 occurred during *in-planta* incubation and extraction. This band is consistent with previous studies which demonstrated expression of BPV-1 in plants and insect cells respectively (Love et al., 2012; Shafti-Keramat et al., 2009). Smearing was also observed in the blot lanes, indicating incomplete L1 protein denaturation. BPV-1 L1 has more inter-capsomeric disulphide bonds than other PVs when assembled (Buck, Pastrana, et al., 2005; Wolf et al., 2010). The resistance to denaturation observed here is thus likely due to BPV-1 particle stability. Although western blot analysis was necessary for elucidation of protein expression patterns, it was limited here by the lack of a functional antibody as an old anti-L1 antibody known to produce inconsistent results was used.

The assembly of BPV-1 L1 and L2 into VLPs and PsVs *in planta* was investigated using TEM (Figure 2.7). The distinct size limits of BPV-1 VLPs (20 - 30 nm) and PsVs (40 - 60 nm) allow distinguishment between the two particle types (Pietersen et al., 2020). Micrographs revealed the presence of a heterogenous population of 40 - 60 nm structures resembling BPV-1 T=7 PsVs made in Pietersen et al. (2020) for strategies 4a, 4A, 6a, and 6A (yellow arrows). There were no clear differences observed between the PsVs obtained from these strategies, indicating that an increased acetosyringone concentration and extended *in planta* maturation have little effect on PsV yield and assembly. For majority of the strategies, the highest concentration of assembled particles was observed in fraction 9. This consistent representation was expected as fraction 9 corresponds to the 27-33% Optiprep™ interface that BPV-1 PsVs are observed to migrate to, based on their density (Pietersen et al., 2020). However, very few putative PsVs were observed, indicating a low PsV yield following purification. Furthermore, the morphology of the putative PsVs varied, with majority appearing to be loosely packed, misshapen, and misassembled. TEM additionally revealed the presence of L1 aggregates, indicating that particle misassembly occurred *in planta* during PsV production (Varsani et al., 2006). Moreover, VLPs resembling those shown in Love et al. (2012) were observed across the strategies, with a particularly high concentration observed in 4a (Figure 2.7A). Production of BPV-1 PsVs in mammalian cells is associated with an estimated encapsidation efficiency of 5% (Buck et al., 2004). The presence of T=1 VLPs and few T=7 PsVs across the PsV production strategies tested here suggest that plant-based pseudogenome packaging by BPV-1 L1/L2 is also associated with low efficiency. A study by Adams et al. (2023) showed that pRIC3-

mSEAP, with a replicon size of 4.8 kb, is ideal for plant-based papillomavirus PsV expression. BPV-1 may deviate from this paradigm. Studies by Zhao et al. (1999) and Zhao et al. (2000) demonstrate that a region on the virus' E2 sequence contains an encapsidation signal that enhances viral assembly. On the contrary, a study by Buck et al. (2004) found that inclusion of the E2 signal is not necessary for intracellular expression of BPV-1 particles. Therefore, exclusion of the E2 sequence in this study could account for the lowered encapsidation efficiency observed but should not prevent BPV-1 PsV production entirely.

No putative PsVs were observed in the heat shock treated groups. Moreover, TEM analysis revealed the presence of 10 nm capsomeric structures in the heat shock groups, with a particularly high concentration detected in 6aH. Furthermore, the heat shock PsV preparations appeared to contain a high number of putative VLPs, indicating effective assembly of L1 and L2 into empty capsids. In summary, these results indicate that, while the heat-shock treatment likely promotes uptake of L1- and L2-encoding DNA into plant cells and subsequent protein synthesis, the treatment could hinder SEAP replicon formation and replication. Consequently, pseudogenome encapsidation for the assembly of functional PsVs could be affected. This finding is consistent with previous studies that suggest HSP up-regulation negatively impacts DNA expression and integrity by inhibiting DNA-binding activity, nucleotide excision repair, and replication fork progression (Schmidt-Rose et al., 1999; Sozhamannan & Chattoraj, 1993; Velichko et al., 2012).

An inconsistency between the western blot and TEM results is apparent in Figure 2.7. The lack of L1 bands in the blots of groups 4A, 4AH, and 6a is incongruent with the corresponding micrographs, which show the existence of particles assembled from L1. This is almost certainly a consequence of the western blot limitations discussed above. Following TEM analysis, A SEAP reporter gene assay was carried out to evaluate the functionality and infectivity of plant-made BPV-1 PsVs *in vitro*. Reporter assays are a useful tool to assess whether PsVs can deliver encapsidated DNA to mammalian cells for reporter gene expression (Lee et al., 2003). The results revealed extremely low SEAP signals in the cell supernatants following PsV infection despite the positive transfection control exhibiting a high expression level (Figure 2.8). The data was contradictory to results reported by Pietersen et al. (2020), in which a SEAP signal

>1.2 x10^6 RLUs was observed for BPV-1 PsV fraction 9, and Lamprecht et al. (2016), in which cells infected with HPV-16 PsVs produced a SEAP signal of >1.3 x10^5 RLUs. The lack of reporter gene expression observed in this study could suggest ineffective pseudogenome packaging. Despite observing putative T=7 PsVs with TEM analysis, it is not conclusive evidence that SEAP replicons were successfully incorporated into the particles.

Rolling circle amplification (RCA) can be used to confirm successful pseudogenome encapsidation (Chabeda et al., 2018; Lamprecht et al., 2016). This technique could therefore be implemented in this study for further characterisation of BPV-1 PsVs. An alternative explanation for the lack of SEAP expression seen here is that the reporter gene expression levels are below the detectable threshold, indicating a low yield of functional PsVs. This would correlate with the TEM results discussed above. Alternatively, the plant-made BPV-1 PsVs could lack the ability to infect host cells. BPVs enter cells via clathrin-dependent endocytosis (Day et al., 2003). Cell surface interactions between L1/L2 capsids and host cell proteins are necessary for PsV uptake and subsequent pseudogenome release and expression (Horvath et al., 2010). Correct assembly of T=7 icosahedral virions is critical for these interactions to occur (Nguyen et al., 2007). In this study, partially assembled and misassembled PsVs were observed in TEM (Figure 2.7), possibly indicating a lack of infectivity. Finally, SEAP expression could have been impacted by the quality of the cells used in the assay. An increase in passage number has been associated with a decrease in cell health with possible consequences for exogenous gene expression (Briske-Anderson et al., 1997; Clynes, 1998). In this chapter, HEK293TT cells of a high passage number (>100) were utilised. Subsequent SEAP signals observed for the positive controls (biological repeats not shown) were 10- to 100-fold lower than those observed in previous PV studies in the laboratory (Lamprecht et al., 2016; Pietersen et al., 2020). While the high passage number could have resulted in attenuated SEAP expression, cell growth and morphology reflected that of completely healthy cells. It is therefore unlikely that the lack of reporter gene expression observed here is a consequence of compromised cell health.

The objective of this chapter was to determine whether varying combinations of the different PsV expression strategies reported on in Pietersen et al. (2020) resulted in

increased PsV production. The results reported on here indicate that incubating recombinant *Agrobacterium* cultures with 500 µM acetosyringone, as opposed to 200 µM, prior to agro-infiltration has an inconsequential effect on L1 expression and PsV formation as no significant difference was observed in terms of L1 expression levels and particles observed with TEM analysis. Heat-shock treatment of plants at 2 dpi, on the other hand, does appear to influence recombinant protein expression. An increase in BPV-1 L1 protein production was observed in heat shocked plants, likely a result of up-regulated heat shock proteins driving protein expression and stability. TEM analysis, however, revealed that the treatment resulted in a poor yield of T=7 PsVs, indicating that the heat-shock treatment hinders PsV formation. Although the exact mechanism driving this interference is unknown, it may be related to HSP up-regulation and gene silencing due to plant stress responses at higher temperatures. Finally, the effects of *in planta* maturation of six days, as opposed to four days, was assessed and the results were inconclusive. However, the high levels of necrosis observed at 6 dpi indicate that an extended maturation could be detrimental to L1 protein accumulation within plants. Therefore, for future studies, infiltrated plants should be closely monitored for signs of death.

Without reporter gene expression data, there is insufficient evidence to conclusively state whether the strategies investigated improve *Agrobacterium*-mediated BPV-1 PsV production in *N. benthamiana*. As there is no clear explanation for the lack of SEAP expression observed, further investigation is required to determine whether it is the result of low encapsidation efficiencies, poor infectivity, minimal PsV yields, or a combination of these factors.

3 Chapter 3: Expression of BPV-1 and HPV-35 pseudovirions encapsidating HPV-16 E7SH in *N. benthamiana*

3.1 Introduction

Over the past twenty years, there has been extensive research into plant-based production of papillomavirus vaccine candidates, specifically of high-risk HPV types. An early breakthrough in the field occurred when Varsani et al. (2003) used transgenic *N. tabacum* for expression of a gene encoding full-length native HPV-16 L1 and found that the protein accumulated to 4 µg/kg wet leaf weight (ww) and assembled into VLPs that could be visualised using electron microscopy. Following this discovery, Warzecha et al. (2003) investigated transgenic expression of a gene encoding a plant codon-optimised HPV-11 L1 protein in potatoes. The resulting VLPs accumulated to 20 µg/kg ww and displayed poor immunogenicity following oral immunisation in mice. A third group explored expression of a human codon-optimised HPV-16 *l1* gene (*hl1*) in transgenic tobacco plants (Biemelt et al., 2003). Resulting hL1 protein levels reached 20 mg/kg and the assembled particles were strongly immunogenic in mice following caesium chloride gradient purification (Biemelt et al., 2003; Giorgi et al., 2010).

Maclean et al. (2007) also investigated codon optimisation as well as intracellular targeting of the HPV-16 *L1* gene and *Agrobacterium*-mediated transient expression in *N. benthamiana*. The authors' findings were clear – human codon-optimisation, paired with the inclusion of a chloroplast localisation signal, resulted in the highest accumulation of L1 in plants with >500 mg/kg of soluble leaf material. The authors also showed that VLPs were appropriately assembled and bound conformation-specific mAbs (Maclean et al., 2007; Rybicki, 2010).

Expression of therapeutic HPV vaccines has been explored. The HPV-16 E7 oncoprotein is the major target of therapeutics as it functions during mid-to-late infection, plays a predominant role in oncogenic transformation, and is constitutively expressed in cervical cancer lesions (Khallouf et al., 2014). Franconi et al. (2002) led this investigation with the use of a potato virus X (PVX) viral vector to express E7 in well-established PVX plant hosts. The highest level of protein accumulated in *N.*

benthamiana at 3-4 µg/g fresh leaf weight. Additionally, 40% of mice vaccinated with plant extract containing E7 displayed protection against an HPV-16 E7-expressing cell line and protection was accompanied by a powerful cytotoxic T-cell response (Franconi et al., 2002; Rybicki, 2014).

In response to possible concerns regarding the use of a native oncoprotein in vaccines, a method to circumvent the risk of viral oncogenesis of HPV vaccines was developed by Ohlschlager et al. (2006). The HPV-16 *e7* gene sequence was shuffled in a way that allows for expression of putative epitopes while deactivating the subsequent E7SH protein. Whitehead et al. (2014) tested a plant-produced E7SH protein fused to Zera®, a protein-body forming peptide that accumulates to high levels in the ER, increases fusion protein yield, and protects against protein degradation (Geli et al., 1994; Torrent et al., 2009). Whitehead et al. (2014) found that the vaccine candidate acted both prophylactically and therapeutically in mice, by eliciting a E7-specific CTL and antibody response that both protected mice from HPV-16 challenge and reduced established tumours. Additionally, the protein bodies formed in the presence of Zera® peptides were shown to enhance the immune response and thus have adjuvanting properties (Chabeda, 2017; Whitehead et al., 2014).

Following the optimisation of BPV-1 PsV expression in *N. benthamiana* in Chapter 2, it was investigated whether plant-made BPV-1 and HPV-35 particles could encapsidate a Zera®-E7SH DNA vaccine candidate and deliver the DNA to mammalian cells. Expression of HPV-35 PsVs were included following the success of Chabeda (2017) in generating a potential plant-made HPV-35 vaccine candidate encapsidating Zera®E7SH. To assess infectivity of the PsVs in mammalian cells, various reporter genes were incorporated into the Zera®-E7SH mammalian expression cassette downstream of E7SH. An HPV-16 E7SH construct lacking Zera® was also developed to assess whether the Zera® peptide affected protein expression and subsequent detection on western blots. Additionally, this chapter describes an optimised strategy to determine if purified BPV-1 and HPV-35 PsVs encapsidated recombinant E7SH DNA.

3.2 Materials and methods

3.2.1 Synthesis of HPV-16 E7SH constructs by In-Fusion cloning

In-Fusion cloning (Takara) is a cloning technique designed for rapid, directional cloning of one or more DNA fragments into any vector. The technique involves linearisation of a vector backbone, design of gene-specific primers with vector-homologous extensions, amplification of the gene of interest, and joining of the amplified gene and linearised vector in an In-Fusion Cloning reaction (Park et al., 2015). In this study, the technique was used to facilitate cloning of five E7SH-based constructs.

3.2.1.1 Primer design

Forward (Fwd) and reverse (Rev) primer sets specific to the genes of interest were designed to incorporate 5' 15 bp extensions complementary to the ends of the linearised vector to facilitate In-Fusion cloning (Table 3.1). In the Fwd primers, a single cytosine nucleotide was incorporated between the vector and gene insert sequences to keep the gene of interest in frame. The primers were tested *in silico* using SnapGene software (www.snapgene.com) and synthesised by Inqaba Biotech (Oligo Synthesis).

Table 3.1: Sequences and PCR annealing temperatures of primers used in this study

Primer name	Orientation	5' → 3' sequence	PCR T_a (°C)	Function
pTRAc	Fwd	CATTTCATTTGGAGAGGACACG	59	Colony PCR and sequencing of pRIC 3.0 constructs
	Rev	GAACTACTCACACATTATTCTGG		
pTH	Fwd	TAG TAA TCA ATT ACG GGG TCA TTA G	60	Colony PCR of pTH constructs
	Rev	GCC ATA GAG CCC ACC GCA		
eGFP	Fwd	acctgctcctgctcccATGGTGAGCAAGGGCGAG	60/65	In-Fusion cloning of eGFP into pRIC3-mZera®E7SH
	Rev	gcagaattctgtcgaTTACTTGTACAGCTCGTCCAT		
G-luciferase	Fwd	acctgctcctgctcccATGGGAGTCAAAGTTCTGTTT	60/65	In-Fusion cloning of G-luciferase into pRIC3-mZera®E7SH
	Rev	gcagaattctgtcgaTTAGTCACCACCGGCCCC		
SEAP	Fwd	acctgctcctgctcccATGCTGCTGCTGCTGCTG	60/65	In-Fusion cloning of SEAP into pRIC3-mZera®E7SH
	Rev	gcagaattctgtcgaTCATGTCTGCTCGAAGCGGC		
E7SH	Fwd	cgaagcttATGCACGGCGACACCCCC	60	Addition of *Hind*III to the 5' end & *Xba*I to the 3' end of E7SH
	Rev	gccctctagaTTATGGTTTCTGAGAACAGA		
mE7SH	Fwd	aaaaaaaaaaacATGTAGTAATCAATTACGGGGTCA	60	In-Fusion cloning of mE7SH into pRIC 3.0
	Rev	ctctagagagctcgaGCCATAGAGCCCACCGCA		

3.2.1.2 PCR amplification

PCR amplification was performed using Phusion™ Hot Start II High-Fidelity DNA Polymerase (Thermo Fisher Scientific), as per the manufacturer's instructions. Gene-specific primer sets were added at a final concentration of 1 µM to amplify 10 ng of template DNA. PCR amplification conditions are specified in Table 3.1 and 3.2. PCR products were confirmed on 1% agarose gels and purified using the NucleoSpin® Gel and PCR Clean-up kit (Macherey-Nagel), as per the manufacturer's instructions with DNA eluted in 10 mM Tris buffer heated to 65°C.

Table 3.2: PCR conditions used throughout this study

Cycle step	Temperature (°C)	Time	Cycles
Initial denaturation	95	5 min	1
Denaturation	95	30s	30-35
Annealing	Primer specific	30s	
Extension	72	1 – 2 min	
Final extension	72	5 min	1
Hold	20	∞	1

3.2.1.3 Linearisation of destination plasmid

The destination plasmids were linearised by RE digestion using restriction enzymes shown in Table 3.3. Linearised vector fragments were confirmed on 1% agarose gels and purified using the NucleoSpin® Gel and PCR Clean-up kit (Macherey-Nagel), as per the manufacturer's instructions with an adaptation whereby DNA was eluted in Tris buffer (10 mM Tris base, pH 7.5) heated to 65°C.

Table 3.3: Summary of cloning and construct properties

Construct name	Insert	Parent vector	Destination vector	RE sites Insert (5'/3')	RE sites Vector (5'/3')	Construct size (kb)
pRIC3-mZera®E7SH	mZeraE7SH	pUC57	pRIC 3.0	*Afl*III/*Xho*I	*Afl*III/*Xho*I	8.61
pRIC3-mZera®E7SHeGFP	eGFP	peGFP	pRIC3-mZera®E7SH	-	*Nco*I/*Sal*I	9.32
pRIC3-mZera®E7SHgluc	Gaussia-luciferase	pRIC 3.0	pRIC3-mZera®E7SH	-	*Nco*I/*Sal*I	9.16
pRIC3-mZera®E7SHSEAP	mSEAP	pRIC 3.0	pRIC3-mZera®E7SH	-	*Nco*I/*Sal*I	10.16
pTH-mE7SH	E7SH	pUC57-mZeraE7SH	pTH	-	*Hind*III/*Xba*I	5.27
pRIC3-mE7SH	mE7SH	pTH	pRIC 3.0	-	*Afl*III/*Xho*I	8.17

3.2.1.4 In-fusion cloning and *E. coli* transformation

The strategy for cloning respective reporter genes into the mammalian cassette of pRIC3-mZera®E7SH is outlined in Figure 3.1 and the two-part strategy for developing a pRIC3-mE7SH construct without Zera® is shown in Figure 3.2. Purified linearised vectors and inserts were fused by using the In-Fusion HD Cloning kit (Takara Bio) according to the manufacturer's instructions. Two microlitres of vector and gene insert, respectively, were mixed with 2 µL of 5x In-Fusion HD Enzyme Premix in a final volume of 10 µL and incubated at 50°C for 15min. Five microlitres of the In-Fusion reaction was then transformed into Stellar™ Competent *E. coli* Cells (Takara Bio). Transformed cells were plated on LA plates supplemented with ampicillin (100 µg/mL) and incubated overnight at 37°C. Positive colonies were confirmed using cPCR as described in section 3.1.3.

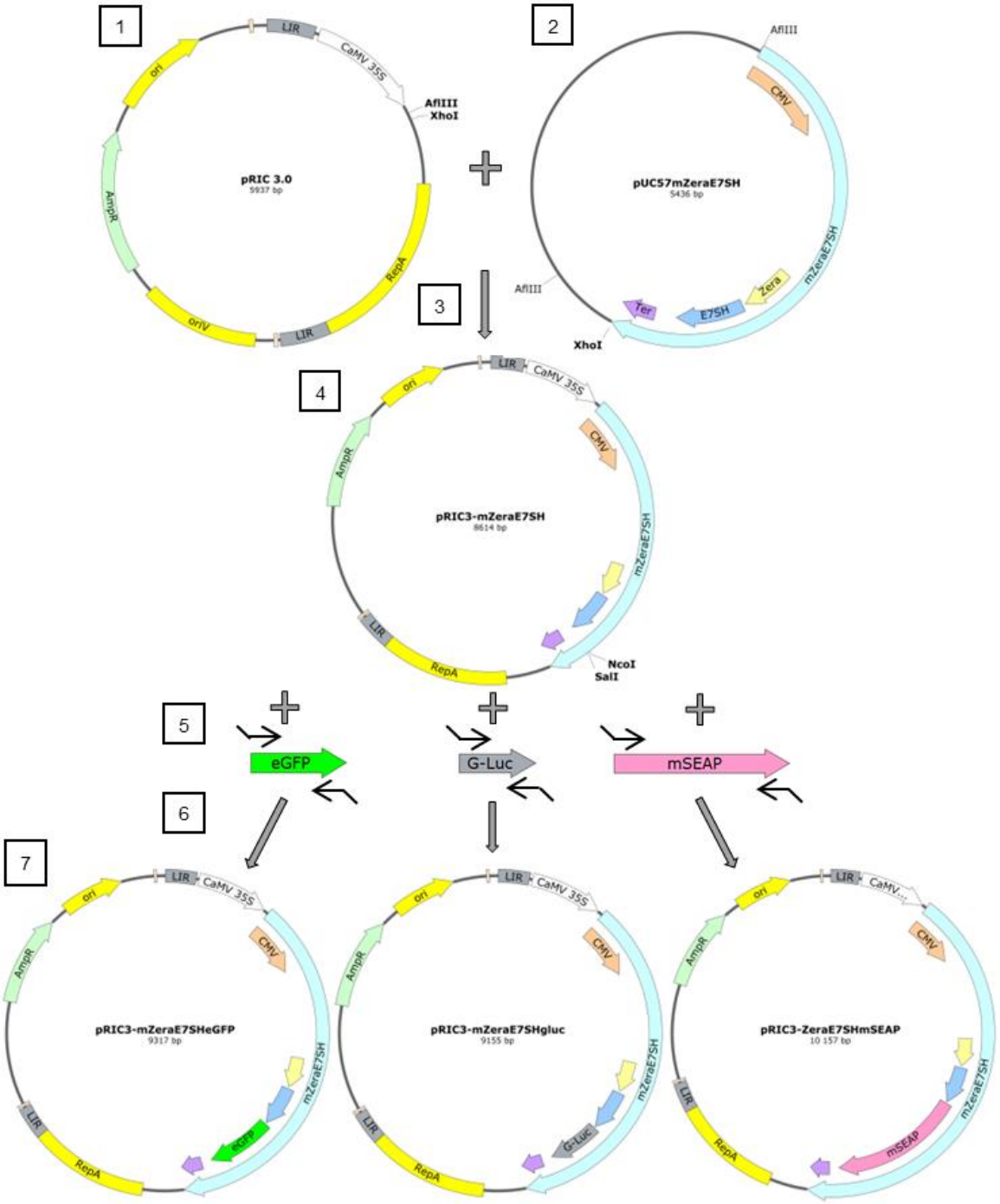

Figure 3.1: In-Fusion plasmid assembly of pRIC3-mZera®E7SH reporter clones. 1) pRIC 3.0 was linearised and **2)** mZera®E7SH was excised from pUC57 with *Afl*III and *Xho*I, and **3)** ligated to form **4)** pRIC3 mZera®E7SH which was then linearised with *Nco*I and *Sal*I. **5)** eGFP, g-luciferase, and mSEAP were PCR amplified out of their respective parent vectors with gene-specific primers and **6)** In-Fusion cloned into linearised pRIC 3.0 to form **7)** pRIC3-mZera®E7SH-eGFP, -gluc, and -mSEAP. The final plasmids also contain: LIR, BeYDV long intergenic region; CaMV 35S, cauliflower mosaic virus intron/enhancer/promoter element; CMV, cytomegalovirus intron/enhancer/promoter element; BGHpolyA, bovine growth hormone polyadenylation signal; RepA, BeYDV rep gene; AmpR, ampicillin resistance gene; and ori, *E. coli* origin of replication.

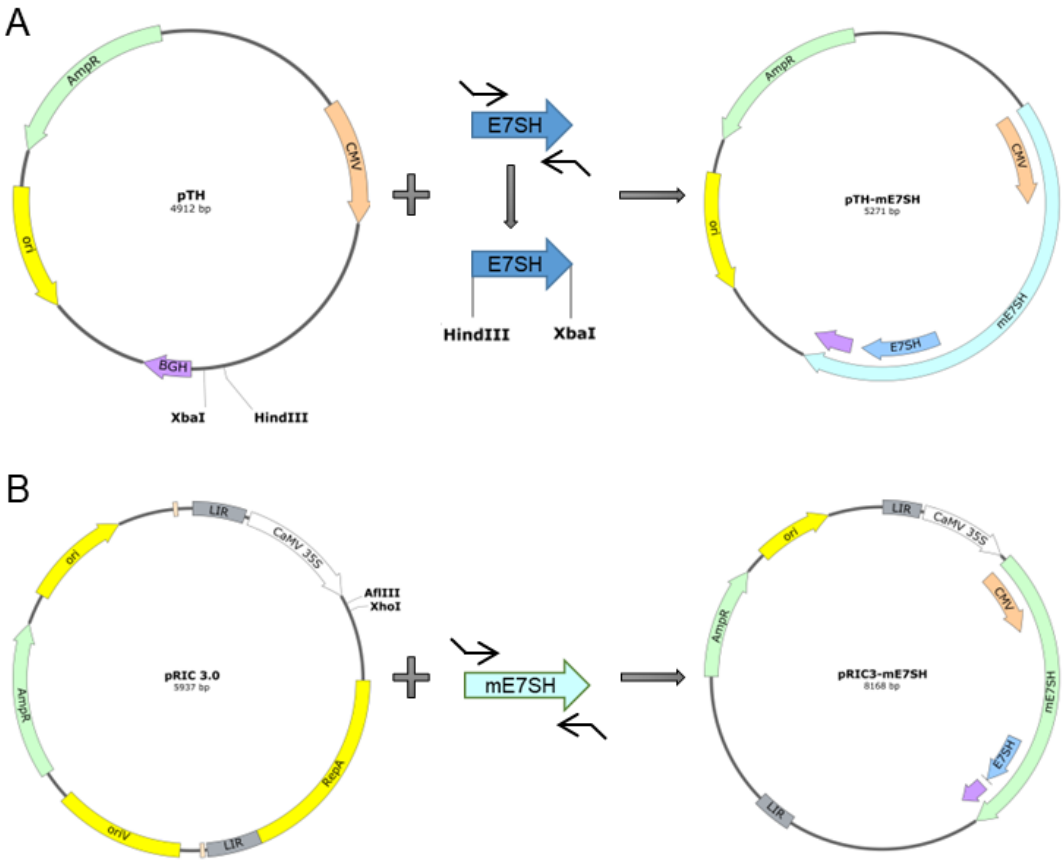

Figure 3.2: Two-step plasmid assembly of pRIC3-mE7SH. To assemble pTH-mE7SH **A)** E7SH was PCR amplified with gene-specific primers to include *Xba*I and *Hind*III RE sites. E7SHamp and pTH were then digested with *Xba*I and *Hind*III and ligated. **B)** mE7SH was PCR amplified from pTH-mE7SH with gene-specific primers and In-Fusion cloned into linearised pRIC 3.0. The plasmids contain: LIR, BeYDV long intergenic region; CaMV 35S, cauliflower mosaic virus intron/enhancer/promoter element; CMV, cytomegalovirus intron/enhancer/promoter element; E7SH, gene of interest encoding HPV-16 E7SH; BGHpolyA, bovine growth hormone polyadenylation signal; ori, *E. coli* origin of replication; oriV, *Agrobacterium* origin of replication; RepA, BeYDV rep gene; AmpR, ampicillin resistance gene; and mE7SH, mammalian cassette containing CMV, HPV-16 E7SH and BGH sequences.

3.2.2 DNA extraction, plasmid isolation, restriction enzyme digestion, and gel electrophoresis

All plasmid DNA in this study was isolated using the QIAprep® Spin Miniprep kit (Qiagen) as per the manufacturer's instructions. All restriction enzyme digests were performed using restriction enzymes (REs) from Thermo Fisher Scientific or New England BioLabs® (NEB) according to the manufacturer's instructions. All PCR and RE digestion products were separated on 0.8-1% TBE [10.8 g/L Tris base, 5.5 g/L boric acid, 0.5 M EDTA, pH 8.0] agarose gels by electrophoresis. Electrophoresed gel

products were excised using long-wave (365 nm) UV light and imaged using short-wave (254 nm) UV light. Extraction of DNA fragments from agarose gels was performed using the QiAquick® Gel Extraction kit (Qiagen) as per the manufacturer's instructions.

3.2.3 Ligation and transformation of *E. coli*

Ligation reactions were performed using T4 DNA Ligase (Thermo Fisher Scientific) according to the manufacturer's instructions. These reactions were transformed into DH5-α chemically competent *E. coli* cells (E. cloni™, Lucigen) and recombinant clones were selected on LB agar (LA) plates containing ampicillin (100 µg/mL).

3.2.4 Confirmation of recombinant constructs by PCR

Bacterial colonies from overnight plates were screened for selection of recombinant clones using colony PCR (cPCR). For cPCR reactions, Taq DNA Polymerase 2x Master Mix RED (Ampliqon) with a final $MgCl_2$ concentration of 1.5 mM was used, as per the manufacturer's instructions. Vector-specific primers, as described in Table 3.1, were added at a final concentration of 0.2 µM each.

PCR cycling conditions used throughout this study are outlined in Table 3.2. Positive clones were confirmed with RE digests and sequencing at Macrogen Inc. (Netherlands).

3.2.5 Sequencing of recombinant clones

Recombinant plasmids were sequenced (Macrogen Inc., Netherlands) using vector-specific primers shown in Table 3.1. Sequences were aligned and analysed to confirm successful amplification and cloning using CLC Main Workbench 6 (Qiagen).

3.2.6 Transformation of *A. tumefaciens*

Electrocompetent *Agrobacterium* cells of strain GV3101::pMP90RK were electroporated with recombinant DNA as described in Chapter 2, section 2.2.1.1. The transformed cells were spread plated onto LB agar plates supplemented with rifampicin (50 µg/mL), kanamycin (30 µg/mL), and carbenicillin (50 µg/mL) and

incubated at 27°C for 2-3 days. Colonies were screened by cPCR, as described in section 3.2.4, using primers shown in Table 3.1, and PCR cycling conditions as outlined in Table 3.2.

3.2.7 *Agrobacterium*-mediated expression of BPV-1 and HPV-35 PsVs

Twenty-four to thirty *N. benthamiana* plants were vacuum infiltrated with recombinant *Agrobacterium* cultures as described in Chapter 2, section 2.1.1.1. The pRIC3-mZera®E7SH construct used as a pseudogenome for encapsidation into BPV-1 and HPV-35 PsVs *in planta,* referred to as GB-pRIC-mZera®E7SH in this study, was assembled with GoldenBraid technology and transformed into *A. tumefaciens* strain EHA105 (Chabeda, 2017). Recombinant *Agrobacterium* cultures were propagated in media supplemented with rifampicin (50 µg/mL), kanamycin (30 µg/mL), and carbenicillin (50 µg/mL), except for the GB-pRIC-mZera®E7SH culture media which was supplemented with spectinomycin (50 µg/mL) and rifampicin (50 µg/mL). Recombinant *Agrobacterium* strains harbouring BPV-1 pTRAc-hL1/hL2 or HPV-35 pTRAc-hL1/hL2 were co-infiltrated with E7SH-based constructs at the OD_{600} values specified in Table 3.4. The cell densities used for infiltration of HPV-35 hL1 and hL2, and the recombinant E7SH constructs were selected based on work done by Lamprecht et al. (2016) and (Chabeda, 2017). An acetosyringone concentration of 200 µM was used to induce cell suspension mixtures. Plants were grown at 22°C under 16hr light: 8hr dark cycles and leaf material was harvested 5 dpi and frozen at -80°C until further processing.

Table 3.4: Culture concentrations (OD_{600}) and combinations of recombinant *Agrobacterium* cultures for expression of BPV-1 and HPV-35 PsVs

	pTRAc-hL1	pTRAc-hL2	pRIC3-mE7SH	GB-pRIC-mZera®E7SH	pRIC3-mZera®E7SH eGFP	Product
OD_{600}	0.25	0.05	-	-	-	VLP control
			0.50	-	-	mE7SH PsVs
			-	0.50	-	mZera®E7SH PsVs
			-	-	0.50	mZera®E7SHeGFP PsVs

3.2.8 Extraction and purification, L1 protein detection, and TEM analysis of purified PsVs

Frozen biomass was homogenised and clarified in HSNaOAc (pH 5.2) as described in Chapter 2, section 2.1.1.2. Clarified crude extracts were loaded onto 30% (5 mL) and 50% (1 mL) sucrose cushions and ultracentrifuged at 174,500 *x g* at 15°C for 45min. The 30% cushions were collected and dialysed overnight at 4°C in HSPBS (pH 7.4), after which dialysed samples were pooled and loaded onto discontinuous iodixanol gradients as shown in Chapter 2, Figure 2.3. Loaded dialysates were purified via centrifugation as described in Chapter 2, section 2.1.1.2, after which 13 x 1 mL fractions were collected from the bottom of the tubes. Dot blot and western blot analysis of purified BPV-1 and HPV-35 fractions was performed as described in Chapter 2, sections 2.1.3.1 and 2.1.3.2. BPV-1 hL1 was probed with BPV-1/1H8 + CAMVIR primary antibody (1:1000) and anti-mouse IgG secondary antibody (1:10,000). HPV-35 hL1 was probed with H16.J4 MAb primary antibody (1:5000) provided by Dr Neil Christensen, and anti-mouse IgG secondary antibody (1:10,000). Fractions with the highest L1 protein concentration were prepared and viewed by TEM as described in Chapter 2, section 2.1.3.3.

3.2.9 Reporter gene encapsidation analysis of BPV-1 and HPV-35 PsVs

3.2.9.1 Denaturation of PsVs

Due to particle stability, a viral capsid lysis step was employed prior to rolling circle amplification (RCA) to allow for analysis of replicon encapsidation. DNA was extracted from particles using the QIAprep® Spin Miniprep kit (Qiagen), as per the manufacturer's instructions with adaptations. Briefly, 50 µL of purified sample was added to 250 µL of Resuspension Buffer P1 in a microcentrifuge tube and mixed thoroughly by inverting the tube 4-6 times. Capsid proteins were then digested in 250 µL Lysis Buffer P2 supplemented with 10 µL recombinant PCR Grade Proteinase K (2.5 units/mg, Roche) at room temperature for 5min. Following this, samples were neutralised in 350 µL Buffer N3 by mixing thoroughly, and resulting flocculent was pelleted by centrifugation for 8min at 17,900 *x g* in a table-top microcentrifuge. The supernatant was applied to the QIAprep® Spin Column and microcentrifuged for 1min at 17,900 *x g*. The column was washed twice with 750 µL Buffer PE and bound DNA

was eluted into a microcentrifuge tube in 30 µL Buffer EB (10 mM Tris-Cl, pH 8.5) heated to 65°C.

3.2.9.2 Amplification and RE digestion of replicons

RCA of purified replicons was performed using the illustra™ Templiphi™ DNA Amplification Kit (Cytiva), as per the manufacturer's instructions. Briefly, 0.5 µL of purified DNA was added to a microcentrifuge tube with 5 µL sample buffer and denatured at 95°C for 3min. In a separate tube, a reaction premix was prepared with 5 µL reaction buffer and 0.2 µL enzyme mix. Denatured samples were cooled to room temperature and 5 µL reaction premix was added to the tube. The reactions were incubated at 30°C for 18hr, after which the enzyme was deactivated at 65°C for 10min. For RCA analysis, 5 µL of amplified mE7SH, mZera®E7SH, and mZera®E7SHeGFP DNA was digested with *Hind*III to yield linear products of 5.2, 5.6, and 6.6 kb respectively. Products were electrophoresed and visualised on a 0.8% agarose gel.

3.2.10 Expression analysis of E7SH-based PsVs in mammalian cells

3.2.10.1 Infection and transfection of HEK293TT cells

HEK293TT cells were maintained as described in Chapter 2, section 2.1.4.1, and 24-well plates were seeded at $1x10^5$ cells/mL and incubated overnight as described in Chapter 2, section 2.1.4.2. Purified BPV-1 and HPV-35 PsV sample fractions F8-11 and F4-7, respectively, were prepared for infection by diluting 1:5 in DMEM and added to cells in triplicate at 500 µL/well. Purified PsV fractions and RCA samples were prepared for transfection by adding 30 µL of PsVs and 8 µL RCA DNA to 100 µL DMEM with 2 µL X-tremeGENE™ respectively. Mixtures were incubated at room temperature for 20min and added to cells in triplicate. For the positive controls, 1 µg of pTH-mZera®E7SH (Whitehead et al., 2014), GB-pRIC-mZera®E7SH, and pRIC3-mZera®E7SHeGFP plasmid DNA were transfected as described. The plates of cells were incubated for a further 72hr, after which cells were harvested and processed for protein detection.

3.2.10.2 Harvesting and western blot detection of E7 and eGFP

Supernatants were aspirated from each well and cells were lysed in 200 µL PBP3 buffer (50 mM KCl, 6mM MgCl2, 10 mM EDTA, 0.4 M NaCl, 100 mM Tris, pH 8) supplemented with 0.5% SDS and 200 mM DTT (Torrent et al., 2009). The lysate was transferred to a microcentrifuge tube and 20 µL lysozyme (1 mg/mL, Roche) and 0.5 µL benzonase nuclease (250 units/µL, Sigma-Aldrich) was added (Chabeda, 2017). Samples were incubated for 1hr at room temperature with agitation, after which cell debris was removed by pelleting in a microcentrifuge at 10,000 *x g* for 30min. The resultant supernatants were denatured with 5x SAB at 95°C for 10min and loaded onto 10% SDS-PAGE gels. Western blot analysis was performed as described in Chapter 2, section 2.1.3.2. For detection of E7, blots were probed with a commercially available anti-HPV-16 (E7) mouse monoclonal antibody [TVG 701Y] (AB20191) (1:1000) and anti-mouse IgG as a secondary antibody (1:10,000).

3.3 Results

3.3.1 Generation and confirmation of recombinant E7SH constructs

To prepare HPV-16 E7SH-based DNA constructs for subsequent encapsidation in PV structural proteins using plant-based expression, the mammalian expression cassette containing Zera®E7SH was sub-cloned from the pUC57 maintenance vector and ligated into pRIC 3.0, a plant expression vector. The mammalian cassette comprised of Zera®E7SH under the control of a CMV mammalian promoter and BGH polyadenylation signal. Positive pRIC3-mZera®E7SH clones were confirmed by colony PCR, RE digest, and sequencing (data not shown).

3.3.1.1 pRIC3-mZera®E7SH-eGFP/gLuc/SEAP

To generate mZera®E7SH constructs with reporter genes included downstream of E7SH within the mammalian expression cassette, pRIC3-CMV-Zera®E7SH-BGH plasmid DNA was linearised with *Nco*I/*Sal*I to produce a band of 8.6 kb. A smeared band of >10 kb was observed for digested pRIC3-mZera®E7SH (blue arrow, Figure 3.3). This pattern of migration is likely due to the retardation in mobility of high molecular weight DNA within 1% agarose gels intended for use with smaller DNA sizes (Stellwagen & Stellwagen, 2009). Three primer sets were synthesised for PCR amplification of eGFP, Gaussia-luciferase, and SEAP reporter genes from their respective plasmids (Table 3.1 & 3.2). Bands representing amplified eGFP, Gaussia-luciferase, and SEAP was observed at ~700 bp (green arrow, Figure 3.3), ~500 bp (orange arrow, Figure 3.3) and ~1.5 kb (yellow arrow, Figure 3.3), respectively. As expected, no bands were observed in the negative control lanes. No difference in the yield of amplified DNA was observed between the primer annealing temperatures tested, namely 60°C and 65°C. The 65°C bands were arbitrarily selected for ligation with linearised pRIC3-mZera®E7SH by In-Fusion cloning.

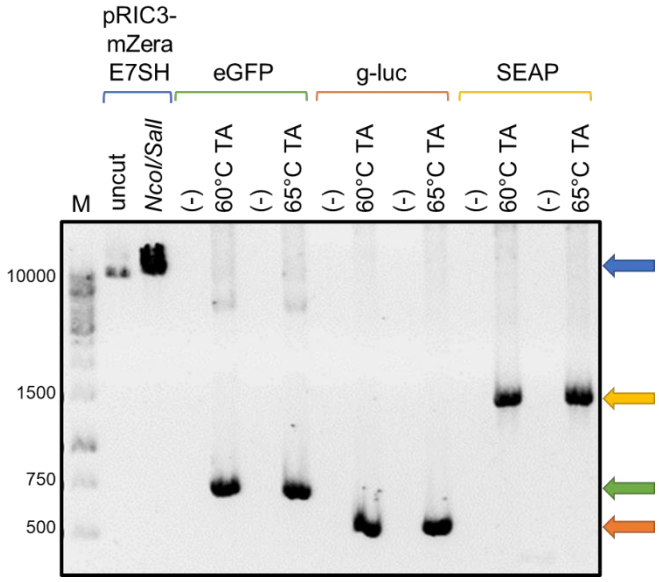

Figure 3.3: RE digestion of pRIC3-CMV-Zera®E7SH-BGH and PCR amplification of reporter gene inserts for In-Fusion Cloning. Labels: M, molecular weight marker (bp); uncut, negative digest control with no REs added; (-), no template DNA negative control; TA, In-Fusion primer annealing temperature; blue arrow, *Nco*I/*Sal*I digested pRIC3-mZera®E7SH (>10 kb); green arrow, amplified eGFP gene (~700 bp); orange arrow, amplified g-luc gene (~500 bp); and yellow arrow, amplified SEAP gene (~1500 bp).

Following ligation and transformation, *E. coli* colonies were screened for positive clones by colony PCR. The expected eGFP, gLuc, and SEAP gene inserts of ~4.5 kb, 4.25 kb, and 5.5 kb were observed after colony PCR (black arrows, Figure 3.4). Bands of ~3.5 kb and ~2 kb were observed for pRIC3-mZEeGFP C6 and pRIC3-mZESEAP colony 14 respectively (white arrows, Figure 3.4), indicating negative clones. Faint bands of >100 bp were observed in the lanes of all 3 constructs (grey arrows, Figure 3.4), indicating the presence of primer dimers. Positive clones of each reporter gene construct were chosen and further confirmed by RE digest and sequencing (data not shown).

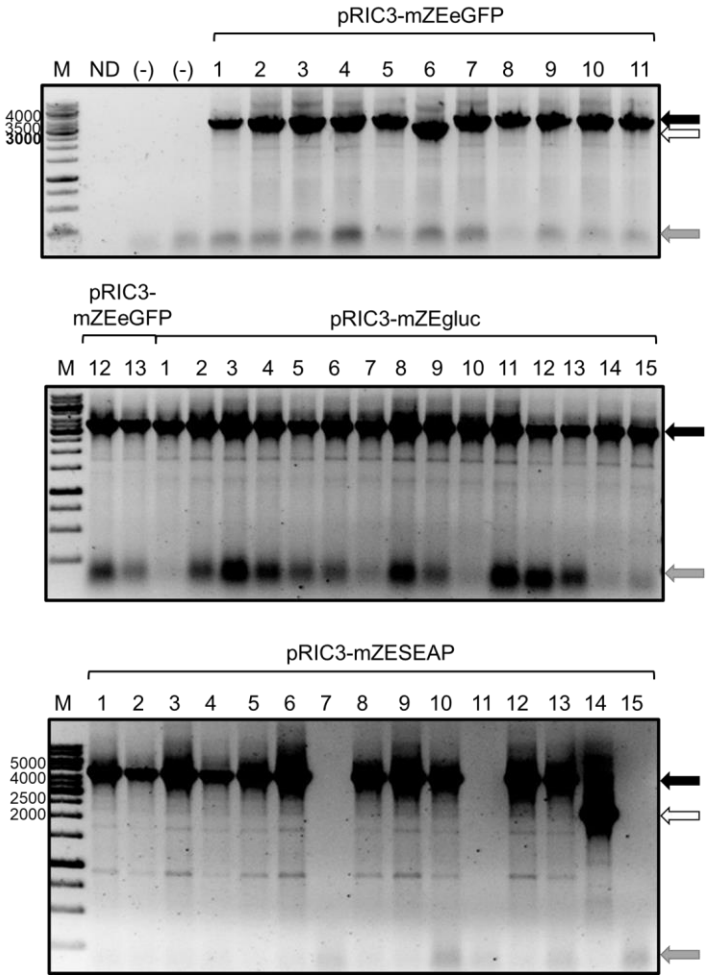

Figure 3.4: Colony PCR confirmation of In-Fusion cloned pRIC-mZera®E7SH reporter constructs in *E. coli*. Colonies were screened with pTRAc primer. Labels: M, molecular weight marker (bp); ND, no template DNA control; (-), no primers control; black arrows, positive pRIC3-mZera®E7SHeGFP (pRIC3-mZEeGFP) (~4.5 kb), pRIC3-mZeraE7SHgluc (pRIC3-mZEgluc) (~4.25 kb), and pRIC3-mZera®E7SHSEAP (pRIC3-mZESEAP) (~5.5 kb) clones; white arrows, negative pRIC3-mZera®E7SH clones; and grey arrow, primer dimers (<100 bp).

3.3.1.2 pRIC3-mE7SH

To assess the effect of Zera® on mammalian expression of E7SH protein, a mE7SH-based construct lacking Zera® was created for comparison with expression of mZera®E7SH. To generate pRIC3-mE7SH, a two-step cloning process with 2 sets of primers was required (Table 3.1). The E7SH gene was amplified from pRIC-mZera®E7SH (1) and pTHZera®E7SH (2) with 5' *Hind*III and 3' *Xba*I RE sites incorporated by PCR and produced bands of ~450 bp (black arrow, Figure 3.5A). To create pTH-mE7SH, pTH plasmid DNA already containing the CMV-BGH mammalian cassette and amplified E7SH were digested with *Hind*III and *Xba*I to produce bands of ~5.9 kb and ~450 bp respectively (black arrows, Figure 3.4B). Following ligation and

E. coli transformation, positive pTH-E7SH clones were confirmed by colony PCR and RE digest (data not shown). Three positive clones were chosen for generation of pRIC3-mE7SH, respectively, to increase the likelihood of successful ligation. CMV-E7SH-BGH was amplified from pTH-E7SH by PCR and an expected band of ~2.3 kb was observed (black arrow, Figure 3.5C). pRIC 3.0 plasmid DNA was digested with *Afl*III/*Xho*I and a linear band of ~5.9 kb was observed (black arrow, Figure 3.5D), after which the vector backbone and mE7SH was joined by In-Fusion cloning.

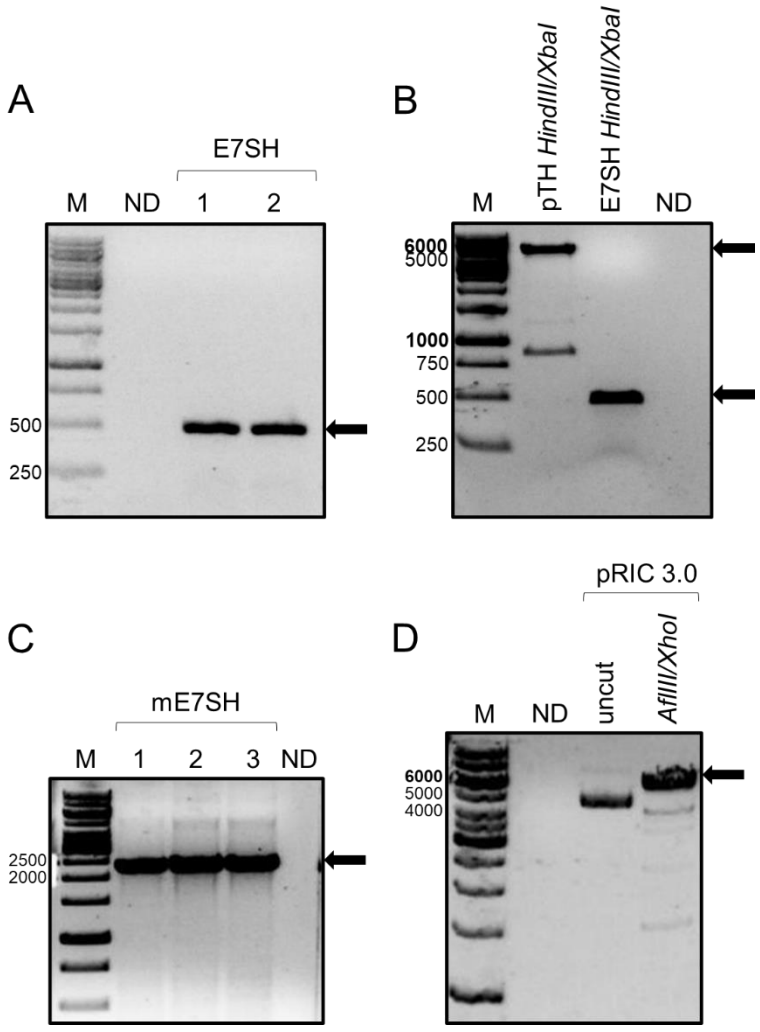

Figure 3.5: PCR amplification of gene inserts and RE digestion of vector backbones for In-Fusion Cloning. A) PCR amplified E7SH gene. 1, E7SH amplified from pRIC3-m Zera®E7SH; 2, E7SH amplified from pTH-mZera®E7SH; and black arrow, E7SH product (~450 bp). **B)** pTH and E7SH digested with *Hind*III/*Xba*I. Black arrows, linearised pTH (~5.9 kb) and digested E7SH (~450 bp). **C)** PCR amplified mE7SH cassette. 1-3, mE7SH amplified from purified pTH-mE7SH clones; and black arrow, mE7SH product (~2.3 kb). **D)** *Afl*III/*Xho*I digested pRIC 3.0. Black arrow, linearised pRIC 3.0 (5.9 kb). Labels: M, molecular weight marker (bp); ND, no template DNA control; and uncut, negative digest control with no REs added.

Colonies were screened for positive pRIC-mE7SH clones by PCR with pTRAc primers (Table 3.1). The expected mE7SH gene insert was observed at ~2.3 kb (black arrow, Figure 3.6). Light bands of >100 bp were observed in the lanes of all 3 constructs (grey arrows, Figure 3.6), indicating primer dimers. Positive clones were further confirmed by RE digest and sequencing (data not shown).

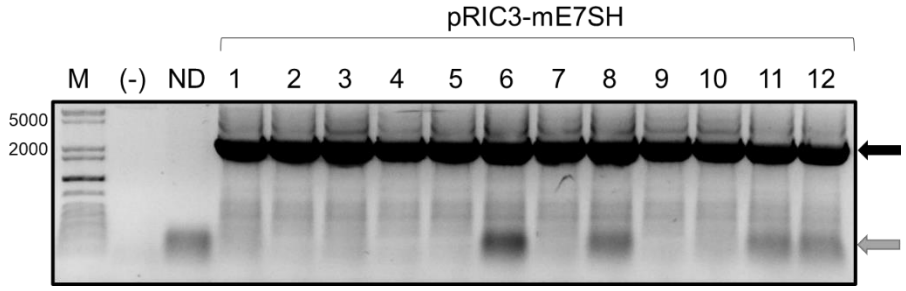

Figure 3.6: Colony PCR confirmation of the In-Fusion cloned pRIC3-mE7SH construct in *E. coli*. Colonies were screened with pTRAc primers. Labels: M, molecular weight marker (bp); (-), no primers control; ND, no template DNA control; black arrow, positive pRIC3-mE7SH (~2.3 kb) clones; and grey arrow, primer dimers (<100 bp).

3.3.2 Confirmation of recombinant constructs in *Agrobacterium*

Recombinant pRIC3-mZeraE7SHeGFP/gLuc/SEAP and pRIC3-mE7SH constructs were electroporated into *A. tumefaciens* strain GV3101::pMP90RK. Colonies were screened by colony PCR. Recombinant *Agrobacterium* colonies containing HPV-35 pTRAc-hL1 and -hL2 from the Biopharming Research Unit culture collection were also screened for confirmation. pRICmZeraE7SH plasmid DNA was included as a positive control (Figure 3.7A). Expected bands of ~1.75 kb (blue rectangle, Figure 3.7A) and ~1.65 kb (purple rectangle, Figure 3.7A) were observed for HPV-35 pTRAc-hL1 and -hL2 respectively. A band of ~4.5 kb was observed for pRIC-mZEeGFP (green arrow, Figure 3.7A). For pRIC-mZEgLuc, a band of ~4.25 kb was observed (orange arrow, Figure 3.7A). For pRIC-mZESEAP, a band of ~5.5 kb was observed (yellow arrow, Figure 3.7A). In Figure 3.7B, bands of ~2.3 kb were observed for pRIC3-mE7SH (black arrows), confirming positive clones. pRIC 3.0 plasmid DNA was included as a negative control with a band of ~250 bp observed (white arrow, Figure 3.7B).

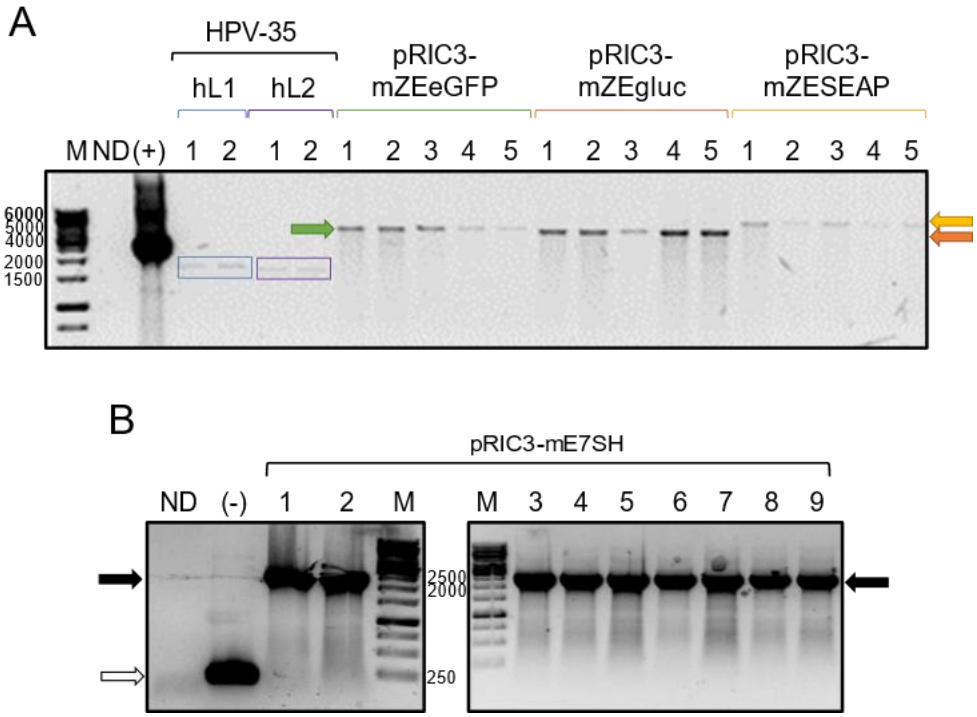

Figure 3.7: Colony PCR confirmation of *Agrobacterium* transformed with In-Fusion cloned recombinants and HPV-35 constructs. A) PCR of HPV-35 pTRAc-hL1 and pTRAc-hL2, and pRIC-mZera®E7SH reporter colonies. (+), purified pRIC-mZera®E7SH DNA (~2.8 kb); blue rectangle, positive HPV-1 hL1 clones (~1.75 kb); purple rectangle, positive HPV-1 hL2 clones (~1.65 kb); green arrow, positive pRIC3-mZera®E7SHeGFP clones (4.5 kb); orange arrow, positive pRIC3-mZera®E7SHgluc clones (4.25 kb); and yellow arrow, pRIC3-mZera®E7SHSEAP clones (5.5 kb). **B)** PCR of *Agrobacterium* transformed pRIC3-mE7SH. (-), purified pRIC 3.0 DNA (~250 bp) indicated by white arrow; and black arrow, positive pRIC3-mE7SH clones (~2.3 kb). Labels: M, molecular weight marker (bp); and ND, no template DNA control.

3.3.3 Purification and L1 expression analysis of BPV-1 and HPV-35 PsVs

To investigate BPV-1 and HPV-35 L1/L2 expression, assembly, and encapsidation of plasmid DNA within a plant-based expression system, *N. benthamiana* plants were co-infiltrated with recombinant *A. tumefaciens* cultures of BPV-1 or HPV-35 pTRAc-hL1/-hL2 with pRIC3-mE7SH, GB-pRIC-mZera®E7SH, or pRIC3-mZera®E7SHeGFP respectively. Due to time and cost constraints associated with the reporter gene assays, the pRIC3-mZera®E7SHgLuc and pRIC3-mZera®E7SHSEAP reporter constructs were excluded from the plant expression studies. For expression of BPV-1 and HPV-35 VLPs, plants were co-infiltrated with pTRA-hL1 and -hL2 recombinant *Agrobacterium* cultures only. The VLPs were produced to serve as a positive L1 expression control in plants and a negative mammalian cell expression control as it did not encapsidate any DNA. The plants across all the groups, except those of the

HPV-35 VLP control, displayed signs of necrosis and chlorosis at day 5 post-infiltration (Figure 3.8), possibly indicating an accumulation of L1 protein. Additionally, severe wilting was observed across the BPV-1 and HPV-35 PsV groups, suggesting early signs of plant death.

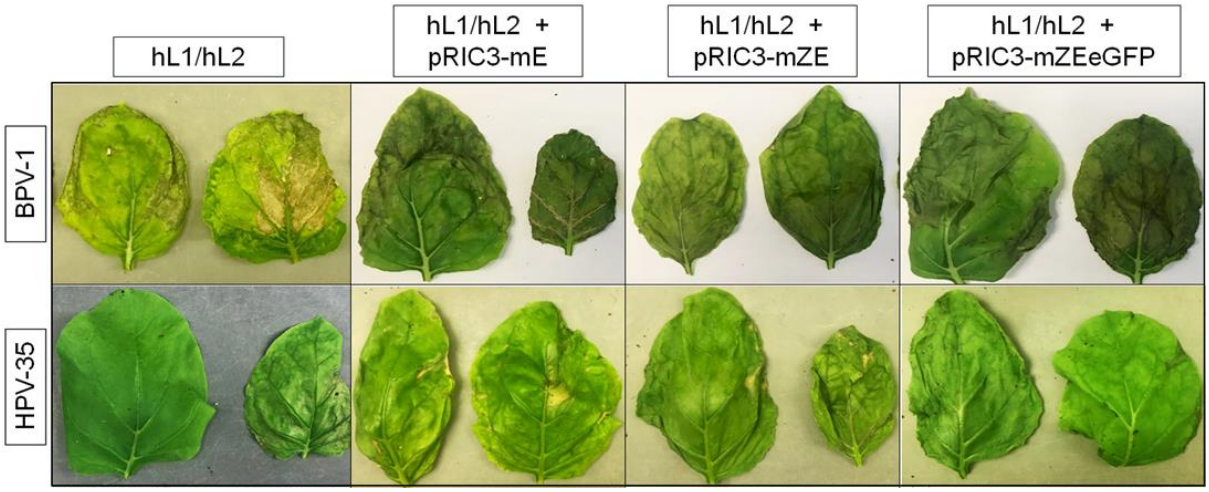

Figure 3.8: Comparison of physiological effects of BPV-1 and HPV-35 PsV production on *N. benthamiana*. Representative samples of leaves indicate differences in physiology of vacuum infiltrated plants co-expressing BPV-1 or HPV-35 pTRAc-hL1/hL2 with pRIC3-mE7SH/-mZera®E7SH/-mZera®E7SHeGFP constructs. Labels: Z, Zera®; and E, E7SH.

BPV-1 and HPV-35 PsVs were extracted and purified in 1x HSPBS, and L1 protein expression was evaluated. Based on dot blot analysis, the strongest L1 signals were observed in fractions 7-12 for all BPV-1 PsV iterations, except for mZEeGFP PsVs where the highest L1 levels were detected in F8-13, and F3-7 for all HPV-35 PsV groups (data not shown). These fractions were selected for further L1 protein analysis by western blotting. Equal volumes of sample were loaded on 10% SDS-PAGE gels and BVP-1 and HPV-35 hL1 proteins (56 kDa) were detected with CAMVIR anti-L1 antibody and H16.J4 Mab respectively (Figure 3.9). BPV-1 VLP F7-12 and HPV-35 VLP F3-6 were loaded as positive controls. A band corresponding to L1 protein was observed at 56 kDa for all BPV-1 PsV groups (blue arrows, Figure 3.9A) with strong signals seen for mE7SH and mZera®E7SH PsVs, possibly indicating a high yield of PsVs in these fractions. A peak in BPV-1 L1 expression was observed in F10 for the VLP control, F8-9 for mE7SH PsVs, F8-10 for mZera®E7SH PsVs, and F10-11 for mZera®E7SHeGFP PsVs. A uniformly distributed L1 band pattern was observed for HPV-35 PsV groups (blue arrows, Figure 3.9B) with no clear peak in protein expression detected. The strongest L1 signal was detected for mZEeGFP PsV

fractions, possibly indicating the highest yield of PsVs in this group. A L1 degradation product was observed at ~52 kDa for all BPV-1 and HPV-35 PsV groups (clear arrows, Figure 3.9). Interestingly, an intense band was detected at 52 kDa for BPV-1 mZEeGFP F8, possibly indicating a high level of L1 protein degradation in this fraction. Additionally, protein smears were detected across PsV groups, possibly indicating high particle stability resulting in incomplete denaturation of the samples prior to blotting.

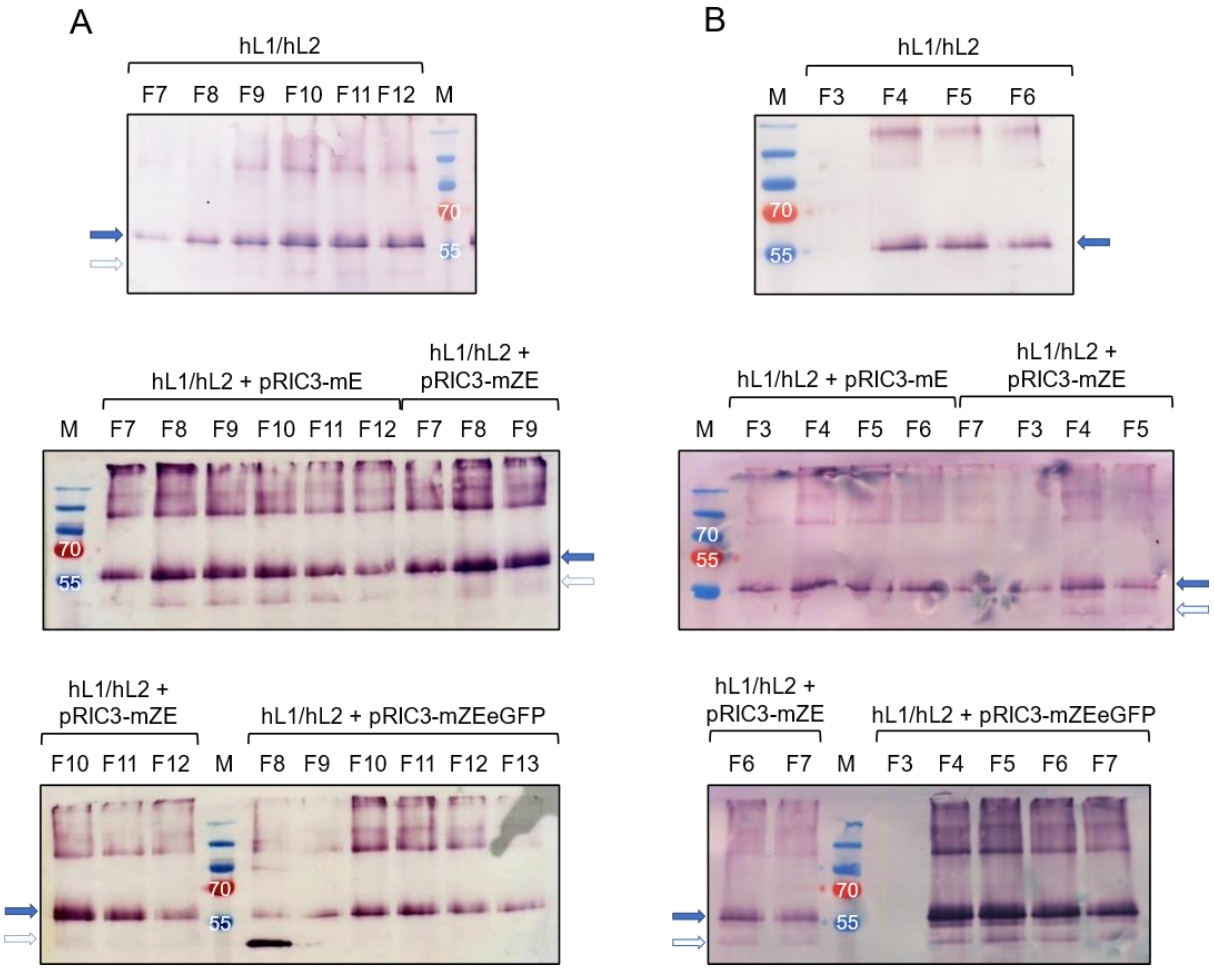

Figure 3.9: Western blot detection of L1 in plant-purified BPV-1 and HPV-35 particles. BPV-1 L1 protein expression is shown in **A)** and HPV-35 L1 expression is shown in **B).** BPV-1 L1 protein (56 kDa) was probed with Camvir anti-L1 antibody (1:1000) and HPV-35 L1 protein (56 kDa) was probed with H16.J14 anti-L1 Mab (1:5000). Labels: M, molecular weight marker (kDa); F3-13, fractions 3 to 13 collected from discontinuous iodixanol gradients; blue arrow, band of interest; and white arrow, degradation product.

3.3.4 TEM analysis of BPV-1 and HPV-35 PsVs

Following successful detection of L1, purified BPV-1 and HPV-35 fractions were assessed for the presence of assembled particles by TEM. Putative BPV-1 PsVs were

observed across the BPV-1 PsV preparations (Figure 3.10, orange boxes). Heterogenous populations of PsVs were observed for BPV mE and mZE F9 and F10, with particles ranging from 40-50 nm in size (yellow arrows). The lowest concentration of BPV-1 particles was observed in the mZEeGFP preparation, possibly due to lowered encapsidation efficiency associated with replicons >6 kb (Adams et al., 2023). The mZEeGFP preparation, however, demonstrated a homogenous population of putative BPV-1 PsVs, with particles 50 nm in size. Structures resembling ~10 nm capsomeres, which appeared to form chains and protein aggregates, as well as VLPs were additionally observed across the BPV-1 preparations.

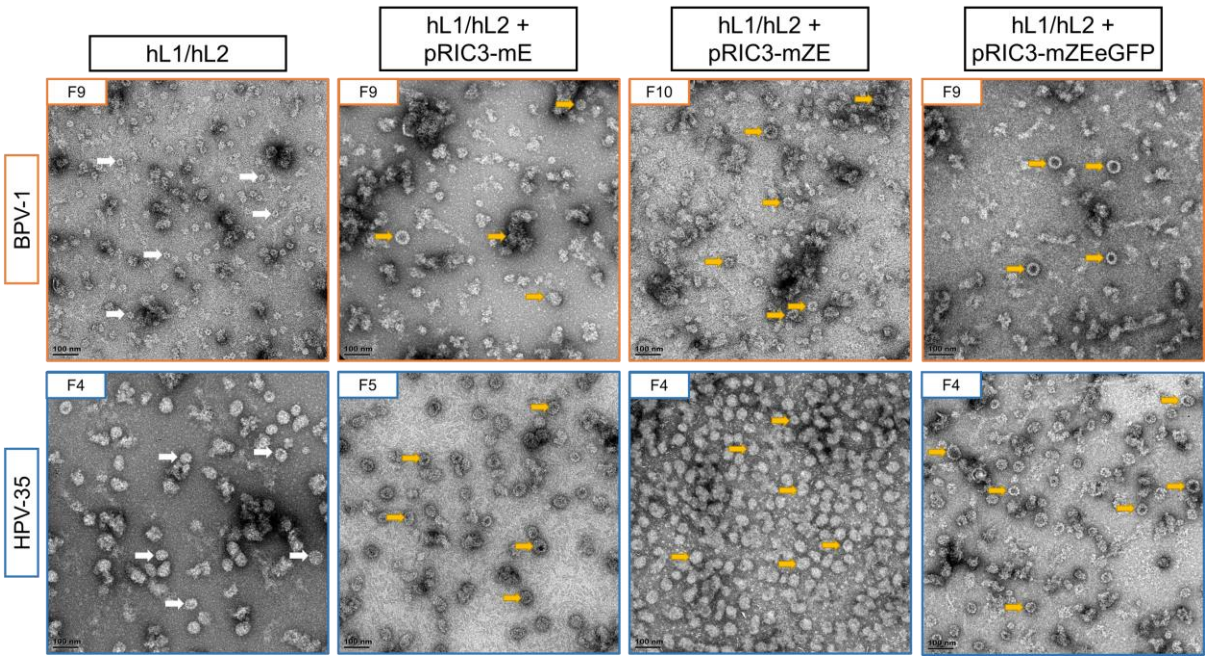

Figure 3.10: Transmission electron micrographs of purified BPV-1 and HPV-35 PsVs. Fractions of BPV-1 and HPV-35 hL1/hL2 + pRIC3-mE7SH/(GB)-mZera®E7SH/-mZera®E7SHeGFP respectively purified on iodixanol gradients in 1x HSPBS buffer. Samples were negatively stained with 2% uranyl acetate. Labels: F4-10, purified BPV-1, and HPV-35 fractions; Z, Zera®; E, E7SH; white arrows, putative T=1 VLPs (HPV-35, 40-60 nm; BPV-1, 20-30 nm); yellow arrows, putative T=7 PsVs (40-60 nm); and scale bar 100 nm.

Particles resembling HPV VLPs and PsVs observed in literature were detected in the HPV-35 fraction preparations (Figure 3.10, blue boxes) (Lamprecht et al., 2016; Shi et al., 2001; Spoden et al., 2013). Putative T=7 PsVs were observed (Figure 3.10, yellow arrows). Relatively homogenous populations of particles ranging in 40-60 nm in size were observed in the HPV-35 mE, mZE, and mZEeGFP preparations, with the highest concentration of particles being detected in mZE F4. Additionally, very few capsomeric

structures were observed in the HPV-35 preparations. Due to the lack of morphological distinctions between HPV VLPs and PsVs, it is unclear whether the particles observed in the PsV fractions are indeed PsVs. Further evaluation of these structures is therefore necessary for particle characterisation.

3.3.5 Confirmation of encapsidated E7SH replicons

PsVs are VLPs capable of packaging plasmid DNA that express a gene of interest. Successful HPV pseudovirion encapsidation of plasmid DNA *in planta* was first demonstrated by Lamprecht et al. (2016) whereby the presence of SEAP was confirmed by inverse PCR following proteinase K digestion of the viral capsids. Here, BPV-1 and HPV-35 PsV fractions were assessed for encapsidated E7SH-based replicons using RCA (Figure 3.11). Prior to RCA screening, PsVs were lysed with a modified lysis treatment in the presence of Proteinase K to release the encapsidated DNA. This optimised treatment was employed as no DNA amplification was observed with use of standard RCA denaturation methods or Proteinase K alone (results not shown). The pRIC3-mE7SH, GB-pRIC-mZera®E7SH, and pRIC3-mZera®E7SHeGFP replicons are 5.2 kb, 4.5 kb, and 6.6 kb in size respectively. Following RCA on lysed fractions, samples were digested with *Hind*III and linearised DNA bands of ~5 kb, ~4.5 kb, and ~6.6 kb corresponding to the size of encapsidated replicons were observed for pRIC3-mE, -mZE and -mZEeGFP respectively (blue arrows). Fragments were present in all fractions, except for BPV-1 mZEeGFP F11, possibly due to loss of DNA during lysis or incomplete lysis. The most intense bands were observed for BPV-1 -mZE F7-9, suggesting a higher concentration of PsVs or more efficient DNA extraction within these fractions. Purified pUC19 DNA was used as a positive RCA reaction control and displayed an expected band of ~2.6 kb (yellow arrows). Bands of >10 kb were observed (green arrows) and represent undigested plasmid DNA.

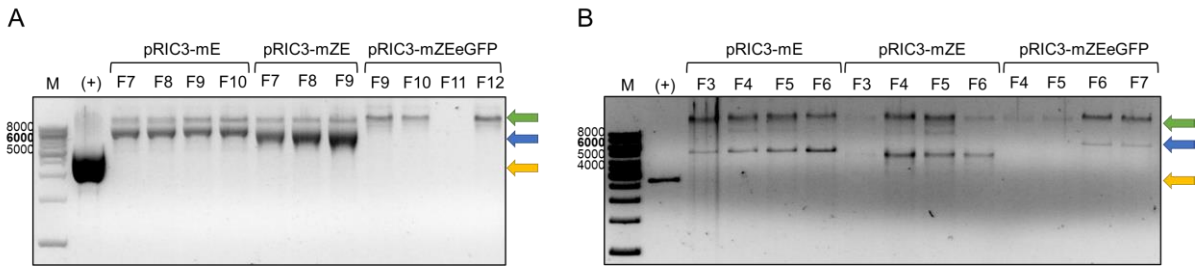

Figure 3.11: Rolling circle amplification of BPV-1 and HPV-35 PsV fractions. Amplification was performed on DNA extracted from **A)** BPV-1 and **B)** HPV-35 fractions run on 0.8% agarose gels after digestion with *Hind*III. Bands of sizes ~5 kb, 4.5 kb, and ~6.6 kb were observed for digested pRIC3-mE7SH, pRIC3-mZera®E7SH and pRIC3-mZera®E7SHeGFP respectively. Labels: M, molecular weight marker (bp); (+) and yellow arrows, positive pUC19 DNA control with an expected band size of 2.6 kb; F3-12, PsV fractions 3-12; green arrow, circular plasmid; and blue arrow, linearised band of interest.

3.3.6 Expression of E7SH PsVs in mammalian cells

To test the ability of plant-made BPV-1 and HPV-35 PsVs to deliver their encapsidated cargo to mammalian cells, HEK293TT cells were infected with PsV fractions confirmed to encapsidate replicons. Additionally, cells were transfected with PsVs and undigested RCA samples to test the ability of the replicons to be expressed as proteins in a mammalian cell system. The original GB-pRIC-mZera®E7SH, pRIC3-mE7SH and pRIC3-mZera®E7SHeGFP plasmids were used as positive transfection controls. Expression of the E7SH-based replicons and positive controls is under control of the mammalian expression cassette containing the CMV promoter and enhancer, and the BGH terminator. Uninfected cells and cells infected with BPV and HPV VLP fractions were used as negative controls. Infected and transfected cells were treated with a SDS and DTT-based lysis buffer 72 hr post-infection, after which cell extracts were resolved on 10% SDS-PAGE gels and proteins were probed with anti-E7SH antibody on western blots (Figure 3.12). In Figure 3.12A, bands corresponding to the E7SH and Zera®E7SH positive controls were observed at 25 kDa (orange arrow) and ~37 kDa (blue arrow) respectively. Although Zera®E7SH is a 29 kDa protein, it has been observed to migrate higher (Chabeda, 2017; Whitehead et al., 2014). No band was observed for the Zera®E7SHeGFP positive control, possibly indicating loss of protein during cell extraction and pelleting. In Figure 3.12B, all positive control bands were observed with E7SH unexpectedly migrating to <25 kDa, Zera®E7SH again migrating to 37 kDa, and Zera®E7SHeGFP migrating to an expected 63.9 kDa. Despite confirmation of DNA encapsidation, no bands indicating protein expression were

detected for cells infected and transfected with BPV and HPV PsVs and RCA products. A negatively developed band was observed across the control and experimental lanes at ~65 kDa (grey arrow). This large protein smear likely corresponds to bovine serum albumin, a 66 kDa protein, with which the 293TT cell growth medium is supplemented.

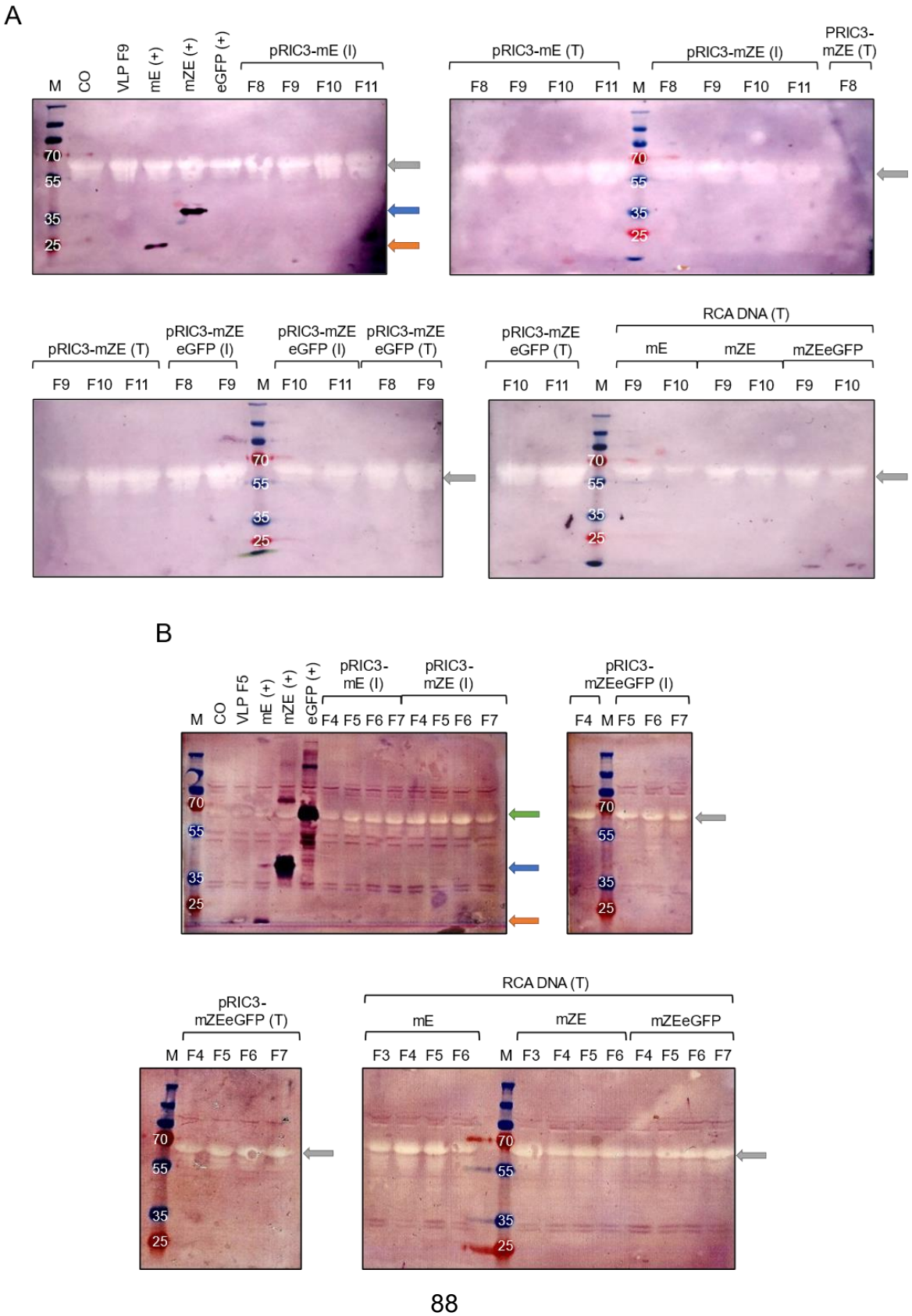

Figure 3.12 (on previous page): Western blot detection of E7SH in HEK293TT cells infected and transfected with BPV-1 and HPV-35 PsVs and RCA samples. Cells were harvested and processed 72hr post-infection/transfection of PsV fractions and RCA DNA. E7SH protein was probed with anti-HPV-16-E7 antibody (1:1000). **A)** BPV-1 PsV and RCA samples. **B)** HPV-35 PsV and RCA samples. Labels: M, molecular weight marker (kDa); CO, cells only control; mE, pRIC3-mE7SH; mZE, GB-pRIC-mZera®E7SH; eGFP, pRIC3-Zera®E7SHeGFP; (+), positive DNA transfection control; F3-11, purified PsV fractions 3 to 11; (I), 293TT infection; (T), 293TT transfection; grey arrow, negative staining (~65 kDa); green arrow, Zera®E7SHeGFP band of interest (63.9 kDa); blue arrow, Zera®E7SH band of interest (37 kDa); and orange arrow, E7SH band of interest (25 kDa).

3.4 Discussion

HPV PsVs have displayed great potential as vehicles for DNA vaccine delivery to several cell types, both *in vitro* and *in vivo* (Ma et al., 2011). HPV PsVs have demonstrated adjuvanting properties and can aid in antigen presenting cell activation and maturation to stimulate both humoral and cellular immune responses (Gurunathan et al., 2000; Peng et al., 2010; Yang et al., 2016). L1 and L2, when co-expressed, can efficiently package heterologous plasmid DNA up to 8 kb in size (Adams et al., 2023; Buck et al., 2004). Previous studies have largely focussed on the use of HPV-16 PsVs for encapsidation and targeting of both homologous and heterologous DNAs to specific cells (Gordon et al., 2012; Graham et al., 2010; Peng et al., 2011; Peng et al., 2010). These studies demonstrate that HPV-16 PsVs can facilitate generation of gene specific T cell responses in animal models. The use of HPV-16 PsVs for gene delivery in humans is limited, however, as a large proportion of the female population has existing immunity to HPV-16 through global vaccination efforts or natural infection with the high-risk PV (Bayer et al., 2018). To address this constraint, studies have investigated the use of non-human PVs for efficient DNA plasmid delivery. PsVs based on *Puma concolor* papillomavirus-1, *Macaca fascicularis* papillomavirus-11, *Mus musculus* papillomavirus-1, BPV-1 and CRPV have been shown to deliver reporter genes efficiently with expression levels rivalling those of HPV-16 *in vivo* (Bayer et al., 2018; Brendle et al., 2021; Handisurya et al., 2012).

While the accepted method for papillomavirus PsV production utilises HEK293TT cells, studies in the laboratory have shown transient protein expression in *N. benthamiana* plants to be an attractive alternative (Lamprecht et al., 2016; Pietersen et al., 2020). The development of DNA replicon systems has largely enabled plant-based production of PsVs (Hefferon, 2017). The pRIC vector (Regnard et al., 2010) is a BeYDV-based autonomously replicating DNA shuttle shown to greatly boost transient protein expression levels in plants (Chabeda, 2017). The vector facilitates continuous replicon formation and replication in plants cells through a rolling circle mechanism (Regnard et al., 2010).

In this study, the pRIC 3.0 vector is the backbone on which In-Fusion technology was applied to generate several recombinant HPV-16 E7SH reporter gene constructs

(Figure 3.1 and 3.2). Reporter genes encoding Gaussia-luciferase, eGFP and mSEAP, respectively, were incorporated into the mammalian expression cassette of Zera®E7SH using In-Fusion cloning (Figure 3.3 and 3.4). Additionally, a pRIC-based E7SH construct lacking Zera® was generated (Figure 3.5 and 3.6). The four E7SH-based pseudogenome constructs were successfully cloned and electroporated into *A. tumefaciens* for transient expression in plants (Figure 3.7). Among the constructs generated, only pRIC3-mE7SH and pRIC3-mZera®E7SHeGFP were selected for use in BPV-1 and HPV-35 PsV production. eGFP has numerous advantages over other reporters for use as a pseudogenome. The auto-fluorescent system is highly sensitive and allows for rapid detection and real time analysis (Ramiro et al., 1998; Rookes & Cahill, 2004). Moreover, detection of eGFP expression is a relatively simple and affordable process (Tang et al., 2009; Zhang et al., 1996).

While L1 expression in plants is sufficient for spontaneous assembly of VLPs, it has been well established that both L1 and L2 are required for effective DNA encapsidation and subsequent PsV formation (Kirnbauer et al., 1993). Co-expression of BPV-1 L1 and L2 showed a 50-fold increase in exogenous DNA packaging compared to L1 expression alone (Zhao et al., 1998). Plant-based expression of L1 and L2 PsVs has been described, wherein human codon-optimised genes showed greater levels of protein accumulation than the wild-type versions (Lamprecht et al., 2016; Maclean et al., 2007). With these findings in mind, PsVs were produced with human codon-optimised sequences encoding L1 and L2 proteins of BPV-1 and HPV-35 respectively. Plants were co-infiltrated with hL1 and hL2, and pRIC constructs harbouring E7SH, Zera®E7SH, and Zera®E7SHeGFP mammalian cassettes respectively. Leaves of plants infiltrated for PsV production were necrotic at 5 days post-infiltration (Figure 3.8), possibly indicating protein degradation. Moreover, these plants were severely wilted compared to the VLP controls, indicating dehydration.

The presence of hL1 in purified BPV-1 and HPV-35 PsV fractions was confirmed by western blotting (Figure 3.9). For both PV types, a band at 56 kDa confirmed successful hL1 expression and purification. The presence of a lower band at ~52 kDa indicates L1 protein degradation likely caused by endogenous plant proteases, of which thousands exist (Jutras et al., 2020). The presence of L2 could not be confirmed as BPV-1 and HPV-35 anti-L2 antibodies were not available.

Purified PsV fractions were next analysed for the presence of assembled L1 and L2 particles by TEM (Figure 3.10). Micrographs of grids trapped with purified BPV-1 and HPV-35 PsV fractions revealed the presence of putative PsVs resembling PV particles previously produced in plants (Cerqueira et al., 2017; Lamprecht et al., 2016; Pietersen et al., 2020). Plant-made BPV-1 and HPV-35 PsVs accumulate within different layers of the discontinuous Optiprep™ gradients on which they are purified. Full HPV-35 capsids (PsVs) have a density of 1.20 g/mL and typically accumulate in fractions 3 - 5 (32% - 36% Optiprep™) (Axis-Shield, 2016; Buck et al., 2006). Assembled BPV-1 particles appear to be more buoyant than their HPV counterparts and, as a result, accumulate between the 27% - 33% Optiprep™ layers, in F8 - F11 (Pietersen et al., 2020; Pyeon et al., 2005). Empty PV capsids (VLPs) display higher densities than their full counterparts (PsVs) within Optiprep™, and, as a result, VLPs typically accumulate below PsVs within the discontinuous gradients (Buck et al., 2004). Previous studies indicate, however, that fully assembled capsids can exist across a range of overlapping densities (Pietersen et al., 2020; Pyeon et al., 2005). Here, HPV-35 PsVs F4 and F5 (Figure 3.10, blue boxes) showed homogenous populations of 40-60 nm particles resembling PsVs. In contrast, BPV-1 PsVs F9 and F10 displayed a heterogenous assortment of structures resembling capsomeric aggregates, 20-30 nm VLPs, and 40-60 nm PsVs (Figure 3.10, orange boxes). Additionally, homogenous populations of VLPs of the expected sizes were observed in HPV-35 and BPV-1 hL1/hL2 fractions 4 and 9 respectively. These results indicate that VLPs accumulated within roughly the same Optiprep™ layers as their corresponding PsVs and, therefore, could not be fully separated from the PsVs during purification. Encapsidation analysis of the PsV fractions imaged with TEM was thus necessary for further PsV classification.

Successful encapsidation of plasmid DNA within HPV PsVs *in planta* was first demonstrated by Lamprecht et al. (2016) whereby the authors used inverse PCR to confirm the presence of SEAP DNA. The authors stated that a Proteinase K treatment prior to DNA amplification was necessary for complete PsV capsid degradation and subsequent pseudogenome release. The authors suggested that the need for this treatment indicated that the particles were highly thermostable and attributed this to the use of a plant expression system. Following this study, Chabeda (2017) used RCA

to assess encapsidation of GB-pRIC-Zera®E7SH DNA within plant-made HPV-16 and HPV-35 PsVs. RCA is an efficient technique for amplification of plasmid DNA templates (Dean et al., 2001; Lizardi et al., 1998). In the present study, RCA was used to investigate the presence of packaged DNA in BPV-1 and HPV-35 PsVs. Initial screening revealed minimal DNA amplification (data not shown). Little improvement was observed following inclusion of a Proteinase K treatment (data not shown). A modified protein denaturation treatment in the presence of Proteinase K was therefore employed to ensure complete lysis of the particle capsids for assessment of DNA encapsidation. RCA was subsequently performed on BPV-1 and HPV-35 pRIC3-mE7SH, -mZeraE7SH, and -mZeraE7SHeGFP PsV fractions (Figure 3.11). Digestion of RCA products with *Hind*III revealed linear fragments corresponding to the expected sizes of the respective E7SH replicons. The presence of these bands confirmed the presence of encapsidated DNA within the plant-produced PsVs. Moreover, the lack of amplification prior to treatment indicates that there was no DNA associated on the outside of the particles. A second band was additionally observed above those of the expected replicon sizes. These bands likely indicate incomplete digestion with *Hind*III due to insufficient incubation time with the restriction enzyme. Although PsV treatment with DNase was not investigated, the data presented here is sufficient to conclude that the plant-made BPV-1 and HPV-35 PsVs packaged the E7SH replicons.

Expression of L1 (Figure 3.9), PsV assembly (Figure 3.10), and encapsidation of E7SH-based replicons (Figure 3.11) was detected for the BPV-1 and HPV-35 fractions investigated. These results suggest that the plant-produced particles observed were indeed PsVs encapsidating the DNA cargo that could be capable of infecting mammalian cells. Expression of Zera®E7SH following HEK293TT infection with plant-made HPV-16 and HPV-35 PsVs has been observed by Chabeda (2017), suggesting that plant-made PsVs are capable of delivering their cargo to mammalian cells. Protein expression levels following PsV infection were extremely low, however, and the author suggests that this indicates a poor yield of PsVs. In the present study, infection of 293TT cells with BPV-1 and HPV-35 PsVs was investigated, and no E7 bands were detected during subsequent western blot analysis (Figure 3.12). Next, transfection of 293TT cells with PsVs in the presence of a DNA transfection reagent was investigated. The reagent used here is liposomal-based and functions by forming positively charged lipid clusters around nucleic acid for efficient entry into host cells through their

phospholipid membranes (Chong et al., 2021; Kim & Eberwine, 2010). Transfection resulted in no E7 bands being observed, indicating that no E7 expression occurred *in vitro* following DNA transfection. The lack of expression observed following PsV transfection could be attributable to the X-tremeGENE™ reagent used which functions by specifically forming complexes with DNA for mammalian cell delivery (Roche, 2020). As PsVs are composed of protein capsids, a protein transfection reagent could be better suited for delivery of PsVs to mammalian cells. However, transfection of RCA products (replicon DNA) into 293TT cells was additionally assessed and, once again, no bands corresponding to E7SH, Zera®E7SH, or Zera®E7SHeGFP were observed on anti-E7 blots (Figure 3.12), due to very low DNA yields. Prior to assaying, quantification of the amplified replicon samples revealed <80 ng of DNA was transfected while a minimum amount of 500 ng DNA is recommended for successful 293TT transfection (Roche, 2020). In contrast, intense bands of 25 kDa, 37 kDa, and 63.9 kDa were observed for GB-pRIC-mZera®E7SH (blue arrows, Figure 3.12), pRIC3-mE7SH (orange arrows, Figure 3.12) and pRIC3-mZera®E7SHeGFP (green arrow, Figure 3.12B), respectively, following 293TT transfection with 1 µg of purified plasmid DNA. The high level of E7 expression observed following plasmid DNA transfection indicates that the plasmid DNA used to form replicons for PsV assembly *in planta* was functional and, additionally, that the DNA transfection reagent worked efficiently. PVs have a highly specified tropism for squamous epithelial cells (Cerqueira & Schiller, 2017). Considering this, the use of HaCaT cells for PsV infection assays was assessed and, as with the 293TT cells, no protein expression was observed on anti-E7 blots (data not shown). As both BPV and HPV are organotropic, the use of HeLa, CaSki and NIKS cell lines could additionally be explored for assessment of PsV infectivity (De Gregorio et al., 2020). For successful PsV infection of mammalian cells, proteolysis of L2 by furin at the cell membrane is essential (Day et al., 2004; Peng et al., 2010). In this study, the presence of L2 in the plant-made PsVs could not be directly confirmed. It is well established, however, that L2 is required for packaging of DNA within PsVs (Buck et al., 2004; Day & Schiller, 2009; Roden et al., 2000). Encapsidation of E7SH-based replicons was confirmed (Figure 3.11), suggesting L2 is integrated into the PsVs. Furthermore, sequence alignment confirmed the presence of furin cleavage sites within the BPV-1 and HPV-35 *L2* sequences (data not shown).

From data presented here, plant-produced BPV-1 and HPV-35 L1 and L2 are capable of encapsidating plasmid DNA to form highly stable particles that should be proficient at infecting mammalian cells. The lack of E7SH expression observed following HEK293TT infection and transfection of PsVs and replicons could therefore indicate a low yield of plant-produced PsVs. Alternatively, the plant-derived PsVs may lack features essential for successful mammalian cell infection. Additional analysis of these particles is necessary to elucidate whether the lack of expression observed here is due to low yield alone or additionally impacted by poor infectivity.

4 Chapter 4: Plant versus mammalian cell-produced pseudovirions

4.1 Introduction

Despite the development of alternative expression systems, mammalian cell-based systems continue to dominate the commercial biopharmaceutical market. Between 2018 and 2022, 85% of the novel recombinant proteins approved for human use were produced in mammalian systems (Walsh & Walsh, 2022). The ‘gold standard’ of high-titre papillomavirus PsV production involves the use of a mammalian expression system (Lamprecht et al., 2016). Buck et al. (2004) developed a method for intracellular PsV production utilising HEK293TT cells. While this production system is effective, robust, and allows for post-translational modifications, it is also a cost-intensive and time-consuming system with complex cell growth requirements and a relatively high risk of contamination (Daniell et al., 2009; Lamprecht et al., 2016; Marsian & Lomonossoff, 2016; Sohrab et al., 2017). The construction and scaling-up of manufacturing facilities also require a large capital investment ("GAVI injects new life into HPV vaccine rollout," 2013; Lai & Chen, 2012). These factors particularly limit the use of mammalian cell-based expression in developing countries and drive the need for development of more cost-effective, scalable, and efficient protein expression alternatives (Chen & Lai, 2013; "GAVI injects new life into HPV vaccine rollout," 2013).

The final research chapter of this study describes a comparative analysis of plant-produced BPV-1 and HPV-35 PsVs (pPsVs) containing mSEAP replicons versus mammalian cell-produced BPV-1 and HPV-35 PsVs (mPsVs) containing YSEAP replicons. This involved the production of BPV-1 hL1/hL2 or HPV-35 hL1/hL2 structural proteins encapsidating a SEAP reporter plasmid in (1) *N. benthamiana* plants and (2) HEK293TT mammalian cells. Protein expression, encapsidation, and gene delivery analyses were performed to elucidate the lack of expression following mammalian cell infection and transfection with plant-produced BPV-1 and HPV-35 pPsVs containing Zera®E7SH in Chapter 3.

4.2 Materials and methods

4.2.1 Production of BPV-1 and HPV-35 PsVs in *N. benthamiana*

Co-infiltration of plants with recombinant *Agrobacterium* suspensions containing BPV-1 pTRAC-hL1 and hL2 or HPV-35 pTRAc hL1 and hL2 with pRIC3-mSEAP was carried out as described in Chapter 3, section 3.1.7. Cell cultures were mixed as follows: hL1 at OD_{600} 0.25, hL2 at OD_{600} 0.05, and pRIC3-mSEAP at OD_{600} 0.70 with a total OD_{600} of 1.00. Infiltrated plants were incubated for 5 days at 22°C under 16hr light: 8hr dark cycles.

4.2.2 Extraction and purification of plant-produced PsVs

Extraction and purification of BPV-1 and HPV-35 PsVs from frozen leaf material was performed using a 30/50% sucrose cushion and discontinuous Optiprep™ gradient as described in Chapter 3, section 3.1.8. Samples were collected in 1 mL fractions from the bottom of the tube and stored at -80°C for head-to-head analysis with mammalian cell-produced PsVs.

4.2.3 Pseudovirion production in mammalian cells

BPV-1 and HPV-35 PsVs were produced according to a protocol developed by Buck, Pastrana, et al. (2005) and described in *Production of Papillomaviral Vectors (Pseudoviruses)*, revised June 2015 (Laboratory of Cellular Oncology, https://home.ccr.cancer.gov/lco/pseudovirusproduction.htm). Plasmid DNA encoding L1 and L2 of BPV-1 (Buck et al., 2004), HPV-35 (Draper et al., 2011), and pYSEAP (Pastrana et al., 2004) was prepared using the E.Z.N.A.® Endo-Free Plasmid DNA Maxi Kit (Omega Bio-Tek) as per the manufacturer's instructions. The pYSEAP vector contains a mammalian expression cassette under the control of the EF-1α promoter and the SV40 polyadenylation signal. The cassette is identical to that of mSEAP (Kennedy, 2013). Names and associated antibiotic resistance of plasmids are shown in Table 4.1.

Table 4.1: Plasmids used to make mPsVs

Plasmid	PV type	Gene	Antibiotic resistance
p1sheLL	BPV-1	L1 & L2	Kanamycin (30 µg/mL)
p35sheLL	HPV-35	L1 & L2	Ampicillin (100 µg/mL)
pYSEAP	n/a	SEAP	Blasticidin (75 µg/mL)

4.2.3.1 Transfection of HEK293TT cells

HEK293TT cells were maintained in cDMEM and incubated at 37°C with 5% CO_2 as described in Chapter 2, section 2.1.4.1. Cells were seeded into 4x T75 flasks per PV type and grown to 50-70% confluency. Each flask was transfected as follows: 19 µg PV plasmid and 19 µg pYSEAP were mixed in 2 mL serum-free DMEM (A), and 80 µL Xtreme-GENE™ was added to 2 mL DMEM (B). (A) and (B) were incubated at room temperature for 20min, combined, and incubated for a further 20min. The resulting mixture was added to the flask and cells were incubated with the DNA/lipid complexes overnight at 37°C. The following day, the media was replaced with cDMEM and cells were incubated for a further 30hr.

4.2.3.2 Harvesting and maturation of PsVs

To harvest cells, culture medium was transferred to a 50 mL sterile tube, and cells adhered to the flask were trypsinised (0.05% Trypsin-EDTA, Gibco) and added to the tube. Cells were pelleted by centrifugation at 2000 *x g* for 3min and the supernatant was discarded. The pellet was resuspended in 500 µL 1x Dulbecco's PBS (DPBS) (Sigma-Aldrich) and transferred to a 1.5 mL siliconized microcentrifuge tube. The 50 mL tube was rinsed with a further 500 µL DPBS. This was added to the cell suspension, after which the cells were centrifuged, and the supernatant discarded.

For PsV maturation, the pelleted cells were partially resuspended by flicking the microcentrifuge tube, after which 1.5x cell pellet volume of DPBS supplemented with 1x Antibiotic-Antimycotic (Gibco) and 9.5 mM $MgCl_2$ was added. The pellet was further resuspended by flicking, after which cells were lysed in 1/20th pellet volume of 10% Triton X-100 (Sigma-Aldrich), 1/1000th volume RNase mix (Invitrogen), and 1/40th ammonium sulphate (pH 9). The lysate was incubated for 24hr at 37°C and mixed by

gentle inversion twice within the first 3hr. Following maturation, the lysate was chilled on ice and centrifuged at 5000 *x g* for 5min at 4°C. The clarified supernatant was transferred to a siliconized tube and the remaining pellet was washed in 2x pellet volumes of DPBS and further centrifuged. The wash supernatant was combined with the original supernatant and the remaining pellet was vigorously resuspended in 1 volume DPBS and frozen in liquid nitrogen. The suspension was then thawed and re-centrifuged, after which the supernatant was combined with the previous supernatants. The pooled supernatants were re-clarified by centrifugation, and subsequently transferred to a siliconized tube, the remaining pellet was washed in HSPBS (0.8 M NaCl, 1x DPBS, pH 7.4) and re-centrifuged. The supernatant was then added to the pooled supernatants and used for PsV purification.

4.2.3.3 Purification of PsVs

PsVs were purified by ultracentrifugation on discontinuous iodixanol gradients of 27%, 33%, and 39%. Gradients were prepared in HSPBS, under-layered in ultracentrifuge tubes, and left to diffuse for 1hr. The clarified supernatant was over-layered onto the gradients and centrifuged at 234 000 *x g* in a SW 55 Ti rotor (Beckman Coulter Inc.) for 3.5hr at 16°C. Following purification, the bottom of the tube was punctured with a 21-gauge needle and fractions were collected in siliconized tubes as follows: 750 µL in fraction 1, 250 µL in fractions 2-10, and 1 mL in fractions 11-12. Following collection, purified fractions were analysed on dot blots.

4.2.4 Analysis of purified PsVs on dot blots and with TEM

Purified fractions of plant PsVs (pPsVs) and mammalian-produced PsVs (mPsVs) were analysed on dot blots for the presence of L1 and particles were visualised using TEM as described in Chapter 2, section 2.1.3. BPV-1 L1 was probed with BPV-1/1H8 + CAMVIR (1:1000) and HPV-35 was probed with H16.J4 MAb (1:5000). Following hL1 detection, fractions with the highest L1 signals were trapped on grids and negatively stained with uranyl acetate for visualisation with TEM.

4.2.5 Reporter gene encapsidation analysis

BPV-1 and HPV-35 PsVs expressed in *N. benthamiana* and HEK293TT cells were lysed and assayed for the presence of SEAP DNA as described in Chapter 3, section

3.1.9. Pseudogenomes were extracted from PsVs in the presence of Proteinase K and purified DNA was eluted in 30 µL Buffer EB heated to 65°C. Plasmids were amplified by RCA overnight at 30°C, after which the enzyme mix was inactivated at 65°C for 10min. Following this, 5 µL of amplified SEAP DNA was linearised by RE digestion with *Hind*III and subsequently resolved and visualised on a 0.8% agarose gel.

4.2.6 SEAP expression analysis in mammalian cells

HEK293TT cells were maintained as described in Chapter 2, section 2.1.4.1. Three 24-well plates were seeded at $1x10^5$ cells/mL and incubated overnight. For infection of cells, selected fractions of BPV-1 and HPV-35 pPsVs and mPsVs were diluted 1:4 in DMEM and added to cells in triplicate at 500 µL/well. The PsV samples described were prepared for DNA transfection by diluting samples 1:3 in 100 µL DMEM in the presence of X-tremeGENE™ as described in Chapter 3, section 3.1.10.1. For preparation of PsVs for protein transfection, 30 µL of each fraction was added to 100 µL DMEM supplemented with 1.25 µL of the Proteo™Juice™ Protein Transfection Reagent (Sigma-Aldrich) respectively. The protein/lipid mixtures were incubated for 20min and added to cells in triplicate. For preparation of positive expression controls, 1 µg of pYSEAP plasmid DNA was transfected with X-tremeGENE™ and ProteoJuice™ respectively, as described. Cells were then incubated at 37°C for a further 72hr, after which the cell supernatants were assayed for SEAP activity using the Great EscAPe™ kit as described in Chapter 2, section 2.1.4.3. Following this, SEAP signal was detected with a GloMax® 20/20 Luminometer.

4.3 Results

4.3.1 Purification of plant- and mammalian cell-made SEAP PsVs

Both *N. benthamiana*- and HEK293TT-produced particles were purified on discontinuous Optiprep™ gradients, and fractions were collected and subsequently screened for the presence of hL1 on dot blots (Figure 4.1).

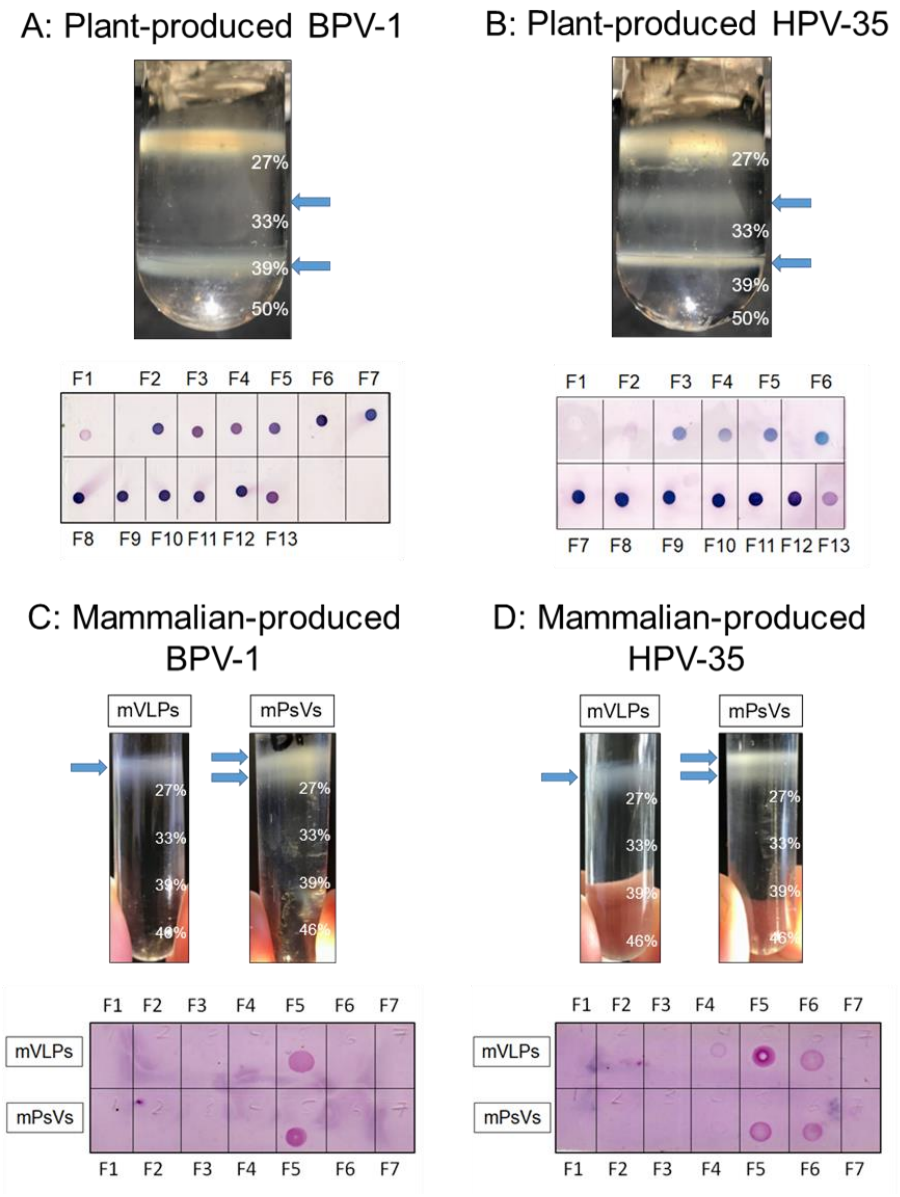

Figure 4.1: Discontinuous gradients and corresponding dot blots for plant and mammalian cell-produced proteins. Purification of BPV-1 and HPV-35 PsVs was performed in 1x HSPBS Optiprep™ gradients. BPV-1 L1 was probed with Camvir anti-L1 antibody (1:1000) and HPV-35 L1 was probed with H16.J14 anti-L1 Mab (1:5000). **A)** Purification and detection of BPV-1 pPsVs from *N. benthamiana*, **B)** Purification and detection of HPV-35 pPsVs from *N. benthamiana*, **C)** Purification and detection of BPV-1 mVLP and mPsV samples from HEK293TT cells, and **D)** Purification and detection of HPV-35 mVLP and mPsV samples from HEK293TT cells. Labels: F1-13, purified fractions 1-13; and blue arrows, opaque bands observed.

Upon visual inspection of the gradient for plant-made BPV-1 pPsVs after centrifugation, two opaque bands were observed at the 27%/33% and 33%/39% interfaces (blue arrows, Figure 4.1A). The corresponding dot blot revealed an intense L1 signal distributed across fractions 2-13 that was readily detected upon the addition of substrate. Despite a less opaque band observed at the 27%/33% Optiprep™ boundary, the highest level of BPV-1 L1 protein was detected in the fractions corresponding to the interface, namely fractions 8-10, as expected. A strong L1 signal was also observed in F6. Two opaque bands were similarly observed at the 27%/33% and 33%/39% interfaces for plant-made HPV-35 pPsVs (blue arrows, Figure 4.1B). The band at the 33/39% interface, corresponding to fractions 3-5, was observed to be the most prominent of the two. HPV-35 L1 protein was readily detected in F3-13 with a peak in the signal uniformly observed across F7-12.

Comparative results were observed between the 27→46% discontinuous gradients of 293TT-produced BPV-1 and HPV-35 particles (Figure 4.1C and D). Upon visual inspection of the mVLP purifications, a single opaque band was observed above the 27% gradient. Within the mPsV gradients, however, two opaque bands were observed (blue arrows). This could indicate the presence of both a VLP and PsV population in the mPsV purifications, spatially separated by the differences in densities between empty and full capsids (Buck, Pastrana, et al., 2005). Following fraction collection, L1 protein was singularly detected in BPV F5 for both mVLPs and mPsVs (Figure 4.1C). For HPV, L1 was observed in F5 and F6 with a stronger signal detected in F5 (Figure 4.1D). To ensure the maximum amount of PsVs, fractions 5 and 6 of HPV-35 were pooled for further analysis.

4.3.2 Confirmation of PsVs encapsidating SEAP

Following confirmation of L1 expression on dot blots, purified BPV and HPV pPsVs and mPsV fractions were screened for encapsidated SEAP DNA by RCA, followed by digestion with *Hind*III and visualisation on agarose gels (Figure 4.2). The mSEAP and pYSEAP replicons are 4.8 kb and 5.3 kb in size, respectively. Purified pUC19 DNA was used as a positive RCA reaction control with an expected band of ~2.6 kb observed (orange arrows). Bands of ~5 kb were observed for HPV pPsV F4 and BPV pPsV F9 with faint bands observed for HPV pPsV F3 (blue arrows, Figure 4.2A),

indicating the presence of SEAP replicons within these samples. The localisation of DNA in these fractions suggests that the plant-made BPV and HPV PsVs were densely compacted at the 27/33% and 33/39% Optiprep™ gradients, respectively. Bands of >10 kb were additionally observed (green arrows) and likely represent undigested replicon DNA. TEM analysis of HPV fraction 4 showed a heterogenous population of particles varying in shape and ranging from 40-50 nm in size, likely indicating a combination of T=1 VLPs and T=7 PsVs. Additionally, 10 nm capsomers and protein aggregates were observed. The micrograph of BPV fraction 9 showed a low yield of 50-60 nm putative T=7 PsVs (yellow arrows, Figure 4.2A). Many 30 nm particles were observed, indicating the presence of T=1 VLPs.

In Figure 4.2B, faint DNA bands of ~5-5.5 kb in size were observed in the lanes corresponding to BPV-1 and HPV-35 mammalian-produced PsV F5, respectively, following RCA and *Hind*III digestion. These bands indicate the presence of pYSEAP replicons within the mPsV fractions. Additionally, dark bands of >10 kb were observed in these lanes (green arrow, Figure 4.2B), likely indicating the presence of undigested products. As expected, no bands were detected for the empty mVLPs. A low concentration of structures resembling PsVs were observed in the TEM micrographs corresponding to BPV and HPV F5 (yellow arrows, Figure 4.2B).

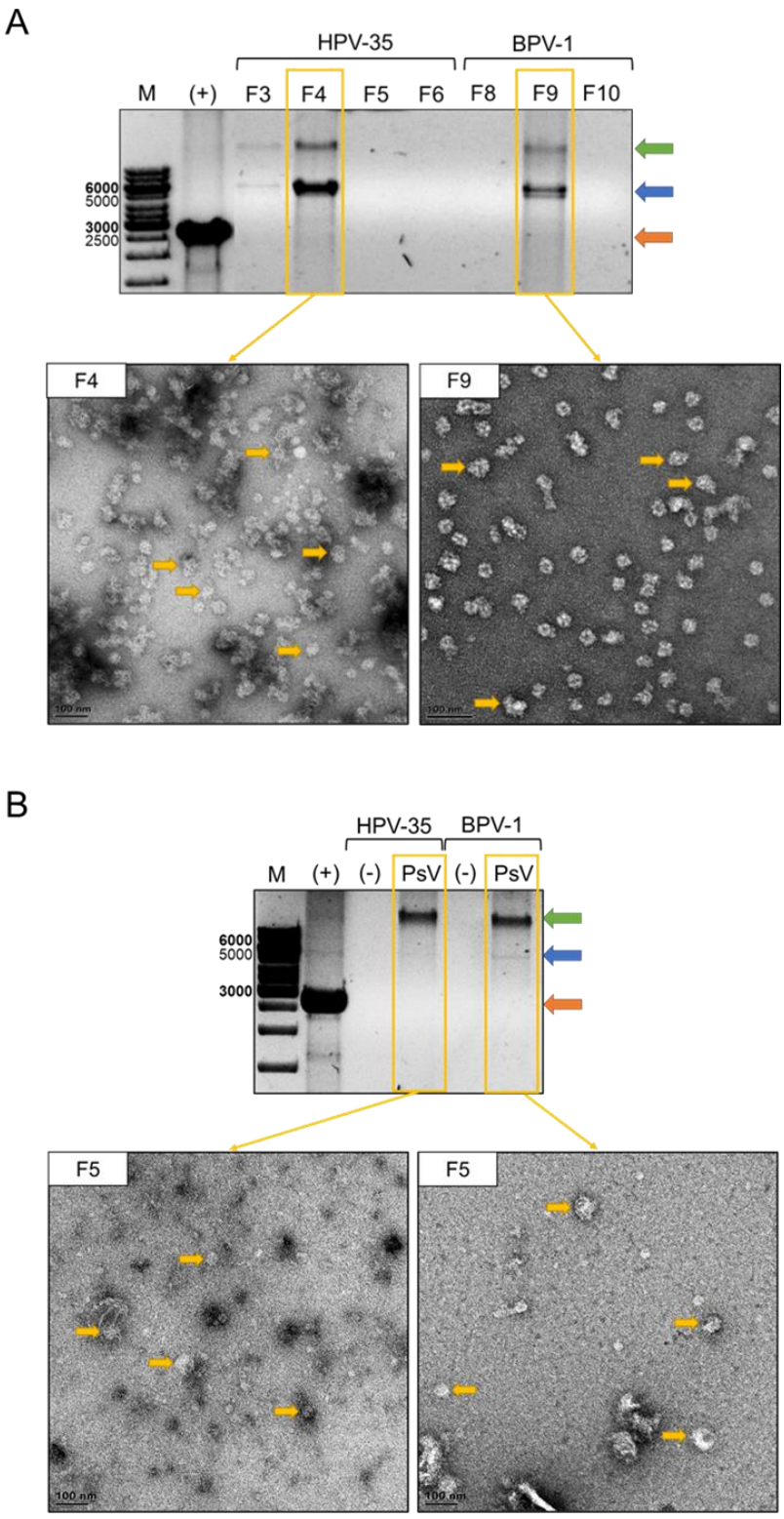

Figure 4.2: RCA of SEAP DNA from plant- and mammalian-produced BPV-1 and HPV-35 PsV fractions, and corresponding TEM images. Replicon presence was confirmed on 0.8% agarose gels following HindIII digestion. **A)** BPV and HPV pPsV fractions purified from N. benthamiana. F3-6 and F8-10, PsV fractions of interest. **B)** BPV and HPV mPsV samples purified from HEK293TT cells. (-), VLP fraction 5; and F5, fraction 5. Labels: M, molecular weight marker (bp); (+) and orange arrow, positive pUC19 DNA control with a band size of 2.6 kb; green arrow, circular plasmid; and blue arrow, linearised band of interest; yellow arrows, putative T=7 PsVs (40-60 nm); and scale bar, 100 nm.

4.3.3 Expression of SEAP in HEK293TT cells

To determine if PsVs could deliver their encapsidated pseudogenome into mammalian cells, HEK293TT cells were infected and transfected with plant-made and 293TT-made PsV fractions shown to successfully encapsidate SEAP DNA (Figure 4.3). Both DNA and protein transfection reagents were investigated to determine whether either reagent was effective at promoting receptor-mediated uptake of PsVs into mammalian cells. The pYSEAP plasmid was used as a positive transfection control and uninfected cells were used as a negative control for the assay. Cell supernatants were assayed for SEAP luminescence in triplicate 72 hr post-infection and transfection. Error bars indicate the standard deviation between the technical repeats. Signals were detected for the positive control (red bars) as well as for the 293TT-produced BPV-1 PsVs (yellow bars) and 293TT-produced HPV-35 PsVs (black bars). Across all conditions, SEAP signals observed for HPV mPsV F5 were at least two-fold that of BPV mPsV F5. This result suggests that either the HPV fraction contains a higher number of functional mPsVs or that the HPV PsVs deliver their cargo to cells more efficiently than those of BPV-1. Transfection of cells in the presence of transfection reagents resulted in very little difference in SEAP expression levels being observed. This suggests that mammalian-produced BPV and HPV PsVs infect cells effectively with no need for the inclusion of a transfection reagent. No SEAP signals were detected in 293TT cells following infection with plant-produced PsVs (Figure 4.3A). Additionally, no improvement in reporter gene expression was observed for cells transfected with pPsVs in the presence of a DNA or protein transfection reagent (Figure 4.3B and C). This lack of SEAP expression associated with both plant-based BPV and HPV PsVs could be indicative of poor PsV assembly and/or yield.

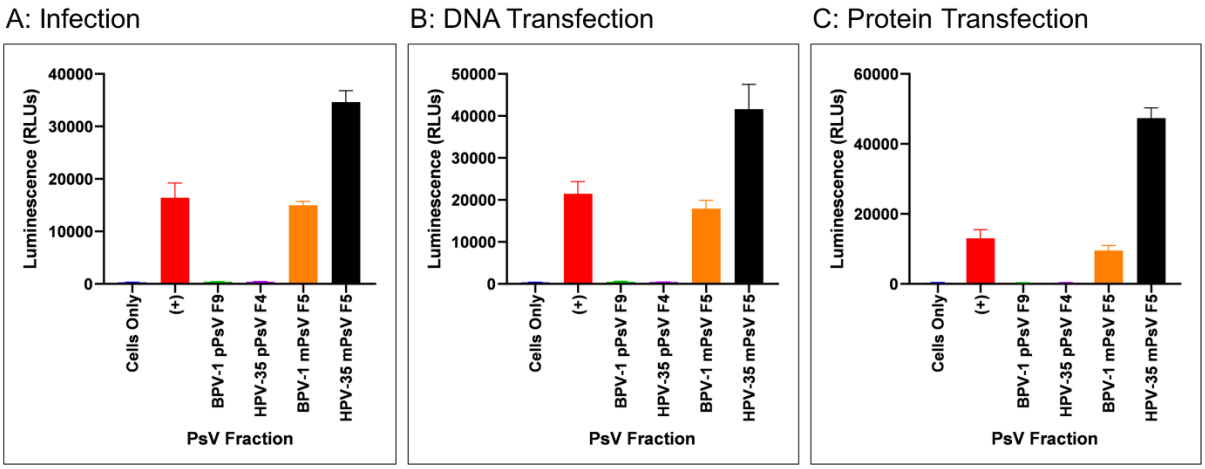

Figure 4.3: SEAP assays of plant- and mammalian cell-produced BPV-1 and HPV-35 PsVs. SEAP expression of cells **A)** infected with PsVs, **B)** transfected with PsVs in the presence of DNA transfection reagent, and **C)** transfected with PsVs in the presence of protein transfection reagent is indicated by luminescence measured in relative light units (RLUs). Labels: (+), positive SEAP expression control; pPsV, plant-produced PsVs; and mPsV, mammalian cell-produced PsVs.

4.4 Discussion

Over the last three decades, plant-based expression systems have shown great promise in the production of recombinant proteins. However, despite boasting benefits of cost efficiency and rapid scalability, mammalian cell-based expression systems continue to dominate commercial vaccine development and papillomavirus research (Moon et al., 2019; Rybicki, 2009). The HEK293TT cell line is a popular choice for recombinant protein expression due to its high transfectability, rapid growth, and strong reproducibility (Buck, Pastrana, et al., 2005; Thomas & Smart, 2005). Following the development of a straightforward HEK293TT transfection method by Buck et al. (2004), the cell line has been used extensively as a tool to generate high titres of highly immunogenic papillomavirus PsVs (Buck, Pastrana, et al., 2005; Graham et al., 2010; Kines et al., 2015; Pastrana et al., 2004). The PsV production strategy involves transfection of 293TT cells with plasmids containing a bicistronic plasmid encoding L1 and L2 genes, and a reporter plasmid encoding SEAP (pYSEAP) (Buck et al., 2004). The authors state that incorporation of both *l1* and *l2* genes within a single ORF on the same plasmid (pSheLL) allows for optimal co-expression of the capsid proteins. Additionally, the authors show that the use of human codon optimised L1- and L2-encoding genes resulted in maximised capsid protein accumulation. Furthermore, the authors demonstrate that inclusion of a SV40 ori in the reporter plasmid allows for the high-level vector replication necessary for efficacious pseudogenome encapsidation. As the HEK293TT-based expression system is the 'gold standard' of PsV production, we utilised it in this study for a head-to-head comparison of papillomavirus PsV production in mammalian cells versus plants. To produce mammalian cell-based BPV-1 and HPV-35 PsVs with SEAP plasmids encapsidated, 293TT cells were co-transfected with human codon-optimised L1/L2-encoding plasmid pSheLL and reporter gene-transfer vector pYSEAP. For production of the plant-based PsVs with SEAP replicons encapsidated, *N. benthamiana* plants were co-infiltrated with human codon-optimised L1 and L2, and replicon-generating mSEAP.

Efficient purification of both plant- and mammalian cell-produced papillomavirus PsV stocks is accomplished through density gradient ultracentrifugation with Optiprep™. Following ultracentrifugation, a yellow-green band was observed above the 27% Optiprep™ layer of both plant-purified gradients (Figure 4.1A and B), showing

successful separation of plant proteins from the BPV-1 and HPV-35 PsVs. Dot blots confirmed the presence of L1 in the plant-purified PsV samples. Visual analysis of the mammalian cell-purified PsV gradients showed two distinct bands above the 27% Optiprep™ gradient (blue arrows, Figure 4.1C and D), indicating the presence of two populations of particles. The density of 293TT-purified PsVs in Optiprep™ is lower than that of empty VLPs (Buck, Pastrana, et al., 2005). The lower band observed here therefore represents a VLP population while the higher band represents PsVs. Although the particle populations existed separately in Optiprep™, they could not be fully separated by fractionation as L1 signals were observed in a single fraction (F5) on BPV-1 dot blots (Figure 4.1C). L1 signals were additionally observed on HPV-35 F5 and F6 blots (Figure 4.1D). While it is possible these samples contained the two separated VLP and PsV populations, it is unlikely that complete separation occurred during fractionation. Fractions 5 and 6 were therefore pooled to ensure the highest number of PsVs possible.

The encapsidation of SEAP DNA into BPV-1 and HPV-35 PsVs was assessed by RCA (Figure 4.2). PsV fractions were prepared for RCA with a modified lysis treatment to ensure complete denaturation of the capsid for the release of encapsidated DNA. Figure 4.2A shows F3-6 and F8-10 of plant-made HPV-35 and BPV-1 PsV samples respectively. Digestion of RCA products with *Hind*III showed linear fragments of 5 kb for HPV-35 fraction 4 and BPV-1 fraction 9 (blue arrow). Additionally, faint bands of 5.5 kb were observed for mammalian cell-produced HPV-35 and BPV-1 PsV samples following linearisation with *Hind*III (blue arrow, Figure 4.2B). These bands of expected sizes confirm the presence of encapsidated DNA within the plant- and HEK293TT-made samples. The presence of dark bands of >10 kb across these samples represents undigested DNA, indicating incomplete digestion following RCA. Previous studies have shown that L1 and L2 can bind and package non-specific DNA (Mallon et al., 1987; Roden et al., 1996; Zhou et al., 1994). Thus, it could be possible for untargeted plasmid DNA to be encapsidated within the PsVs. While the identity of the DNA encapsidated in the PsVs made here could not be confirmed, the sizes of the digested RCA products observed correspond to those expected for mSEAP and YSEAP. Therefore, the packaged DNA detected is likely SEAP pseudogenome specific.

The fractions that were confirmed to contain PsVs harbouring SEAP DNA were trapped on grids and particles were assessed for structure and yield by TEM (Figure 4.2). HPV-35 pPsV fraction 4 revealed a heterogenous population of 40-50 nm VLPs and PsVs, 10 nm L1 capsomers, and large protein aggregates. Since HPV VLPs and PsVs assemble to the same size range, the actual yield of T=7 PsVs was unclear from these results. In contrast, the clear size discrepancies between BPV-1 VLPs and PsVs in TEM revealed a low concentration of T=7 PsVs amongst a homogenous population of 30 nm VLPs. The putative PsVs observed for both the BPV-1 and HPV-35 preparations were misshapen, indicating poor capsid assembly. Surprisingly, very few particles were observed in the mPsV samples. Moreover, the structures did not resemble PV PsVs observed in previous literature (Buck, Pastrana, et al., 2005; Lamprecht et al., 2016; Maclean et al., 2007). The lack of particles observed here is likely a result of poor grid preparation, however, and not a reflection of PsV assembly in mammalian cells.

This head-to-head analysis of plant- and mammalian-based PsVs was conducted to determine the lack of reporter gene expression observed following mammalian cell infection with plant-made PsVs in Chapter 2 and 3. Thus, following confirmation of pseudogenome packaging, PsV infectivity was investigated with a reporter gene assay. PsV preparations were added to HEK293TT cells and SEAP expression levels were assessed after 72 hr. Expression of both YSEAP (within mPsVs) and mSEAP (within pPsVs) is under control of the SV40 early promoter for maximum expression in mammalian cells following PsV infection (Buck, Pastrana, et al., 2005; Kennedy, 2013). Figure 4.3A shows that SEAP signals were detected in 293TT cell supernatants following infection with mammalian-made PsVs but not with plant-made PsVs, indicating that the mPsVs are capable of infecting host cells to deliver their cargo. Furthermore, this result could indicate a low yield of pPsVs or poor infectivity. Poor infectivity may be attributable to the lack of a reassembly step in the presence of nuclear mammalian extract, which has been shown to induce disassembly of empty particles for reassembly around pseudogenome DNA (Schiller et al., 2016). The addition of a disassembly/reassembly step during PsV production could improve PsV assembly and infectivity and should therefore be investigated.

The lack of functional PsVs obtained in plants may be attributable to the absence of a maturation process following protein extraction. Studies by Buck, Thompson, et al. (2005) show that inclusion of a maturation step following cell lysis is necessary for efficient purification of 293TT-produced PsVs. During natural infection, PV capsids undergo an incredibly slow maturation process following assembly (Doorbar, 2005). Disulfide bond formation between L1 proteins in the capsid drives the process and results in virions with increased stability and resistance to proteolytic digestion (Cerqueira & Schiller, 2017). Buck, Thompson, et al. (2005) showed that an overnight incubation in high-salt buffer at 37°C mimics the natural environment in which these bonds form to produce highly stable PsVs. Moreover, the authors showed that failure to include this step resulted in a substantial loss of particles during purification, possibly due to hydrostatic pressure and shearing during ultracentrifugation. Notably, the authors additionally showed that particle maturation does not affect infectivity, as no significant difference in antibody neutralisation between immature and mature PsVs was observed (Buck, Thompson, et al., 2005). This finding is consistent with previous studies in the laboratory whereby antibody neutralisation with plant-made HPV PsVs was observed (Lamprecht et al., 2016; Naupu, 2019). Nonetheless, plant-based production of PV PsVs in the laboratory is associated with poor yields, protein aggregate formation, and proteolytic degradation (Adams, 2020; Chabeda, 2017; Pietersen, 2019). The addition of an overnight maturation step following extraction of plant-made PsVs should therefore be explored.

SEAP expression patterns observed following transfection of PsVs into 293TT cells in the presence of DNA and protein transfection reagents were similar to those observed following infection of 293TT with PsVs (Figure 4.3B and C). The SEAP signals observed for DNA and protein transfection of cells with mPsVs were comparable to the levels achieved following infection, despite using 1/10th of the sample volume. This result indicates that the DNA and protein transfection reagents were highly effective at intracellular delivery of the PsVs. Notably, the SEAP expression levels achieved following infection and transfection with HPV-35 mPsVs were at least two-fold greater than with BPV-1 mPsVs (Figure 4.3), indicating that more SEAP DNA was delivered with the HPV-35 mPsVs. This finding suggests that HPV-35 PsV production in 293TT cells is associated with a higher encapsidation efficiency than that of BPV-1. Additionally, Figure 4.3 revealed no SEAP expression following transfection of cells

with BPV and HPV pPsVs. As the presence of a transfection reagent eliminates the need for PsV infectivity, the lack of SEAP expression following 293TT transfection with pPsVs is likely due to too little DNA being delivered, indicating a low encapsidation efficiency and/or poor PsV yield. Quantitative analysis is needed to determine the actual yield of PsVs and encapsidated DNA. An Enzyme-linked Immunosorbent Assay (ELISA) could be used to quantify L1 protein concentration in the PsV samples (Adams et al., 2023). While L1 concentration does not directly correlate to PsV yield, since L2 incorporation is also necessary for PsV formation, it would give an estimation of the concentration of PsVs within the sample. Moreover, the concentration of encapsidated DNA within the sample could be efficiently measured using qPCR (Bayer et al., 2018; Cerqueira et al., 2017). Furthermore, by using the ratio of encapsidated DNA to L1 concentration, the efficiency of DNA packaging within PsVs could be estimated (Adams et al., 2023).

In conclusion, this study found that, while high levels of plant-made L1 protein accumulation was observed following purification, only a small percentage assembled into PsVs, possibly explaining the lack of reporter gene expression observed following mammalian cell infection and transfection with the plant-made PsVs. Moreover, most particles observed were aberrantly assembled and accompanied by large populations of L1 aggregates. Further optimisation of plant-based expression and purification should therefore be explored to improve PsV yield and encapsidation efficiency.

5 Chapter 5: General discussion and conclusions

5.1 General discussion

Cervical cancer is the second most frequently diagnosed cancer in women with an estimated 604,000 new cases reported in 2020 alone (Sung et al., 2021). A large proportion of these incidences emerged in Sub-Saharan Africa (SSA) where the burden of cervical cancer is extremely high, and still rising (Jedy-Agba et al., 2020). Persistent exposure to high-risk HPV subtypes is the primary cause of persistent cervical cancer (zur Hausen, 2002). Despite the great burden developing countries face, HPV infection with high-risk types is entirely preventable. Global prophylactic vaccination strategies in high income regions such as North America and Australia have been extremely successful in the eradication of HPV infection (Bray et al., 2005). This success is largely attributable to commercially available VLP-based vaccines such as Gardasil 4®, Gardasil 9®, and Cervarix™. However, these vaccines are ineffective at reducing already established infections (Hildesheim et al., 2016). Moreover, the commercially available vaccines are costly and intervention measures are resource intensive (Bruni et al., 2016). As a result, the incidence rates of HPV infection and cervical neoplasia development remain high in developing countries such as South Africa. It is therefore necessary to explore therapeutic treatments to address the burden of high-risk HPVs in these lower income countries.

DNA vaccines are appealing candidates for therapeutic treatments as they are safe, easy to produce, and stimulate antigen-specific T-cell immunity (Gurunathan et al., 2000). However, naked DNA vaccines are associated with inefficient presentation to APCs. This limitation can be overcome by using PsVs as delivery vehicles for DNA vaccines (Peng et al., 2011). PsVs based on HPV, particularly HPV-16, have been shown to efficiently infect immune cells for delivery of DNA vaccines *in vivo* (Graham et al., 2010; Kines et al., 2016; Ma et al., 2011; Peng et al., 2010). High-risk HPVs are, however, precluded from use as gene delivery vehicles due to a large proportion of the female population having existing immunity through natural infection and worldwide vaccination efforts (Bayer et al., 2018). Delivery systems based on non-human PV PsVs should therefore be explored.

HPV-16 PsVs have successfully been produced in plants (Lamprecht et al., 2016). Plant expression systems are associated with lower costs, increased scalability, and a lowered risk of human pathogen contamination than the mammalian cell-based expression systems that dominate the biopharmaceutical market (Giorgi et al., 2010; Lomonossoff & D'Aoust, 2016; Rybicki, 2014). The use of plants for the production of a PsV-based therapeutic vaccine could therefore be advantageous for low-income countries like South Africa. Therefore, this study aimed to investigate plant-based production of BPV-1 PsVs encapsidating a HPV-16 DNA vaccine candidate. Moreover, this study aimed to test the ability of the plant-made PsVs to deliver their encapsidated pseudogenome to mammalian cells.

Firstly, an optimisation study to determine the ideal conditions for BPV-1 PsV production in plants, using a SEAP reporter plasmid, was investigated (Chapter 2). Several modifications of a plant-based HPV PsV production and extraction method developed by Lamprecht et al. (2016) were investigated to maximise particle yield. Strategies such as increased acetosyringone concentration for recombinant *Agrobacterium* induction, heat-shock treatment of post-infiltrated plants, and extended *in planta* maturation were explored. The results of this study indicated that *Agrobacterium* induction using an increased acetosyringone concentration resulted in no improvement of L1 protein accumulation and PsV yield, thus the strategy was not implemented for further PsV production. The results further showed that, while heat shock treatment was associated with an increase in L1 production, the treatment appeared to hinder PsV assembly. Therefore, the treatment was not implemented. Finally, conclusions on whether to implement a six day *in planta* maturation could not be reached as the plants became necrotic at 5 – 6 dpi. While putative BPV-1 PsVs were observed for some of the strategies tested, encapsidation of the SEAP pseudogenome was not confirmed and no reporter gene expression was observed following mammalian cell infection.

Next, a proof-of-concept study to address the need for cost-effective and efficacious therapeutic vaccines, using a HPV-16 E7SH-based DNA vaccine delivered by plant-produced PsVs, was examined (Chapter 3). The E7 oncoprotein is an ideal target for therapeutic vaccine development due to its role in oncogenic transformation and constitutive expression in cervical cancer lesions (Whitehead et al., 2014). Several

recombinant self-replicating E7SH-based reporter plasmids were constructed using In-Fusion cloning technology (Park et al., 2015). BPV-1 and HPV-35 L1/L2 were assessed for their ability to package the E7SH-based pseudogenomes for PsV production in plants. HPV-35 was selected as it has been shown to encapsidate a Zera®E7SH DNA vaccine in plants for delivery to mammalian cells *in vitro* (Chabeda, 2017). PsVs were successfully produced in plants and resembled PsVs produced in mammalian systems. However, very few PsVs were observed and these were accompanied by misassembled particles, L1 aggregates, and capsomeric structures. BPV-1 and HPV-35 PsVs successfully encapsidated the E7SH-based pseudogenomes. However, the E7SH replicons showed no E7 expression following transfection of mammalian cells. Furthermore, no E7 expression was observed following infection of mammalian cells with plant-made BPV-1 and HPV-35 PsVs.

Lastly, a comparative analysis to elucidate the lack of expression following DNA vaccine delivery with plant-made PsVs into mammalian cells, using HEK293TT-made PsVs, was explored (Chapter 4). The 293TT cell line has been shown to be highly successful for generating high-titres of PV-based PsVs (Buck, Pastrana, et al., 2005). These PsVs are highly capable of delivering their pseudogenome into host cells both *in vitro* and *in vivo* (Graham et al., 2010; Kines et al., 2015; Pastrana et al., 2004). BPV-1 and HPV-35 PsVs were successfully produced in both plants and mammalian cells. As in previous studies, the plant-produced PsVs displayed poor yield and structural integrity. While the PsVs produced in both systems showed successful encapsidation of their respective SEAP pseudogenomes, only the 293TT-produced PsVs showed SEAP expression following mammalian cell infection. Moreover, transfection of mammalian cells with plant-made PsVs resulted in no SEAP expression being observed.

5.2 Conclusions and future work

These studies have shown that, while PsVs capable of pseudogenome encapsidation were successfully produced in plants, the PsVs were ineffective at delivering their packaged DNA into mammalian cells. Moreover, low yields of plant-made PsVs were consistently achieved despite high levels of L1 protein accumulation observed following PsV purification. These findings show that L1 accumulation is not necessarily

indicative of PsV yield and that PsV production in plants is associated with poor encapsidation efficiency and aberrant particle assembly. Future research could focus on disassembly/assembly of plant-produced PsVs in the presence of mammalian cell nuclear extract during PsV production for increased encapsidation efficiency and assembly (Schiller et al., 2016). In addition, research should target optimisation of the PV PsV purification process with inclusion of a maturation step to increase particle stability and thus potentially improve PsV yield (Buck, Thompson, et al., 2005; Cardone et al., 2014).

In this study, the identity of the encapsidated pseudogenomes in the plant-produced PsVs could not be conclusively confirmed. Future work should therefore include sequencing of the DNA extracted from PsVs to confirm successful replicon formation and functionality. Moreover, PsV yield and encapsidated DNA could not be quantified in this study. Future studies could include ELISA and qPCR experiments to determine the concentration of L1 protein and encapsidated DNA obtained following plant-based production. The ratio of these values would give an indication of the encapsidation efficiency associated with the PsVs. Inclusion of these experiments would therefore be extremely valuable for further elucidation of the results discussed in study.

In this study, the ability of plant-made PsVs to deliver their encapsidated pseudogenomes into mammalian cells was assessed in an *in vitro* model. Future work could focus on animal studies to investigate the immunogenicity of plant-made PV PsVs in comparison to mammalian cell-produced PsVs within an *in vivo* model. The immune system is extremely complex and immune cell responses cannot accurately be replicated in cultured cells (Day et al., 2010). The use of an *in vivo* system would therefore provide more accurate information on the interactions between PV PsVs and the host cells they target.

In conclusion, this research contributes towards the development of plant-produced PsVs as potential delivery vehicles for therapeutic HPV vaccines. However, more research is required to overcome potential limitations of plant-produced PsVs highlighted in this study, in order to explore this application further.

Bibliography

References

Adams, A. (2020). *Optimization and characterisation of plant produced Human Papillomavirus pseudovirions in Nicotiana benthamiana.* University of Cape Town.

Adams, A., Hendrikse, M., Rybicki, E. P., & Hitzeroth, II. (2023). Optimal size of DNA encapsidated by plant produced human papillomavirus pseudovirions. *Virology*, *580*, 88-97. https://doi.org/10.1016/j.virol.2023.02.003

Antonishyn, N. A. (2007). The utility of hpv typing and relative quantification of HPV-16 transcripts for monitoring HPV vaccine efficacy and improving colposcopy triage of women with abnormal cervical cytology. In.

Auewarakul, P., Gissmann, L., & Cid-Arregui, A. (1994). Targeted expression of the E6 and E7 oncogenes of human papillomavirus type 16 in the epidermis of transgenic mice elicits generalized epidermal hyperplasia involving autocrine factors. *Mol Cell Biol*, *14*(12), 8250-8258. https://doi.org/10.1128/mcb.14.12.8250-8258.1994

Bachmann, M. F., & Zinkernagel, R. M. (1996). The influence of virus structure on antibody responses and virus serotype formation. *Immunol Today*, *17*(12), 553-558. https://doi.org/10.1016/s0167-5699(96)10066-9

Bachmann, M. F., & Zinkernagel, R. M. (1997). Neutralizing antiviral B cell responses. *Annu Rev Immunol*, *15*, 235-270. https://doi.org/10.1146/annurev.immunol.15.1.235

Bagarazzi, M. L., Yan, J., Morrow, M. P., Shen, X., Parker, R. L., Lee, J. C., Giffear, M., Pankhong, P., Khan, A. S., Broderick, K. E., Knott, C., Lin, F., Boyer, J. D., Draghia-Akli, R., White, C. J., Kim, J. J., Weiner, D. B., & Sardesai, N. Y. (2012). Immunotherapy against HPV16/18 generates potent TH1 and cytotoxic cellular immune responses. *Sci Transl Med*, *4*(155), 155ra138. https://doi.org/10.1126/scitranslmed.3004414

Baghban, R., Farajnia, S., Rajabibazl, M., Ghasemi, Y., Mafi, A., Hoseinpoor, R., Rahbarnia, L., & Aria, M. (2019). Yeast Expression Systems: Overview and Recent Advances. *Mol Biotechnol*, *61*(5), 365-384. https://doi.org/10.1007/s12033-019-00164-8

Baker, T. S., Newcomb, W. W., Olson, N. H., Cowsert, L. M., Olson, C., & Brown, J. C. (1991). Structures of bovine and human papillomaviruses. Analysis by cryoelectron microscopy and three-dimensional image reconstruction. *Biophys J*, *60*(6), 1445-1456. https://doi.org/10.1016/s0006-3495(91)82181-6

Barber, G. N. (2011). Cytoplasmic DNA innate immune pathways. *Immunol Rev*, *243*(1), 99-108. https://doi.org/10.1111/j.1600-065X.2011.01051.x

Baulcombe, D. (2004). RNA silencing in plants. *Nature*, *431*(7006), 356-363. https://doi.org/10.1038/nature02874

Bayer, L., Gumpel, J., Hause, G., Muller, M., & Grunwald, T. (2018). Non-human papillomaviruses for gene delivery in vitro and in vivo. *PLoS One*, *13*(6), e0198996. https://doi.org/10.1371/journal.pone.0198996

Bernard, H. U. (1994). Coevolution of papillomaviruses with human populations. *Trends Microbiol*, *2*(4), 140-143. https://doi.org/10.1016/0966-842x(94)90602-5

Bernard, H. U. (2005). The clinical importance of the nomenclature, evolution and taxonomy of human papillomaviruses. *J Clin Virol*, *32 Suppl 1*, S1-6. https://doi.org/10.1016/j.jcv.2004.10.021

Bernard, H. U., Burk, R. D., Chen, Z., van Doorslaer, K., zur Hausen, H., & de Villiers, E. M. (2010). Classification of papillomaviruses (PVs) based on 189 PV types and proposal of taxonomic amendments. *Virology*, *401*(1), 70-79. https://doi.org/10.1016/j.virol.2010.02.002

Bertani, G. (1951). Studies on Lysogenesis I. *Journal of Bacteriology*, *62*(3), 293-300. https://doi.org/doi:10.1128/jb.62.3.293-300.1951

Best, S. R., Peng, S., Juang, C. M., Hung, C. F., Hannaman, D., Saunders, J. R., Wu, T. C., & Pai, S. I. (2009). Administration of HPV DNA vaccine via electroporation elicits the strongest CD8+ T cell immune responses compared to intramuscular injection and intradermal gene gun delivery. *Vaccine*, *27*(40), 5450-5459. https://doi.org/10.1016/j.vaccine.2009.07.005

Beutner, K. R., & Tyring, S. (1997). Human papillomavirus and human disease. *Am J Med*, *102*(5A), 9-15. https://doi.org/10.1016/s0002-9343(97)00178-2

Bian, T., Wang, Y., Lu, Z., Ye, Z., Zhao, L., Ren, J., Zhang, H., Ruan, L., & Tian, H. (2008). Human papillomavirus type 16 L1E7 chimeric capsomeres have prophylactic and therapeutic efficacy against papillomavirus in mice. *Mol Cancer Ther*, *7*(5), 1329-1335. https://doi.org/10.1158/1535-7163.MCT-07-2015

Biemelt, S., Sonnewald, U., Galmbacher, P., Willmitzer, L., & Müller, M. (2003). Production of human papillomavirus type 16 virus-like particles in transgenic plants. *J Virol*, *77*(17), 9211-9220. https://doi.org/10.1128/jvi.77.17.9211-9220.2003

Bocaneti, F., Altamura, G., Corteggio, A., Velescu, E., Roperto, F., & Borzacchiello, G. (2016). Bovine Papillomavirus: New Insights into an Old Disease. *Transbound Emerg Dis*, *63*(1), 14-23. https://doi.org/10.1111/tbed.12222

Bosch, F. X., Lorincz, A., Muñoz, N., Meijer, C. J., & Shah, K. V. (2002). The causal relation between human papillomavirus and cervical cancer. *J Clin Pathol*, *55*(4), 244-265. https://doi.org/10.1136/jcp.55.4.244

Bray, F., Carstensen, B., Møller, H., Zappa, M., Zakelj, M. P., Lawrence, G., Hakama, M., & Weiderpass, E. (2005). Incidence trends of adenocarcinoma of the cervix in 13 European countries. *Cancer Epidemiol Biomarkers Prev*, *14*(9), 2191-2199. https://doi.org/10.1158/1055-9965.Epi-05-0231

Brendle, S., Cladel, N., Balogh, K., Alam, S., Christensen, N., Meyers, C., & Hu, J. (2021). A Comparative Study on Delivery of Externally Attached DNA by

Papillomavirus VLPs and Pseudoviruses. *Vaccines*, *9*(12), 1501. https://www.mdpi.com/2076-393X/9/12/1501

Brentjens, M. H., Yeung-Yue, K. A., Lee, P. C., & Tyring, S. K. (2002). Human papillomavirus: a review. *Dermatol Clin*, *20*(2), 315-331. https://doi.org/10.1016/s0733-8635(01)00028-6

Briske-Anderson, M. J., Finley, J. W., & Newman, S. M. (1997). The influence of culture time and passage number on the morphological and physiological development of Caco-2 cells. *Proc Soc Exp Biol Med*, *214*(3), 248-257. https://doi.org/10.3181/00379727-214-44093

Brisson, M., Kim, J. J., Canfell, K., Drolet, M., Gingras, G., Burger, E. A., Martin, D., Simms, K. T., Bénard, É., Boily, M. C., Sy, S., Regan, C., Keane, A., Caruana, M., Nguyen, D. T. N., Smith, M. A., Laprise, J. F., Jit, M., Alary, M., Hutubessy, R. (2020). Impact of HPV vaccination and cervical screening on cervical cancer elimination: a comparative modelling analysis in 78 low-income and lower-middle-income countries. *Lancet*, *395*(10224), 575-590. https://doi.org/10.1016/s0140-6736(20)30068-4

Bruni, L., Diaz, M., Barrionuevo-Rosas, L., Herrero, R., Bray, F., Bosch, F. X., de Sanjosé, S., & Castellsagué, X. (2016). Global estimates of human papillomavirus vaccination coverage by region and income level: a pooled analysis. *The Lancet Global Health*, *4*(7), e453-e463. https://doi.org/10.1016/s2214-109x(16)30099-7

Buck, C. B., Pastrana, D. V., Lowy, D. R., & Schiller, J. T. (2004). Efficient intracellular assembly of papillomaviral vectors. *J Virol*, *78*(2), 751-757. https://doi.org/10.1128/jvi.78.2.751-757.2004

Buck, C. B., Pastrana, D. V., Lowy, D. R., & Schiller, J. T. (2005). Generation of HPV pseudovirions using transfection and their use in neutralization assays. *Methods Mol Med*, *119*, 445-462. https://doi.org/10.1385/1-59259-982-6:445

Buck, C. B., Pastrana, D. V., Lowy, D. R., & Schiller, J. T. (2006). Generation of HPV Pseudovirions Using Transfection and Their Use in Neutralization Assays. In C. Davy & J. Doorbar (Eds.), *Human Papillomaviruses: Methods and Protocols* (pp. 445-462). Humana Press. https://doi.org/10.1385/1-59259-982-6:445

Buck, C. B., Thompson, C. D., Pang, Y. Y., Lowy, D. R., & Schiller, J. T. (2005). Maturation of papillomavirus capsids. *J Virol*, *79*(5), 2839-2846. https://doi.org/10.1128/JVI.79.5.2839-2846.2005

Campo, M. S. (2002). Animal models of papillomavirus pathogenesis. *Virus Res*, *89*(2), 249-261. https://doi.org/10.1016/s0168-1702(02)00193-4

Campo, M. S., & Roden, R. B. (2010). Papillomavirus prophylactic vaccines: established successes, new approaches. *J Virol*, *84*(3), 1214-1220. https://doi.org/10.1128/JVI.01927-09

Canfell, K., Kim, J. J., Brisson, M., Keane, A., Simms, K. T., Caruana, M., Burger, E. A., Martin, D., Nguyen, D. T. N., Bénard, É., Sy, S., Regan, C., Drolet, M., Gingras, G., Laprise, J. F., Torode, J., Smith, M. A., Fidarova, E., Trapani, D., Hutubessy, R. (2020). Mortality impact of achieving WHO cervical cancer elimination targets: a comparative modelling analysis in 78 low-income and

lower-middle-income countries. *Lancet*, *395*(10224), 591-603. https://doi.org/10.1016/s0140-6736(20)30157-4

Cardone, G., Moyer, A. L., Cheng, N., Thompson, C. D., Dvoretzky, I., Lowy, D. R., Schiller, J. T., Steven, A. C., Buck, C. B., & Trus, B. L. (2014). Maturation of the human papillomavirus 16 capsid. *mBio*, *5*(4), e01104-01114. https://doi.org/10.1128/mBio.01104-14

Cerqueira, C., & Schiller, J. T. (2017). Papillomavirus assembly: An overview and perspectives. *Virus Res*, *231*, 103-107. https://doi.org/10.1016/j.virusres.2016.11.010

Cerqueira, C., Thompson, C. D., Day, P. M., Pang, Y. S., Lowy, D. R., & Schiller, J. T. (2017). Efficient Production of Papillomavirus Gene Delivery Vectors in Defined In Vitro Reactions. *Mol Ther Methods Clin Dev*, *5*, 165-179. https://doi.org/10.1016/j.omtm.2017.04.005

Chabeda, A., Yanez, R. J. R., Lamprecht, R., Meyers, A. E., Rybicki, E. P., & Hitzeroth, II. (2018). Therapeutic vaccines for high-risk HPV-associated diseases. *Papillomavirus Res*, *5*, 46-58. https://doi.org/10.1016/j.pvr.2017.12.006

Chabeda, E. A. (2017). *Immunogenic assessment of plant-produced Human papillomavirus type 16 chimaeric L1:L2 virus-like particles and the production of an encapsidated therapeutic DNA vaccine candidate*. University of Cape Town.

Chambers, G., Ellsmore, V. A., O'Brien, P. M., Reid, S. W. J., Love, S., Campo, M. S., & Nasir, L. (2003). Association of bovine papillomavirus with the equine sarcoid. *J Gen Virol*, *84*(Pt 5), 1055-1062. https://doi.org/10.1099/vir.0.18947-0

Chargelegue, D., Drake, P. M., Obregon, P., Prada, A., Fairweather, N., & Ma, J. K. (2005). Highly immunogenic and protective recombinant vaccine candidate expressed in transgenic plants. *Infect Immun*, *73*(9), 5915-5922. https://doi.org/10.1128/IAI.73.9.5915-5922.2005

Chen, C. H., Ji, H., Suh, K. W., Choti, M. A., Pardoll, D. M., & Wu, T. C. (1999). Gene gun-mediated DNA vaccination induces antitumor immunity against human papillomavirus type 16 E7-expressing murine tumor metastases in the liver and lungs. *Gene Ther*, *6*(12), 1972-1981. https://doi.org/10.1038/sj.gt.3301067

Chen, Q., He, J., Phoolcharoen, W., & Mason, H. S. (2011). Geminiviral vectors based on bean yellow dwarf virus for production of vaccine antigens and monoclonal antibodies in plants. *Human vaccines*, *7*(3), 331-338.

Chen, Q., & Lai, H. (2013). Plant-derived virus-like particles as vaccines. *Hum Vaccin Immunother*, *9*(1), 26-49. https://doi.org/10.4161/hv.22218

Chen, Q., Lai, H., Hurtado, J., Stahnke, J., Leuzinger, K., & Dent, M. (2013). Agroinfiltration as an Effective and Scalable Strategy of Gene Delivery for Production of Pharmaceutical Proteins. *Adv Tech Biol Med*, *1*(1). https://doi.org/10.4172/atbm.1000103

Chen, Q., Tacket, C., Mason, H., Mor, T., Cardineau, G., & Arntzen, C. (2009). New Generation Vaccines.

Chen, X. S., Garcea, R. L., Goldberg, I., Casini, G., & Harrison, S. C. (2000). Structure of small virus-like particles assembled from the L1 protein of human papillomavirus 16. *Mol Cell*, *5*(3), 557-567. https://doi.org/10.1016/s1097-2765(00)80449-9

Cheng, M. A., Farmer, E., Huang, C., Lin, J., Hung, C. F., & Wu, T. C. (2018). Therapeutic DNA Vaccines for Human Papillomavirus and Associated Diseases. *Hum Gene Ther*, *29*(9), 971-996. https://doi.org/10.1089/hum.2017.197

Chong, Z. X., Yeap, S. K., & Ho, W. Y. (2021). Transfection types, methods and strategies: a technical review. *PeerJ*, *9*, e11165. https://doi.org/10.7717/peerj.11165

Christensen, N. D., Dillner, J., Eklund, C., Carter, J. J., Wipf, G. C., Reed, C. A., Cladel, N. M., & Galloway, D. A. (1996). Surface conformational and linear epitopes on HPV-16 and HPV-18 L1 virus-like particles as defined by monoclonal antibodies. *Virology*, *223*(1), 174-184. https://doi.org/10.1006/viro.1996.0466

Cladel, N. M., Hu, J., Balogh, K., Mejia, A., & Christensen, N. D. (2008). Wounding prior to challenge substantially improves infectivity of cottontail rabbit papillomavirus and allows for standardization of infection. *J Virol Methods*, *148*(1-2), 34-39. https://doi.org/10.1016/j.jviromet.2007.10.005

Clynes, M. (1998). *Animal Cell Culture Techniques* (1st 1998. ed.). Springer Berlin Heidelberg : Imprint: Springer.

Crum, C. P. (1998). Detecting every genital papilloma virus infection: what does it mean? *Am J Pathol*, *153*(6), 1667-1671. https://doi.org/10.1016/S0002-9440(10)65679-9

Cubie, H. A. (2013). Diseases associated with human papillomavirus infection. *Virology*, *445*(1-2), 21-34. https://doi.org/10.1016/j.virol.2013.06.007

D'Aoust, M. A., Lavoie, P. O., Couture, M. M., Trepanier, S., Guay, J. M., Dargis, M., Mongrand, S., Landry, N., Ward, B. J., & Vezina, L. P. (2008). Influenza virus-like particles produced by transient expression in Nicotiana benthamiana induce a protective immune response against a lethal viral challenge in mice. *Plant Biotechnol J*, *6*(9), 930-940. https://doi.org/10.1111/j.1467-7652.2008.00384.x

Da Silva, D. M., Schiller, J. T., & Kast, W. M. (2003). Heterologous boosting increases immunogenicity of chimeric papillomavirus virus-like particle vaccines. *Vaccine*, *21*(23), 3219-3227. https://doi.org/10.1016/s0264-410x(03)00237-8

Dadar, M., Chakraborty, S., Dhama, K., Prasad, M., Khandia, R., Hassan, S., Munjal, A., Tiwari, R., Karthik, K., Kumar, D., Iqbal, H. M. N., & Chaicumpa, W. (2018). Advances in Designing and Developing Vaccines, Drugs and Therapeutic Approaches to Counter Human Papilloma Virus. *Front Immunol*, *9*, 2478. https://doi.org/10.3389/fimmu.2018.02478

Daniell, H., Singh, N. D., Mason, H., & Streatfield, S. J. (2009). Plant-made vaccine antigens and biopharmaceuticals. *Trends Plant Sci*, *14*(12), 669-679. https://doi.org/10.1016/j.tplants.2009.09.009

Day, P. M., Baker, C. C., Lowy, D. R., & Schiller, J. T. (2004). Establishment of papillomavirus infection is enhanced by promyelocytic leukemia protein (PML) expression. *Proc Natl Acad Sci U S A*, *101*(39), 14252-14257. https://doi.org/10.1073/pnas.0404229101

Day, P. M., Kines, R. C., Thompson, C. D., Jagu, S., Roden, R. B., Lowy, D. R., & Schiller, J. T. (2010). In vivo mechanisms of vaccine-induced protection against HPV infection. *Cell Host Microbe*, *8*(3), 260-270. https://doi.org/10.1016/j.chom.2010.08.003

Day, P. M., Lowy, D. R., & Schiller, J. T. (2003). Papillomaviruses infect cells via a clathrin-dependent pathway. *Virology*, *307*(1), 1-11. https://doi.org/10.1016/s0042-6822(02)00143-5

Day, P. M., & Schiller, J. T. (2009). The role of furin in papillomavirus infection. *Future Microbiol*, *4*(10), 1255-1262. https://doi.org/10.2217/fmb.09.86

De Gregorio, V., Urciuolo, F., Netti, P. A., & Imparato, G. (2020). In Vitro Organotypic Systems to Model Tumor Microenvironment in Human Papillomavirus (HPV)-Related Cancers. *Cancers (Basel)*, *12*(5). https://doi.org/10.3390/cancers12051150

de Martel, C., Ferlay, J., Franceschi, S., Vignat, J., Bray, F., Forman, D., & Plummer, M. (2012). Global burden of cancers attributable to infections in 2008: a review and synthetic analysis. *Lancet Oncol*, *13*(6), 607-615. https://doi.org/10.1016/S1470-2045(12)70137-7

de Villiers, E. M. (2013). Cross-roads in the classification of papillomaviruses. In: Virology.

de Villiers, E. M., Fauquet, C., Broker, T. R., Bernard, H. U., & zur Hausen, H. (2004). Classification of papillomaviruses. *Virology*, *324*(1), 17-27. https://doi.org/10.1016/j.virol.2004.03.033

De Vuyst, H., Alemany, L., Lacey, C., Chibwesha, C. J., Sahasrabuddhe, V., Banura, C., Denny, L., & Parham, G. P. (2013). The burden of human papillomavirus infections and related diseases in sub-saharan Africa. *Vaccine*, *31 Suppl 5*(05), F32-46. https://doi.org/10.1016/j.vaccine.2012.07.092

Dean, F. B., Nelson, J. R., Giesler, T. L., & Lasken, R. S. (2001). Rapid amplification of plasmid and phage DNA using Phi 29 DNA polymerase and multiply-primed rolling circle amplification. *Genome Res*, *11*(6), 1095-1099. https://doi.org/10.1101/gr.180501

Della Torre, G., Pilotti, S., de Palo, G., & Rilke, F. (1978). Viral particles in cervical condylomatous lesions. *Tumori*, *64*(5), 549-553. https://doi.org/10.1177/030089167806400513

Dennis, S. J., O'Kennedy, M. M., Rutkowska, D., Tsekoa, T., Lourens, C. W., Hitzeroth, II, Meyers, A. E., & Rybicki, E. P. (2018). Safety and immunogenicity of plant-produced African horse sickness virus-like particles in horses. *Vet Res*, *49*(1), 105. https://doi.org/10.1186/s13567-018-0600-4

Ding, D. C., Chiang, M. H., Lai, H. C., Hsiung, C. A., Hsieh, C. Y., & Chu, T. Y. (2009). Methylation of the long control region of HPV16 is related to the severity of

cervical neoplasia. *Eur J Obstet Gynecol Reprod Biol*, *147*(2), 215-220. https://doi.org/10.1016/j.ejogrb.2009.08.023

Donnelly, J. J., Ulmer, J. B., Shiver, J. W., & Liu, M. A. (1997). DNA vaccines. *Annu Rev Immunol*, *15*, 617-648. https://doi.org/10.1146/annurev.immunol.15.1.617

Doorbar, J. (2005). The papillomavirus life cycle. *J Clin Virol*, *32 Suppl 1*, S7-15. https://doi.org/10.1016/j.jcv.2004.12.006

Doorbar, J. (2006). Molecular biology of human papillomavirus infection and cervical cancer. *Clin Sci (Lond)*, *110*(5), 525-541. https://doi.org/10.1042/CS20050369

Doorbar, J. (2016). Model systems of human papillomavirus-associated disease. *J Pathol*, *238*(2), 166-179. https://doi.org/10.1002/path.4656

Doorbar, J., Quint, W., Banks, L., Bravo, I. G., Stoler, M., Broker, T. R., & Stanley, M. A. (2012). The biology and life-cycle of human papillomaviruses. *Vaccine*, *30 Suppl 5*, F55-70. https://doi.org/10.1016/j.vaccine.2012.06.083

Draper, E., Bissett, S. L., Howell-Jones, R., Edwards, D., Munslow, G., Soldan, K., & Beddows, S. (2011). Neutralization of non-vaccine human papillomavirus pseudoviruses from the A7 and A9 species groups by bivalent HPV vaccine sera. *Vaccine*, *29*(47), 8585-8590. https://doi.org/10.1016/j.vaccine.2011.09.021

Dürst, M., Gissmann, L., Ikenberg, H., & zur Hausen, H. (1983). A papillomavirus DNA from a cervical carcinoma and its prevalence in cancer biopsy samples from different geographic regions. *Proc Natl Acad Sci U S A*, *80*(12), 3812-3815. https://doi.org/10.1073/pnas.80.12.3812

Dyda, A., Shah, Z., Surian, D., Martin, P., Coiera, E., Dey, A., Leask, J., & Dunn, A. G. (2019). HPV vaccine coverage in Australia and associations with HPV vaccine information exposure among Australian Twitter users. *Hum Vaccin Immunother*, *15*(7-8), 1488-1495. https://doi.org/10.1080/21645515.2019.1596712

Edgue, G., Twyman, R. M., Beiss, V., Fischer, R., & Sack, M. (2017). Antibodies from plants for bionanomaterials. *Wiley Interdiscip Rev Nanomed Nanobiotechnol*, *9*(6). https://doi.org/10.1002/wnan.1462

Edwards, A. (2019). *Production of a plant-produced Bovine papillomavirus vaccine candidate: Expression of BPV-1 virus-like particles and Pseudovirions in Nicotiana benthamiana.* University of Cape Town.

Egawa, N., Egawa, K., Griffin, H., & Doorbar, J. (2015). Human Papillomaviruses; Epithelial Tropisms, and the Development of Neoplasia. *Viruses*, *7*(7), 3863-3890. https://doi.org/10.3390/v7072802

Evander, M., Frazer, I. H., Payne, E., Qi, Y. M., Hengst, K., & McMillan, N. A. (1997). Identification of the alpha6 integrin as a candidate receptor for papillomaviruses. *J Virol*, *71*(3), 2449-2456. https://doi.org/10.1128/JVI.71.3.2449-2456.1997

Fifis, T., Gamvrellis, A., Crimeen-Irwin, B., Pietersz, G. A., Li, J., Mottram, P. L., McKenzie, I. F., & Plebanski, M. (2004). Size-dependent immunogenicity: therapeutic and protective properties of nano-vaccines against tumors. *J Immunol*, *173*(5), 3148-3154. https://doi.org/10.4049/jimmunol.173.5.3148

Fischer, R., & Buyel, J. F. (2020). Molecular farming - The slope of enlightenment. *Biotechnol Adv*, *40*, 107519. https://doi.org/10.1016/j.biotechadv.2020.107519

Fischer, R., Vaquero-Martin, C., Sack, M., Drossard, J., Emans, N., & Commandeur, U. (1999). Towards molecular farming in the future: transient protein expression in plants. *Biotechnol Appl Biochem*, *30*(2), 113-116. https://www.ncbi.nlm.nih.gov/pubmed/10512789

Florin, L., Sapp, C., Streeck, R. E., & Sapp, M. (2002). Assembly and translocation of papillomavirus capsid proteins. *J Virol*, *76*(19), 10009-10014. https://doi.org/10.1128/jvi.76.19.10009-10014.2002

Forman, D., de Martel, C., Lacey, C. J., Soerjomataram, I., Lortet-Tieulent, J., Bruni, L., Vignat, J., Ferlay, J., Bray, F., Plummer, M., & Franceschi, S. (2012). Global burden of human papillomavirus and related diseases. *Vaccine*, *30 Suppl 5*, F12-23. https://doi.org/10.1016/j.vaccine.2012.07.055

Franconi, R., Di Bonito, P., Dibello, F., Accardi, L., Muller, A., Cirilli, A., Simeone, P., Donà, M. G., Venuti, A., & Giorgi, C. (2002). Plant-derived human papillomavirus 16 E7 oncoprotein induces immune response and specific tumor protection. *Cancer Res*, *62*(13), 3654-3658.

Frattini, M. G., Lim, H. B., & Laimins, L. A. (1996). In vitro synthesis of oncogenic human papillomaviruses requires episomal genomes for differentiation-dependent late expression. *Proc Natl Acad Sci U S A*, *93*(7), 3062-3067. https://doi.org/10.1073/pnas.93.7.3062

Gardella, B., Gritti, A., Soleymaninejadian, E., Pasquali, M. F., Riemma, G., La Verde, M., Schettino, M. T., Fortunato, N., Torella, M., & Dominoni, M. (2022). New Perspectives in Therapeutic Vaccines for HPV: A Critical Review. *Medicina (Kaunas)*, *58*(7). https://doi.org/10.3390/medicina58070860

Gariglio, P., Gutierrez, J., Cortes, E., & Vazquez, J. (2009). The role of retinoid deficiency and estrogens as cofactors in cervical cancer. *Arch Med Res*, *40*(6), 449-465. https://doi.org/10.1016/j.arcmed.2009.08.002

Garland, S. M., Skinner, S. R., & Brotherton, J. M. (2011). Adolescent and young adult HPV vaccination in Australia: achievements and challenges. *Prev Med*, *53 Suppl 1*, S29-35. https://doi.org/10.1016/j.ypmed.2011.08.015

Geli, M. I., Torrent, M., & Ludevid, D. (1994). Two Structural Domains Mediate Two Sequential Events in [gamma]-Zein Targeting: Protein Endoplasmic Reticulum Retention and Protein Body Formation. *Plant Cell*, *6*(12), 1911-1922. https://doi.org/10.1105/tpc.6.12.1911

Gils, M., Kandzia, R., Marillonnet, S., Klimyuk, V., & Gleba, Y. (2005). High-yield production of authentic human growth hormone using a plant virus-based expression system. *Plant Biotechnology Journal*, *3*(6), 613-620.

Giorgi, C., Franconi, R., & Rybicki, E. P. (2010). Human papillomavirus vaccines in plants. *Expert Rev Vaccines*, *9*(8), 913-924. https://doi.org/10.1586/erv.10.84

Gordon, S. N., Kines, R. C., Kutsyna, G., Ma, Z. M., Hryniewicz, A., Roberts, J. N., Fenizia, C., Hidajat, R., Brocca-Cofano, E., Cuburu, N., Buck, C. B., Bernardo, M. L., Robert-Guroff, M., Miller, C. J., Graham, B. S., Lowy, D. R., Schiller, J. T., & Franchini, G. (2012). Targeting the vaginal mucosa with human

papillomavirus pseudovirion vaccines delivering simian immunodeficiency virus DNA. *J Immunol*, *188*(2), 714-723. https://doi.org/10.4049/jimmunol.1101404

Graham, B. S., Kines, R. C., Corbett, K. S., Nicewonger, J., Johnson, T. R., Chen, M., LaVigne, D., Roberts, J. N., Cuburu, N., Schiller, J. T., & Buck, C. B. (2010). Mucosal delivery of human papillomavirus pseudovirus-encapsidated plasmids improves the potency of DNA vaccination. *Mucosal Immunol*, *3*(5), 475-486. https://doi.org/10.1038/mi.2010.31

Greenstone, H. L., Nieland, J. D., de Visser, K. E., De Bruijn, M. L., Kirnbauer, R., Roden, R. B., Lowy, D. R., Kast, W. M., & Schiller, J. T. (1998). Chimeric papillomavirus virus-like particles elicit antitumor immunity against the E7 oncoprotein in an HPV16 tumor model. *Proc Natl Acad Sci U S A*, *95*(4), 1800-1805. https://doi.org/10.1073/pnas.95.4.1800

Grgacic, E. V., & Anderson, D. A. (2006). Virus-like particles: passport to immune recognition. *Methods*, *40*(1), 60-65. https://doi.org/10.1016/j.ymeth.2006.07.018

Gurunathan, S., Klinman, D. M., & Seder, R. A. (2000). DNA vaccines: immunology, application, and optimization*. *Annu Rev Immunol*, *18*, 927-974. https://doi.org/10.1146/annurev.immunol.18.1.927

Hagensee, M. E., Yaegashi, N., & Galloway, D. A. (1993). Self-assembly of human papillomavirus type 1 capsids by expression of the L1 protein alone or by coexpression of the L1 and L2 capsid proteins. *J Virol*, *67*(1), 315-322. https://doi.org/10.1128/JVI.67.1.315-322.1993

Hammond, E., Khurana, A., Shridhar, V., & Dredge, K. (2014). The Role of Heparanase and Sulfatases in the Modification of Heparan Sulfate Proteoglycans within the Tumor Microenvironment and Opportunities for Novel Cancer Therapeutics. *Front Oncol*, *4*, 195. https://doi.org/10.3389/fonc.2014.00195

Hancock, G., Hellner, K., & Dorrell, L. (2018). Therapeutic HPV vaccines. *Best Pract Res Clin Obstet Gynaecol*, *47*, 59-72. https://doi.org/10.1016/j.bpobgyn.2017.09.008

Handisurya, A., Day, P. M., Thompson, C. D., Buck, C. B., Kwak, K., Roden, R. B., Lowy, D. R., & Schiller, J. T. (2012). Murine skin and vaginal mucosa are similarly susceptible to infection by pseudovirions of different papillomavirus classifications and species. *Virology*, *433*(2), 385-394. https://doi.org/10.1016/j.virol.2012.08.035

Harper, D. M., Franco, E. L., Wheeler, C. M., Moscicki, A. B., Romanowski, B., Roteli-Martins, C. M., Jenkins, D., Schuind, A., Costa Clemens, S. A., Dubin, G., & group, H. P. V. V. S. (2006). Sustained efficacy up to 4.5 years of a bivalent L1 virus-like particle vaccine against human papillomavirus types 16 and 18: follow-up from a randomised control trial. *Lancet*, *367*(9518), 1247-1255. https://doi.org/10.1016/S0140-6736(06)68439-0

Harrison, R. L., & Jarvis, D. L. (2006). Protein N-glycosylation in the baculovirus-insect cell expression system and engineering of insect cells to produce

"mammalianized" recombinant glycoproteins. *Adv Virus Res*, *68*, 159-191. https://doi.org/10.1016/S0065-3527(06)68005-6

Hefferon, K. (2017). Plant Virus Expression Vectors: A Powerhouse for Global Health. *Biomedicines*, *5*(3). https://doi.org/10.3390/biomedicines5030044

Hiatt, A., Cafferkey, R., & Bowdish, K. (1989). Production of antibodies in transgenic plants. *Nature*, *342*(6245), 76-78. https://doi.org/10.1038/342076a0

Hiei, Y., Ohta, S., Komari, T., & Kumashiro, T. (1994). Efficient transformation of rice (Oryza sativa L.) mediated by Agrobacterium and sequence analysis of the boundaries of the T-DNA. *Plant J*, *6*(2), 271-282. https://doi.org/10.1046/j.1365-313x.1994.6020271.x

Hildesheim, A., Gonzalez, P., Kreimer, A. R., Wacholder, S., Schussler, J., Rodriguez, A. C., Porras, C., Schiffman, M., Sidawy, M., Schiller, J. T., Lowy, D. R., Herrero, R., & Costa Rica, H. P. V. V. T. G. (2016). Impact of human papillomavirus (HPV) 16 and 18 vaccination on prevalent infections and rates of cervical lesions after excisional treatment. *Am J Obstet Gynecol*, *215*(2), 212 e211-212 e215. https://doi.org/10.1016/j.ajog.2016.02.021

Hitzeroth II, Chabeda A, Whitehead MP, Graf M and Rybicki EP (2018) Optimizing a Human Papillomavirus Type 16 L1-Based Chimaeric Gene for Expression in Plants. Front. Bioeng. Biotechnol. 6:101. doi: 10.3389/fbioe.2018.00101

Hopkins, T. G., & Wood, N. (2013). Female human papillomavirus (HPV) vaccination: global uptake and the impact of attitudes. *Vaccine*, *31*(13), 1673-1679. https://doi.org/10.1016/j.vaccine.2013.01.028

Horvath, C. A., Boulet, G. A., Renoux, V. M., Delvenne, P. O., & Bogers, J. P. (2010). Mechanisms of cell entry by human papillomaviruses: an overview. *Virol J*, *7*, 11. https://doi.org/10.1186/1743-422x-7-11

Huang, C. F., Monie, A., Weng, W. H., & Wu, T. (2010). DNA vaccines for cervical cancer. *Am J Transl Res*, *2*(1), 75-87. https://www.ncbi.nlm.nih.gov/pubmed/20182584

Huang, Z., Santi, L., LePore, K., Kilbourne, J., Arntzen, C. J., & Mason, H. S. (2006). Rapid, high-level production of hepatitis B core antigen in plant leaf and its immunogenicity in mice. *Vaccine*, *24*(14), 2506-2513. https://doi.org/10.1016/j.vaccine.2005.12.024

Huebbers, J. W., & Buyel, J. F. (2021). On the verge of the market - Plant factories for the automated and standardized production of biopharmaceuticals. *Biotechnol Adv*, *46*, 107681. https://doi.org/10.1016/j.biotechadv.2020.107681

Hung, C. F., Ma, B., Monie, A., Tsen, S. W., & Wu, T. C. (2008). Therapeutic human papillomavirus vaccines: current clinical trials and future directions. *Expert Opin Biol Ther*, *8*(4), 421-439. https://doi.org/10.1517/14712598.8.4.421

Jedy-Agba, E., Joko, W. Y., Liu, B., Buziba, N. G., Borok, M., Korir, A., Masamba, L., Manraj, S. S., Finesse, A., Wabinga, H., Somdyala, N., & Parkin, D. M. (2020). Trends in cervical cancer incidence in sub-Saharan Africa. *Br J Cancer*, *123*(1), 148-154. https://doi.org/10.1038/s41416-020-0831-9

Jeoung, J. M., Krishnaveni, S., Muthukrishnan, S., Trick, H. N., & Liang, G. H. (2002). Optimization of sorghum transformation parameters using genes for green

fluorescent protein and beta-glucuronidase as visual markers. *Hereditas*, *137*(1), 20-28. https://doi.org/10.1034/j.1601-5223.2002.1370104.x

Jutras, P. V., Dodds, I., & van der Hoorn, R. A. L. (2020). Proteases of Nicotiana benthamiana: an emerging battle for molecular farming. *Current Opinion in Biotechnology*, *61*, 60-65. https://doi.org/https://doi.org/10.1016/j.copbio.2019.10.006

Keane-Myers, A. M., & Bell, M. (2014). Evolution of electroporated DNA vaccines. *Methods Mol Biol*, *1121*, 269-278. https://doi.org/10.1007/978-1-4614-9632-8_24

Kennedy, P. (2013). *HPV Pseudovirion Production in Plants.* University of Cape Town.

Khallouf, H., Grabowska, A. K., & Riemer, A. B. (2014). Therapeutic Vaccine Strategies against Human Papillomavirus. *Vaccines (Basel)*, *2*(2), 422-462. https://doi.org/10.3390/vaccines2020422

Khan, S. A. (2005). Plasmid rolling-circle replication: highlights of two decades of research. *Plasmid*, *53*(2), 126-136. https://doi.org/10.1016/j.plasmid.2004.12.008

Kim, T. K., & Eberwine, J. H. (2010). Mammalian cell transfection: the present and the future. *Anal Bioanal Chem*, *397*(8), 3173-3178. https://doi.org/10.1007/s00216-010-3821-6

Kines, R. C., Cerio, R. J., Roberts, J. N., Thompson, C. D., de Los Pinos, E., Lowy, D. R., & Schiller, J. T. (2016). Human papillomavirus capsids preferentially bind and infect tumor cells. *Int J Cancer*, *138*(4), 901-911. https://doi.org/10.1002/ijc.29823

Kines, R. C., Thompson, C. D., Lowy, D. R., Schiller, J. T., & Day, P. M. (2009). The initial steps leading to papillomavirus infection occur on the basement membrane prior to cell surface binding. *Proc Natl Acad Sci U S A*, *106*(48), 20458-20463. https://doi.org/10.1073/pnas.0908502106

Kines, R. C., Zarnitsyn, V., Johnson, T. R., Pang, Y. Y., Corbett, K. S., Nicewonger, J. D., Gangopadhyay, A., Chen, M., Liu, J., Prausnitz, M. R., Schiller, J. T., & Graham, B. S. (2015). Vaccination with human papillomavirus pseudovirus-encapsidated plasmids targeted to skin using microneedles. *PLoS One*, *10*(3), e0120797. https://doi.org/10.1371/journal.pone.0120797

Kirnbauer, R., Booy, F., Cheng, N., Lowy, D. R., & Schiller, J. T. (1992). Papillomavirus L1 major capsid protein self-assembles into virus-like particles that are highly immunogenic. *Proc Natl Acad Sci U S A*, *89*(24), 12180-12184. https://doi.org/10.1073/pnas.89.24.12180

Kirnbauer, R., Taub, J., Greenstone, H., Roden, R., Durst, M., Gissmann, L., Lowy, D. R., & Schiller, J. T. (1993). Efficient self-assembly of human papillomavirus type 16 L1 and L1-L2 into virus-like particles. *J Virol*, *67*(12), 6929-6936. https://doi.org/10.1128/JVI.67.12.6929-6936.1993

Kjemtrup, S., Talarico, T. L., & Ursin, V. (2014). Biotechnology: Pharming. In N. K. Van Alfen (Ed.), *Encyclopedia of Agriculture and Food Systems* (pp. 117-133). Academic Press. https://doi.org/https://doi.org/10.1016/B978-0-444-52512-3.00215-1

Knoff, J., Yang, B., Hung, C. F., & Wu, T. C. (2014). Cervical Cancer: Development of Targeted Therapies Beyond Molecular Pathogenesis. *Curr Obstet Gynecol Rep*, *3*(1), 18-32. https://doi.org/10.1007/s13669-013-0068-1

Koch, C., Ramsauer, A. S., Drogemuller, M., Ackermann, M., Gerber, V., & Tobler, K. (2018). Genomic comparison of bovine papillomavirus 1 isolates from bovine, equine and asinine lesional tissue samples. *Virus Res*, *244*, 6-12. https://doi.org/10.1016/j.virusres.2017.11.005

Komarova, T. V., Baschieri, S., Donini, M., Marusic, C., Benvenuto, E., & Dorokhov, Y. L. (2010). Transient expression systems for plant-derived biopharmaceuticals. *Expert Rev Vaccines*, *9*(8), 859-876. https://doi.org/10.1586/erv.10.85

Kubler, H., Scheel, B., Gnad-Vogt, U., Miller, K., Schultze-Seemann, W., Vom Dorp, F., Parmiani, G., Hampel, C., Wedel, S., Trojan, L., Jocham, D., Maurer, T., Rippin, G., Fotin-Mleczek, M., von der Mulbe, F., Probst, J., Hoerr, I., Kallen, K. J., Lander, T., & Stenzl, A. (2015). Self-adjuvanted mRNA vaccination in advanced prostate cancer patients: a first-in-man phase I/IIa study. *J Immunother Cancer*, *3*, 26. https://doi.org/10.1186/s40425-015-0068-y

Kuck, D., Leder, C., Kern, A., Muller, M., Piuko, K., Gissmann, L., & Kleinschmidt, J. A. (2006). Efficiency of HPV 16 L1/E7 DNA immunization: influence of cellular localization and capsid assembly. *Vaccine*, *24*(15), 2952-2965. https://doi.org/10.1016/j.vaccine.2005.12.023

Kumar, S., Biswas, M., & Jose, T. (2015). HPV vaccine: Current status and future directions. *Med J Armed Forces India*, *71*(2), 171-177. https://doi.org/10.1016/j.mjafi.2015.02.006

Lai, E. M., Shih, H. W., Wen, S. R., Cheng, M. W., Hwang, H. H., & Chiu, S. H. (2006). Proteomic analysis of Agrobacterium tumefaciens response to the Vir gene inducer acetosyringone. *Proteomics*, *6*(14), 4130-4136. https://doi.org/10.1002/pmic.200600254

Lai, H., & Chen, Q. (2012). Bioprocessing of plant-derived virus-like particles of Norwalk virus capsid protein under current Good Manufacture Practice regulations. *Plant Cell Rep*, *31*(3), 573-584. https://doi.org/10.1007/s00299-011-1196-6

Lai, H., Engle, M., Fuchs, A., Keller, T., Johnson, S., Gorlatov, S., Diamond, M. S., & Chen, Q. (2010). Monoclonal antibody produced in plants efficiently treats West Nile virus infection in mice. *Proc Natl Acad Sci U S A*, *107*(6), 2419-2424. https://doi.org/10.1073/pnas.0914503107

Lamprecht, R. L., Kennedy, P., Huddy, S. M., Bethke, S., Hendrikse, M., Hitzeroth, II, & Rybicki, E. P. (2016). Production of Human papillomavirus pseudovirions in plants and their use in pseudovirion-based neutralisation assays in mammalian cells. *Sci Rep*, *6*, 20431. https://doi.org/10.1038/srep20431

Landry, N., Ward, B. J., Trépanier, S., Montomoli, E., Dargis, M., Lapini, G., & Vézina, L. P. (2010). Preclinical and clinical development of plant-made virus-like particle vaccine against avian H5N1 influenza. *PLoS One*, *5*(12), e15559. https://doi.org/10.1371/journal.pone.0015559

Lee, M. R., Kim, Y. J., Hwang, D.-Y., Kang, T. S., Hwang, J. H., Lim, C. H., Kang, H.-K., Goo, J. S., Lim, H.-J., Ahn, K. S., Cho, J. S., Chae, K. R., & Kim, Y. K. (2003). An In Vitro Bioassay for Xenobiotics Using the SXR-Driven Human CYP3A4/lac Z Reporter Gene. *International Journal of Toxicology*, *22*, 207 - 213.

Lemp, J. M., De Neve, J. W., Bussmann, H., Chen, S., Manne-Goehler, J., Theilmann, M., Marcus, M. E., Ebert, C., Probst, C., Tsabedze-Sibanyoni, L., Sturua, L., Kibachio, J. M., Moghaddam, S. S., Martins, J. S., Houinato, D., Houehanou, C., Gurung, M. S., Gathecha, G., Farzadfar, F., Geldsetzer, P. (2020). Lifetime Prevalence of Cervical Cancer Screening in 55 Low- and Middle-Income Countries. *Jama*, *324*(15), 1532-1542. https://doi.org/10.1001/jama.2020.16244

Lin, K., Doolan, K., Hung, C. F., & Wu, T. C. (2010). Perspectives for preventive and therapeutic HPV vaccines. *J Formos Med Assoc*, *109*(1), 4-24. https://doi.org/10.1016/s0929-6646(10)60017-4

Liu, D., Shriver, Z., Qi, Y., Venkataraman, G., & Sasisekharan, R. (2002). Dynamic regulation of tumor growth and metastasis by heparan sulfate glycosaminoglycans. *Semin Thromb Hemost*, *28*(1), 67-78. https://doi.org/10.1055/s-2002-20565

Lizardi, P. M., Huang, X., Zhu, Z., Bray-Ward, P., Thomas, D. C., & Ward, D. C. (1998). Mutation detection and single-molecule counting using isothermal rolling-circle amplification. *Nat Genet*, *19*(3), 225-232. https://doi.org/10.1038/898

Lomonossoff, G. P., & D'Aoust, M. A. (2016). Plant-produced biopharmaceuticals: A case of technical developments driving clinical deployment. *Science*, *353*(6305), 1237-1240. https://doi.org/10.1126/science.aaf6638

Love, A. J., Chapman, S. N., Matic, S., Noris, E., Lomonossoff, G. P., & Taliansky, M. (2012). In planta production of a candidate vaccine against bovine papillomavirus type 1. *Planta*, *236*(4), 1305-1313. https://doi.org/10.1007/s00425-012-1692-0

Ma, B., Roden, R. B., Hung, C. F., & Wu, T. C. (2011). HPV pseudovirions as DNA delivery vehicles. *Ther Deliv*, *2*(4), 427-430. https://doi.org/10.4155/tde.11.28

Maclean, J., Koekemoer, M., Olivier, A. J., Stewart, D., Hitzeroth, II, Rademacher, T., Fischer, R., Williamson, A. L., & Rybicki, E. P. (2007). Optimization of human papillomavirus type 16 (HPV-16) L1 expression in plants: comparison of the suitability of different HPV-16 L1 gene variants and different cell-compartment localization. *J Gen Virol*, *88*(Pt 5), 1460-1469. https://doi.org/10.1099/vir.0.82718-0

Madison, K. C. (2003). Barrier function of the skin: "la raison d'etre" of the epidermis. *J Invest Dermatol*, *121*(2), 231-241. https://doi.org/10.1046/j.1523-1747.2003.12359.x

Mallon, R. G., Wojciechowicz, D., & Defendi, V. (1987). DNA-binding activity of papillomavirus proteins. *J Virol*, *61*(5), 1655-1660. https://doi.org/10.1128/JVI.61.5.1655-1660.1987

Mao, C., Koutsky, L. A., Ault, K. A., Wheeler, C. M., Brown, D. R., Wiley, D. J., Alvarez, F. B., Bautista, O. M., Jansen, K. U., & Barr, E. (2006). Efficacy of human papillomavirus-16 vaccine to prevent cervical intraepithelial neoplasia: a randomized controlled trial. *Obstet Gynecol*, *107*(1), 18-27. https://doi.org/10.1097/01.AOG.0000192397.41191.fb

Marchetti, B., Ashrafi, G. H., Tsirimonaki, E., O'Brien, P. M., & Campo, M. S. (2002). The bovine papillomavirus oncoprotein E5 retains MHC class I molecules in the Golgi apparatus and prevents their transport to the cell surface. *Oncogene*, *21*(51), 7808-7816. https://doi.org/10.1038/sj.onc.1205885

Marsian, J., & Lomonossoff, G. P. (2016). Molecular pharming - VLPs made in plants. *Curr Opin Biotechnol*, *37*, 201-206. https://doi.org/10.1016/j.copbio.2015.12.007

Mason, H. S., Lam, D. M., & Arntzen, C. J. (1992). Expression of hepatitis B surface antigen in transgenic plants. *Proc Natl Acad Sci U S A*, *89*(24), 11745-11749. https://doi.org/10.1073/pnas.89.24.11745

Matsuda, R., Tahara, A., Matoba, N., & Fujiwara, K. (2012). Virus vector-mediated rapid protein production in Nicotiana benthamiana: effects of temperature and photosynthetic photon flux density on hemagglutinin accumulation. *Environmental Control in Biology*, *50*(4), 375-381.

Meisels, A., & Fortin, R. (1976). Condylomatous lesions of the cervix and vagina. I. Cytologic patterns. *Acta Cytol*, *20*(6), 505-509. https://www.ncbi.nlm.nih.gov/pubmed/1069445

Merlin, M., Gecchele, E., Capaldi, S., Pezzotti, M., & Avesani, L. (2014). Comparative evaluation of recombinant protein production in different biofactories: the green perspective. *Biomed Res Int*, *2014*, 136419. https://doi.org/10.1155/2014/136419

Meyers, A., Chakauya, E., Shephard, E., Tanzer, F. L., Maclean, J., Lynch, A., Williamson, A. L., & Rybicki, E. P. (2008). Expression of HIV-1 antigens in plants as potential subunit vaccines. *BMC Biotechnol*, *8*, 53. https://doi.org/10.1186/1472-6750-8-53

Middleton, K., Peh, W., Southern, S., Griffin, H., Sotlar, K., Nakahara, T., El-Sherif, A., Morris, L., Seth, R., Hibma, M., Jenkins, D., Lambert, P., Coleman, N., & Doorbar, J. (2003). Organization of human papillomavirus productive cycle during neoplastic progression provides a basis for selection of diagnostic markers. *J Virol*, *77*(19), 10186-10201. https://doi.org/10.1128/jvi.77.19.10186-10201.2003

Modis, Y., Trus, B. L., & Harrison, S. C. (2002). Atomic model of the papillomavirus capsid. *Embo j*, *21*(18), 4754-4762. https://doi.org/10.1093/emboj/cdf494

Monroy-Garcia, A., Gomez-Lim, M. A., Weiss-Steider, B., Hernandez-Montes, J., Huerta-Yepez, S., Rangel-Santiago, J. F., Santiago-Osorio, E., & Mora Garcia Mde, L. (2014). Immunization with an HPV-16 L1-based chimeric virus-like particle containing HPV-16 E6 and E7 epitopes elicits long-lasting prophylactic and therapeutic efficacy in an HPV-16 tumor mice model. *Arch Virol*, *159*(2), 291-305. https://doi.org/10.1007/s00705-013-1819-z

Moody, C. A., & Laimins, L. A. (2010). Human papillomavirus oncoproteins: pathways to transformation. *Nat Rev Cancer*, *10*(8), 550-560. https://doi.org/10.1038/nrc2886

Moon, K. B., Park, J. S., Park, Y. I., Song, I. J., Lee, H. J., Cho, H. S., Jeon, J. H., & Kim, H. S. (2019). Development of Systems for the Production of Plant-Derived Biopharmaceuticals. *Plants (Basel)*, *9*(1). https://doi.org/10.3390/plants9010030

Moscicki, A. B., Schiffman, M., Burchell, A., Albero, G., Giuliano, A. R., Goodman, M. T., Kjaer, S. K., & Palefsky, J. (2012). Updating the natural history of human papillomavirus and anogenital cancers. *Vaccine*, *30 Suppl 5*, F24-33. https://doi.org/10.1016/j.vaccine.2012.05.089

Munday, J. S. (2014). Bovine and human papillomaviruses: a comparative review. *Vet Pathol*, *51*(6), 1063-1075. https://doi.org/10.1177/0300985814537837

Munday, J. S., Hanlon, E. M., Howe, L., Squires, R. A., & French, A. F. (2007). Feline cutaneous viral papilloma associated with human papillomavirus type 9. *Vet Pathol*, *44*(6), 924-927. https://doi.org/10.1354/vp.44-6-924

Munger, K., & Howley, P. M. (2002). Human papillomavirus immortalization and transformation functions. *Virus Res*, *89*(2), 213-228. https://doi.org/10.1016/s0168-1702(02)00190-9

Naupu, P. N. (2019). *The Immunogenicity of Plant-produced Human Papillomavirus (HPV) Virus-like particles (VLPs) in Mice.* University of Cape Town.

Nguyen, H. D., Reddy, V. S., & Brooks, C. L. (2007). Deciphering the Kinetic Mechanism of Spontaneous Self-Assembly of Icosahedral Capsids. *Nano Letters*, *7*(2), 338-344. https://doi.org/10.1021/nl062449h

Noad, R., & Roy, P. (2003). Virus-like particles as immunogens. *Trends Microbiol*, *11*(9), 438-444. https://doi.org/10.1016/s0966-842x(03)00208-7

Norkunas, K., Harding, R., Dale, J., & Dugdale, B. (2018). Improving agroinfiltration-based transient gene expression in Nicotiana benthamiana. *Plant Methods*, *14*, 71. https://doi.org/10.1186/s13007-018-0343-2

Nosaki, S., Hoshikawa, K., Ezura, H., & Miura, K. (2021a). Transient protein expression systems in plants and their applications. *Plant Biotechnol (Tokyo)*, *38*(3), 297-304. https://doi.org/10.5511/plantbiotechnology.21.0610a

Nosaki, S., Kaneko, M. K., Tsuruta, F., Yoshida, H., Kato, Y., & Miura, K. (2021b). Prevention of necrosis caused by transient expression in Nicotiana benthamiana by application of ascorbic acid. *Plant Physiology*, *186*(2), 832-835. https://doi.org/10.1093/plphys/kiab102

O'Brien, J., & Lummis, S. C. (2004). Biolistic and diolistic transfection: using the gene gun to deliver DNA and lipophilic dyes into mammalian cells. *Methods*, *33*(2), 121-125. https://doi.org/10.1016/j.ymeth.2003.11.010

O'Brien, P. M., & Saveria Campo, M. (2002). Evasion of host immunity directed by papillomavirus-encoded proteins. *Virus Res*, *88*(1-2), 103-117. https://doi.org/10.1016/s0168-1702(02)00123-5

Ohlschlager, P., Pes, M., Osen, W., Durst, M., Schneider, A., Gissmann, L., & Kaufmann, A. M. (2006). An improved rearranged Human Papillomavirus Type

16 E7 DNA vaccine candidate (HPV-16 E7SH) induces an E7 wildtype-specific T cell response. *Vaccine*, *24*(15), 2880-2893. https://doi.org/10.1016/j.vaccine.2005.12.061

Otten, G., Schaefer, M., Doe, B., Liu, H., Srivastava, I., zur Megede, J., O'Hagan, D., Donnelly, J., Widera, G., Rabussay, D., Lewis, M. G., Barnett, S., & Ulmer, J. B. (2004). Enhancement of DNA vaccine potency in rhesus macaques by electroporation. *Vaccine*, *22*(19), 2489-2493. https://doi.org/10.1016/j.vaccine.2003.11.073

Ozaki, T., & Nakagawara, A. (2011). Role of p53 in Cell Death and Human Cancers. *Cancers (Basel)*, *3*(1), 994-1013. https://doi.org/10.3390/cancers3010994

Ozbun, M. A., & Meyers, C. (1998). Temporal usage of multiple promoters during the life cycle of human papillomavirus type 31b. *J Virol*, *72*(4), 2715-2722. https://doi.org/10.1128/JVI.72.4.2715-2722.1998

Park, C. J., & Seo, Y. S. (2015). Heat Shock Proteins: A Review of the Molecular Chaperones for Plant Immunity. *Plant Pathol J*, *31*(4), 323-333. https://doi.org/10.5423/PPJ.RW.08.2015.0150

Park, J., Throop, A. L., & LaBaer, J. (2015). Site-specific recombinational cloning using gateway and in-fusion cloning schemes. *Curr Protoc Mol Biol*, *110*, 3.20.21-23.20.23. https://doi.org/10.1002/0471142727.mb0320s110

Pastrana, D. V., Buck, C. B., Pang, Y. Y., Thompson, C. D., Castle, P. E., FitzGerald, P. C., Kruger Kjaer, S., Lowy, D. R., & Schiller, J. T. (2004). Reactivity of human sera in a sensitive, high-throughput pseudovirus-based papillomavirus neutralization assay for HPV16 and HPV18. *Virology*, *321*(2), 205-216. https://doi.org/10.1016/j.virol.2003.12.027

Peng, S., Ma, B., Chen, S. H., Hung, C. F., & Wu, T. (2011). DNA vaccines delivered by human papillomavirus pseudovirions as a promising approach for generating antigen-specific CD8+ T cell immunity. *Cell Biosci*, *1*, 26. https://doi.org/10.1186/2045-3701-1-26

Peng, S., Monie, A., Kang, T. H., Hung, C. F., Roden, R., & Wu, T. C. (2010). Efficient delivery of DNA vaccines using human papillomavirus pseudovirions. *Gene Ther*, *17*(12), 1453-1464. https://doi.org/10.1038/gt.2010.106

Pietersen, I. (2019). *Working towards a plant-produced Bovine papillomavirus vaccine: Expression of BPV1 virus-like particles and pseudovirions in Nicotiana benthamiana.* University of Cape Town. Cape Town, South Africa.

Pietersen, I., van Zyl, A., Rybicki, E., & Hitzeroth, I. (2020). Novel Production of Bovine Papillomavirus Pseudovirions in Tobacco Plants. *Pathogens*, *9*(12). https://doi.org/10.3390/pathogens9120996

Pillet, S., Racine, T., Nfon, C., Di Lenardo, T. Z., Babiuk, S., Ward, B. J., Kobinger, G. P., & Landry, N. (2015). Plant-derived H7 VLP vaccine elicits protective immune response against H7N9 influenza virus in mice and ferrets. *Vaccine*, *33*(46), 6282-6289. https://doi.org/10.1016/j.vaccine.2015.09.065

Pineo, C. B., Hitzeroth, II, & Rybicki, E. P. (2013). Immunogenic assessment of plant-produced human papillomavirus type 16 L1/L2 chimaeras. *Plant Biotechnol J*, *11*(8), 964-975. https://doi.org/10.1111/pbi.12089

Potera, C. (2012). Vaccine manufacturing gets boost from tobacco plants: Canada-based medicago opens US Facility to exploit its influenza vaccine production method. *Genetic Engineering & Biotechnology News*, *32*(6), 8-10.

Pyeon, D., Lambert, P. F., & Ahlquist, P. (2005). Production of infectious human papillomavirus independently of viral replication and epithelial cell differentiation. *Proceedings of the national academy of sciences*, *102*(26), 9311-9316. https://doi.org/doi:10.1073/pnas.0504020102

Qi, Y. M., Peng, S. W., Hengst, K., Evander, M., Park, D. S., Zhou, J., & Frazer, I. H. (1996). Epithelial cells display separate receptors for papillomavirus VLPs and for soluble L1 capsid protein. *Virology*, *216*(1), 35-45. https://doi.org/10.1006/viro.1996.0032

Ramiro, A. R., de Yébenes, V. G., Trigueros, C., Carrasco, Y. R., & Toribio, M. L. (1998). Enhanced green fluorescent protein as an efficient reporter gene for retroviral transduction of human multipotent lymphoid precursors. *Human gene therapy*, *9 7*, 1103-1109.

Ramoz, N., Rueda, L. A., Bouadjar, B., Montoya, L. S., Orth, G., & Favre, M. (2002). Mutations in two adjacent novel genes are associated with epidermodysplasia verruciformis. *Nat Genet*, *32*(4), 579-581. https://doi.org/10.1038/ng1044

Rector, A., & Van Ranst, M. (2013). Animal papillomaviruses. *Virology*, *445*(1-2), 213-223. https://doi.org/10.1016/j.virol.2013.05.007

Regnard, G. L., Halley-Stott, R. P., Tanzer, F. L., Hitzeroth, II, & Rybicki, E. P. (2010). High level protein expression in plants through the use of a novel autonomously replicating geminivirus shuttle vector. *Plant Biotechnol J*, *8*(1), 38-46. https://doi.org/10.1111/j.1467-7652.2009.00462.x

Rikhotso, R. R., Mitchell, E. M., Wilson, D. T., Doede, A., Matume, N. D., & Bessong, P. O. (2022). Prevalence and distribution of selected cervical human papillomavirus types in HIV infected and HIV uninfected women in South Africa, 1989-2021: A narrative review. *S Afr J Infect Dis*, *37*(1), 363. https://doi.org/10.4102/sajid.v37i1.363

Rivera, A. L., Gómez-Lim, M., Fernández, F., & Loske, A. M. (2012). Physical methods for genetic plant transformation. *Phys Life Rev*, *9*(3), 308-345. https://doi.org/10.1016/j.plrev.2012.06.002

Roberts, J. N., Buck, C. B., Thompson, C. D., Kines, R., Bernardo, M., Choyke, P. L., Lowy, D. R., & Schiller, J. T. (2007). Genital transmission of HPV in a mouse model is potentiated by nonoxynol-9 and inhibited by carrageenan. *Nat Med*, *13*(7), 857-861. https://doi.org/10.1038/nm1598

Roden, R. B., Greenstone, H. L., Kirnbauer, R., Booy, F. P., Jessie, J., Lowy, D. R., & Schiller, J. T. (1996). In vitro generation and type-specific neutralization of a human papillomavirus type 16 virion pseudotype. *J Virol*, *70*(9), 5875-5883. https://doi.org/10.1128/JVI.70.9.5875-5883.1996

Roden, R. B., Kirnbauer, R., Jenson, A. B., Lowy, D. R., & Schiller, J. T. (1994). Interaction of papillomaviruses with the cell surface. *J Virol*, *68*(11), 7260-7266. https://doi.org/10.1128/JVI.68.11.7260-7266.1994

Roden, R. B., Lowy, D. R., & Schiller, J. T. (1997). Papillomavirus is resistant to desiccation. *J Infect Dis*, *176*(4), 1076-1079. https://doi.org/10.1086/516515

Roden, R. B., Yutzy, W. H. t., Fallon, R., Inglis, S., Lowy, D. R., & Schiller, J. T. (2000). Minor capsid protein of human genital papillomaviruses contains subdominant, cross-neutralizing epitopes. *Virology*, *270*(2), 254-257. https://doi.org/10.1006/viro.2000.0272

Rogowsky, P. M., Close, T. J., Chimera, J. A., Shaw, J. J., & Kado, C. I. (1987). Regulation of the vir genes of Agrobacterium tumefaciens plasmid pTiC58. *J Bacteriol*, *169*(11), 5101-5112. https://doi.org/10.1128/jb.169.11.5101-5112.1987

Roman, A., & Munger, K. (2013). The papillomavirus E7 proteins. *Virology*, *445*(1-2), 138-168. https://doi.org/10.1016/j.virol.2013.04.013

Rookes, J. E., & Cahill, D. M. (2004). A PAL1 Gene Promoter–Green Fluorescent Protein Reporter System to Analyse Defence Responses in Live Cells of Arabidopsis thaliana. *European Journal of Plant Pathology*, *109*, 83-94.

Roozendaal, R., Mebius, R. E., & Kraal, G. (2008). The conduit system of the lymph node. *Int Immunol*, *20*(12), 1483-1487. https://doi.org/10.1093/intimm/dxn110

Rosales, C., & Rosales, R. (2017). Prophylactic and Therapeutic Vaccines against Human Papillomavirus Infections. In *Vaccines*. https://doi.org/10.5772/intechopen.69548

Rozov, S. M., & Deineko, E. V. (2022). Increasing the Efficiency of the Accumulation of Recombinant Proteins in Plant Cells: The Role of Transport Signal Peptides. *Plants (Basel)*, *11*(19). https://doi.org/10.3390/plants11192561

Rybicki, E. P. (2009). Plant-produced vaccines: promise and reality. *Drug Discov Today*, *14*(1-2), 16-24. https://doi.org/10.1016/j.drudis.2008.10.002

Rybicki, E. P. (2010). Plant-made vaccines for humans and animals. *Plant Biotechnol J*, *8*(5), 620-637. https://doi.org/10.1111/j.1467-7652.2010.00507.x

Rybicki, E. P. (2014). Plant-based vaccines against viruses. *Virol J*, *11*, 205. https://doi.org/10.1186/s12985-014-0205-0

Sainsbury, F., & Lomonossoff, G. P. (2014). Transient expressions of synthetic biology in plants. *Curr Opin Plant Biol*, *19*, 1-7. https://doi.org/10.1016/j.pbi.2014.02.003

Sambrook, J., Fritsch, E. F., & Maniatis, T. (1989). *Molecular cloning: a laboratory manual*. Cold spring harbor laboratory press.

Schafer, M., & Werner, S. (2008). Cancer as an overhealing wound: an old hypothesis revisited. *Nat Rev Mol Cell Biol*, *9*(8), 628-638. https://doi.org/10.1038/nrm2455

Schiller, J. T., Castellsague, X., & Garland, S. M. (2012). A review of clinical trials of human papillomavirus prophylactic vaccines. *Vaccine*, *30 Suppl 5*, F123-138. https://doi.org/10.1016/j.vaccine.2012.04.108

Schiller, J. T., Cerqueira, C., Pang, Y. Y., Day, P. M., Thompson, C. D., Buck, C. B., & Lowy, D. R. (2016). A Cell-Free Assembly System for Generating Infectious Human Papillomavirus 16 Capsids Implicates a Size Discrimination Mechanism for Preferential Viral Genome Packaging. *J Virol*, *90*(2), 1096-1107. https://doi.org/10.1128/JVI.02497-15

Schiller, J. T., & Davies, P. (2004). Delivering on the promise: HPV vaccines and cervical cancer. *Nat Rev Microbiol*, *2*(4), 343-347. https://doi.org/10.1038/nrmicro867

Schiller, J. T., Day, P. M., & Kines, R. C. (2010). Current understanding of the mechanism of HPV infection. *Gynecol Oncol*, *118*(1 Suppl), S12-17. https://doi.org/10.1016/j.ygyno.2010.04.004

Schiller, J. T., & Müller, M. (2015). Next generation prophylactic human papillomavirus vaccines. *The Lancet Oncology*, *16*(5), e217-e225. https://doi.org/10.1016/s1470-2045(14)71179-9

Schmidt-Rose, T., Pollet, D., Will, K., Bergemann, J., & Wittern, K. P. (1999). Analysis of UV-B-induced DNA damage and its repair in heat-shocked skin cells. *Journal of photochemistry and photobiology. B, Biology*, *53 1-3*, 144-152.

Schwarz, E., Dürst, M., Demankowski, C., Lattermann, O., Zech, R., Wolfsperger, E., Suhai, S., & zur Hausen, H. (1983). DNA sequence and genome organization of genital human papillomavirus type 6b. *Embo j*, *2*(12), 2341-2348. https://doi.org/10.1002/j.1460-2075.1983.tb01744.x

Schwarz, E., Freese, U. K., Gissmann, L., Mayer, W., Roggenbuck, B., Stremlau, A., & zur Hausen, H. (1985). Structure and transcription of human papillomavirus sequences in cervical carcinoma cells. *Nature*, *314*(6006), 111-114. https://doi.org/10.1038/314111a0

Selinka, H. C., Florin, L., Patel, H. D., Freitag, K., Schmidtke, M., Makarov, V. A., & Sapp, M. (2007). Inhibition of transfer to secondary receptors by heparan sulfate-binding drug or antibody induces noninfectious uptake of human papillomavirus. *J Virol*, *81*(20), 10970-10980. https://doi.org/10.1128/JVI.00998-07

Shafti-Keramat, S., Handisurya, A., Kriehuber, E., Meneguzzi, G., Slupetzky, K., & Kirnbauer, R. (2003). Different heparan sulfate proteoglycans serve as cellular receptors for human papillomaviruses. *J Virol*, *77*(24), 13125-13135. https://doi.org/10.1128/jvi.77.24.13125-13135.2003

Shafti-Keramat, S., Schellenbacher, C., Handisurya, A., Christensen, N., Reininger, B., Brandt, S., & Kirnbauer, R. (2009). Bovine papillomavirus type 1 (BPV1) and BPV2 are closely related serotypes. *Virology*, *393*(1), 1-6. https://doi.org/https://doi.org/10.1016/j.virol.2009.07.036

Shen, W. J., & Forde, B. G. (1989). Efficient transformation of Agrobacterium spp. by high voltage electroporation. *Nucleic Acids Res*, *17*(20), 8385. https://doi.org/10.1093/nar/17.20.8385

Sherman, L., Jackman, A., Itzhaki, H., Stoppler, M. C., Koval, D., & Schlegel, R. (1997). Inhibition of serum- and calcium-induced differentiation of human keratinocytes by HPV16 E6 oncoprotein: role of p53 inactivation. *Virology*, *237*(2), 296-306. https://doi.org/10.1006/viro.1997.8778

Shi, W., Liu, J., Huang, Y., & Qiao, L. (2001). Papillomavirus pseudovirus: a novel vaccine to induce mucosal and systemic cytotoxic T-lymphocyte responses. *J Virol*, *75*(21), 10139-10148. https://doi.org/10.1128/JVI.75.21.10139-10148.2001

Singh, G. K., Azuine, R. E., & Siahpush, M. (2012). Global Inequalities in Cervical Cancer Incidence and Mortality are Linked to Deprivation, Low Socioeconomic Status, and Human Development. *Int J MCH AIDS*, *1*(1), 17-30. https://doi.org/10.21106/ijma.12

Skeate, J. G., Woodham, A. W., Einstein, M. H., Da Silva, D. M., & Kast, W. M. (2016). Current therapeutic vaccination and immunotherapy strategies for HPV-related diseases. *Hum Vaccin Immunother*, *12*(6), 1418-1429. https://doi.org/10.1080/21645515.2015.1136039

Smith, M. A., Winch, K., Canfell, K., & Brotherton, J. M. (2021). Effective HPV vaccination coverage in Australia by number of doses and two-dose spacing: What if one or two doses are sufficient? *Tumour Virus Res*, *11*, 200216. https://doi.org/10.1016/j.tvr.2021.200216

Sohrab, S. S., Suhail, M., Kamal, M. A., Husen, A., & Azhar, E. I. (2017). Recent Development and Future Prospects of Plant-Based Vaccines. *Curr Drug Metab*, *18*(9), 831-841. https://doi.org/10.2174/1389200218666170711121810

Sozhamannan, S., & Chattoraj, D. K. (1993). Heat shock proteins DnaJ, DnaK, and GrpE stimulate P1 plasmid replication by promoting initiator binding to the origin. *Journal of Bacteriology*, *175*, 3546 - 3555.

Spoden, G., Kuhling, L., Cordes, N., Frenzel, B., Sapp, M., Boller, K., Florin, L., & Schelhaas, M. (2013). Human papillomavirus types 16, 18, and 31 share similar endocytic requirements for entry. *J Virol*, *87*(13), 7765-7773. https://doi.org/10.1128/JVI.00370-13

Stacey, S. N., Jordan, D., Williamson, A. J., Brown, M., Coote, J. H., & Arrand, J. R. (2000). Leaky scanning is the predominant mechanism for translation of human papillomavirus type 16 E7 oncoprotein from E6/E7 bicistronic mRNA. *J Virol*, *74*(16), 7284-7297. https://doi.org/10.1128/jvi.74.16.7284-7297.2000

Stander, J., Mbewana, S., & Meyers, A. E. (2022). Plant-Derived Human Vaccines: Recent Developments. *BioDrugs*, *36*(5), 573-589. https://doi.org/10.1007/s40259-022-00544-8

Stauffer, Y., Raj, K., Masternak, K., & Beard, P. (1998). Infectious human papillomavirus type 18 pseudovirions. *J Mol Biol*, *283*(3), 529-536. https://doi.org/10.1006/jmbi.1998.2113

Stellwagen, N. C., & Stellwagen, E. (2009). Effect of the matrix on DNA electrophoretic mobility. *J Chromatogr A*, *1216*(10), 1917-1929. https://doi.org/10.1016/j.chroma.2008.11.090

Sung, H., Ferlay, J., Siegel, R. L., Laversanne, M., Soerjomataram, I., Jemal, A., & Bray, F. (2021). Global Cancer Statistics 2020: GLOBOCAN Estimates of Incidence and Mortality Worldwide for 36 Cancers in 185 Countries. *CA Cancer J Clin*, *71*(3), 209-249. https://doi.org/10.3322/caac.21660

Tang, J., Liang, S., Zhang, J., Gao, Z., & Zhang, S. (2009). pGreen-S: a clone vector bearing absence of enhanced green fluorescent protein for screening recombinants. *Analytical biochemistry*, *388 1*, 173-174.

Thomas, D. R., & Walmsley, A. M. (2018). Plant-Made Veterinary Vaccines for Newcastle Disease Virus. In J. MacDonald (Ed.), *Prospects of Plant-Based*

Vaccines in Veterinary Medicine (pp. 149-167). Springer International Publishing. https://doi.org/10.1007/978-3-319-90137-4_6

Thomas, P., & Smart, T. G. (2005). HEK293 cell line: A vehicle for the expression of recombinant proteins. *Journal of Pharmacological and Toxicological Methods*, *51*(3), 187-200. https://doi.org/https://doi.org/10.1016/j.vascn.2004.08.014

Thuenemann, E. C., Lenzi, P., Love, A. J., Taliansky, M., Bécares, M., Zuñiga, S., Enjuanes, L., Zahmanova, G. G., Minkov, I. N., Matić, S., Noris, E., Meyers, A., Hattingh, A., Rybicki, E. P., Kiselev, O. I., Ravin, N. V., Eldarov, M. A., Skryabin, K. G., & Lomonossoff, G. P. (2013). The use of transient expression systems for the rapid production of virus-like particles in plants. *Curr Pharm Des*, *19*(31), 5564-5573. https://doi.org/10.2174/1381612811319310011

Torrent, M., Llompart, B., Lasserre-Ramassamy, S., Llop-Tous, I., Bastida, M., Marzabal, P., Westerholm-Parvinen, A., Saloheimo, M., Heifetz, P. B., & Ludevid, M. D. (2009). Eukaryotic protein production in designed storage organelles. *BMC Biol*, *7*, 5. https://doi.org/10.1186/1741-7007-7-5

Touze, A., & Coursaget, P. (1998). In vitro gene transfer using human papillomavirus-like particles. *Nucleic Acids Res*, *26*(5), 1317-1323. https://doi.org/10.1093/nar/26.5.1317

Towbin, H., Staehelin, T., & Gordon, J. (1979). Electrophoretic transfer of proteins from polyacrylamide gels to nitrocellulose sheets: procedure and some applications. *Proceedings of the national academy of sciences*, *76*(9), 4350-4354.

Tremblay, R., Wang, D., Jevnikar, A. M., & Ma, S. (2010). Tobacco, a highly efficient green bioreactor for production of therapeutic proteins. *Biotechnol Adv*, *28*(2), 214-221. https://doi.org/10.1016/j.biotechadv.2009.11.008

Trombetta, C. M., Marchi, S., Manini, I., Lazzeri, G., & Montomoli, E. (2019). Challenges in the development of egg-independent vaccines for influenza. *Expert Rev Vaccines*, *18*(7), 737-750. https://doi.org/10.1080/14760584.2019.1639503

Trus, B. L., Roden, R. B., Greenstone, H. L., Vrhel, M., Schiller, J. T., & Booy, F. P. (1997). Novel structural features of bovine papillomavirus capsid revealed by a three-dimensional reconstruction to 9 A resolution. *Nat Struct Biol*, *4*(5), 413-420. https://doi.org/10.1038/nsb0597-413

Tsai, Y. L., Wang, M. H., Gao, C., Klüsener, S., Baron, C., Narberhaus, F., & Lai, E. M. (2009). Small heat-shock protein HspL is induced by VirB protein(s) and promotes VirB/D4-mediated DNA transfer in Agrobacterium tumefaciens. *Microbiology (Reading)*, *155*(Pt 10), 3270-3280. https://doi.org/10.1099/mic.0.030676-0

Tseng, C. W., Trimble, C., Zeng, Q., Monie, A., Alvarez, R. D., Huh, W. K., Hoory, T., Wang, M. C., Hung, C. F., & Wu, T. C. (2009). Low-dose radiation enhances therapeutic HPV DNA vaccination in tumor-bearing hosts. *Cancer Immunol Immunother*, *58*(5), 737-748. https://doi.org/10.1007/s00262-008-0596-0

Tyring, S. K. (2000). Human papillomavirus infections: epidemiology, pathogenesis, and host immune response. *J Am Acad Dermatol*, *43*(1 Pt 2), S18-26. https://doi.org/10.1067/mjd.2000.107807

Tzfira, T., Li, J., Lacroix, B., & Citovsky, V. (2004). Agrobacterium T-DNA integration: molecules and models. *Trends Genet*, *20*(8), 375-383. https://doi.org/10.1016/j.tig.2004.06.004

Ul Haq, S., Khan, A., Ali, M., Khattak, A. M., Gai, W. X., Zhang, H. X., Wei, A. M., & Gong, Z. H. (2019). Heat Shock Proteins: Dynamic Biomolecules to Counter Plant Biotic and Abiotic Stresses. *Int J Mol Sci*, *20*(21). https://doi.org/10.3390/ijms20215321

Usha, R., Rohll, J. B., Spall, V. E., Shanks, M., Maule, A. J., Johnson, J. E., & Lomonossoff, G. P. (1993). Expression of an animal virus antigenic site on the surface of a plant virus particle. *Virology*, *197*(1), 366-374. https://doi.org/10.1006/viro.1993.1598

Vaghchhipawala, Z., Rojas, C. M., Senthil-Kumar, M., & Mysore, K. S. (2011). Agroinoculation and agroinfiltration: simple tools for complex gene function analyses. *Methods Mol Biol*, *678*, 65-76. https://doi.org/10.1007/978-1-60761-682-5_6

Van Doorslaer, K. (2013). Evolution of the papillomaviridae. *Virology*, *445*(1-2), 11-20. https://doi.org/10.1016/j.virol.2013.05.012

van Zyl, A. R., & Hitzeroth, II. (2016). Purification of Virus-Like Particles (VLPs) from Plants. *Methods Mol Biol*, *1404*, 569-579. https://doi.org/10.1007/978-1-4939-3389-1_37

Varsani, A., Williamson, A. L., Rose, R. C., Jaffer, M., & Rybicki, E. P. (2003). Expression of Human papillomavirus type 16 major capsid protein in transgenic Nicotiana tabacum cv. Xanthi. *Arch Virol*, *148*(9), 1771-1786. https://doi.org/10.1007/s00705-003-0119-4

Varsani, A., Williamson, A. L., Stewart, D., & Rybicki, E. P. (2006). Transient expression of Human papillomavirus type 16 L1 protein in Nicotiana benthamiana using an infectious tobamovirus vector. *Virus Res*, *120*(1-2), 91-96. https://doi.org/10.1016/j.virusres.2006.01.022

Velichko, A. K., Petrova, N. V., Kantidze, O. L., & Razin, S. V. (2012). Dual effect of heat shock on DNA replication and genome integrity. *Molecular Biology of the Cell*, *23*, 3450 - 3460.

Voinnet, O., Rivas, S., Mestre, P., & Baulcombe, D. (2003). An enhanced transient expression system in plants based on suppression of gene silencing by the p19 protein of tomato bushy stunt virus. *Plant J*, *33*(5), 949-956. https://doi.org/10.1046/j.1365-313x.2003.01676.x

Walboomers, J. M., Jacobs, M. V., Manos, M. M., Bosch, F. X., Kummer, J. A., Shah, K. V., Snijders, P. J., Peto, J., Meijer, C. J., & Muñoz, N. (1999). Human papillomavirus is a necessary cause of invasive cervical cancer worldwide. *J Pathol*, *189*(1), 12-19. https://doi.org/10.1002/(sici)1096-9896(199909)189:1<12::Aid-path431>3.0.Co;2-f

Walsh, G., & Walsh, E. (2022). Biopharmaceutical benchmarks 2022. *Nature Biotechnology*, *40*(12), 1722-1760. https://doi.org/10.1038/s41587-022-01582-x

Wang, J. W., & Roden, R. B. (2013). Virus-like particles for the prevention of human papillomavirus-associated malignancies. *Expert Rev Vaccines*, *12*(2), 129-141. https://doi.org/10.1586/erv.12.151

Ward, B. J., Makarkov, A., Séguin, A., Pillet, S., Trépanier, S., Dhaliwall, J., Libman, M. D., Vesikari, T., & Landry, N. (2020). Efficacy, immunogenicity, and safety of a plant-derived, quadrivalent, virus-like particle influenza vaccine in adults (18-64 years) and older adults (≥65 years): two multicentre, randomised phase 3 trials. *Lancet*, *396*(10261), 1491-1503. https://doi.org/10.1016/s0140-6736(20)32014-6

Warzecha, H., Mason, H. S., Lane, C., Tryggvesson, A., Rybicki, E., Williamson, A. L., Clements, J. D., & Rose, R. C. (2003). Oral immunogenicity of human papillomavirus-like particles expressed in potato. *J Virol*, *77*(16), 8702-8711. https://doi.org/10.1128/jvi.77.16.8702-8711.2003

Whitehead, M., Ohlschlager, P., Almajhdi, F. N., Alloza, L., Marzabal, P., Meyers, A. E., Hitzeroth, II, & Rybicki, E. P. (2014). Human papillomavirus (HPV) type 16 E7 protein bodies cause tumour regression in mice. *BMC Cancer*, *14*, 367. https://doi.org/10.1186/1471-2407-14-367

Wilson, V. G., West, M., Woytek, K., & Rangasamy, D. (2002). Papillomavirus E1 proteins: form, function, and features. *Virus Genes*, *24*(3), 275-290. https://doi.org/10.1023/a:1015336817836

Wolf, M., Garcea, R. L., Grigorieff, N., & Harrison, S. C. (2010). Subunit interactions in bovine papillomavirus. *Proc Natl Acad Sci U S A*, *107*(14), 6298-6303. https://doi.org/10.1073/pnas.0914604107

Wu, J., Gao, T., Hu, J., Zhao, L., Yu, C., & Ma, F. (2022). Research advances in function and regulation mechanisms of plant small heat shock proteins (sHSPs) under environmental stresses. *Sci Total Environ*, *825*, 154054. https://doi.org/10.1016/j.scitotenv.2022.154054

Yan, J., Harris, K., Khan, A. S., Draghia-Akli, R., Sewell, D., & Weiner, D. B. (2008). Cellular immunity induced by a novel HPV18 DNA vaccine encoding an E6/E7 fusion consensus protein in mice and rhesus macaques. *Vaccine*, *26*(40), 5210-5215. https://doi.org/10.1016/j.vaccine.2008.03.069

Yan, J., Reichenbach, D. K., Corbitt, N., Hokey, D. A., Ramanathan, M. P., McKinney, K. A., Weiner, D. B., & Sewell, D. (2009). Induction of antitumor immunity in vivo following delivery of a novel HPV-16 DNA vaccine encoding an E6/E7 fusion antigen. *Vaccine*, *27*(3), 431-440. https://doi.org/10.1016/j.vaccine.2008.10.078

Yanez, R. J., Lamprecht, R., Granadillo, M., Weber, B., Torrens, I., Rybicki, E. P., & Hitzeroth, I. I. (2017). Expression optimization of a cell membrane-penetrating human papillomavirus type 16 therapeutic vaccine candidate in Nicotiana benthamiana. PLoS One, 12(8), e0183177.

Yang, A., Farmer, E., Wu, T. C., & Hung, C. F. (2016). Perspectives for therapeutic HPV vaccine development. *J Biomed Sci*, *23*(1), 75. https://doi.org/10.1186/s12929-016-0293-9

Zhang, G., Gurtu, V. E., & Kain, S. R. (1996). An enhanced green fluorescent protein allows sensitive detection of gene transfer in mammalian cells. *Biochemical and biophysical research communications*, *227 3*, 707-711.

Zhang, G. G., Rodrigues, L., Rovinski, B., & White, K. A. (2002). Production of HIV-1 p24 protein in transgenic tobacco plants. *Mol Biotechnol*, *20*(2), 131-136. https://doi.org/10.1385/mb:20:2:131

Zhao, K. N., Frazer, I. H., Jun Liu, W., Williams, M., & Zhou, J. (1999). Nucleotides 1506-1625 of bovine papillomavirus type 1 genome can enhance DNA packaging by L1/L2 capsids. *Virology*, *259*(1), 211-218. https://doi.org/10.1006/viro.1999.9714

Zhao, K. N., Hengst, K., Liu, W. J., Liu, Y. H., Liu, X. S., McMillan, N. A., & Frazer, I. H. (2000). BPV1 E2 protein enhances packaging of full-length plasmid DNA in BPV1 pseudovirions. *Virology*, *272*(2), 382-393. https://doi.org/10.1006/viro.2000.0348

Zhao, K. N., Sun, X. Y., Frazer, I. H., & Zhou, J. (1998). DNA packaging by L1 and L2 capsid proteins of bovine papillomavirus type 1. *Virology*, *243*(2), 482-491. https://doi.org/10.1006/viro.1998.9091

Zhou, J., Stenzel, D. J., Sun, X. Y., & Frazer, I. H. (1993). Synthesis and assembly of infectious bovine papillomavirus particles in vitro. *J Gen Virol*, *74 (Pt 4)*, 763-768. https://doi.org/10.1099/0022-1317-74-4-763

Zhou, J., Sun, X. Y., Louis, K., & Frazer, I. H. (1994). Interaction of human papillomavirus (HPV) type 16 capsid proteins with HPV DNA requires an intact L2 N-terminal sequence. *J Virol*, *68*(2), 619-625. https://doi.org/10.1128/JVI.68.2.619-625.1994

zur Hausen, H. (2002). Papillomaviruses and cancer: from basic studies to clinical application. *Nat Rev Cancer*, *2*(5), 342-350. https://doi.org/10.1038/nrc798

Websites and other references

Axis-Shield. (2016). Optiprep - product description. In.

GAVI injects new life into HPV vaccine rollout. (2013). *Lancet*, *381*(9879), 1688. Retrieved May 18, from https://www.ncbi.nlm.nih.gov/pubmed/23683613

Global Cancer Observatory: Cancer Today. (2020). *2022*(14 November). http://gco.iarc.fr/today

Global HPV Vaccine Introduction Overview. (2020). *2022*(15 November). path.org/resources/global-hpv-vaccine-introduction-overview

Medicago Covifenz COVID-19 vaccine. (2022). https://www.canada.ca/en/health-canada/services/drugs-health-products/covid19-industry/drugs-vaccines-treatments/vaccines/medicago.html#shr-pg0

News In Brief. (2006). *Nature Biotechnology*, *24*(3), 233-234. https://doi.org/10.1038/nbt0306-233

Prendiville, W., & Sankaranarayanan, R. (2017). *IARC Technical Publications* (Colposcopy and Treatment of Cervical Precancer, Issue.

Roche. (2020). X-tremeGENE HP DNA Transfection Reagent. In (10 ed.).

Szondy, D. (2013). DARPA produces 10 million flu vaccine doses in one month. Retrieved 06/01/2023, from https://newatlas.com/darpa-flu-vaccine/25966/

WHO. (2016). *Weekly Epidemiological Record* (48). W. H. Organization.

WHO. (2020). *GLOBOCAN 2020*. https://gco.iarc.fr/

WHO Director-General Calls for All Countries to Take Action to Help End the Suffering Caused by Cervical Cancer. (2018). *2022*(15 November). http://who.int/reproductivehealth/call-to-action-elimination-cervical-cancer/en/